FABRICATION OF NANO COMPOSITE HYDROGELS BASED ON POLYVINYL ALCOHOL FOR BIOMEDICAL APPLICATIONS

ALI KARIMI

A THESIS SUBMITTED IN FULFILMENT OF THE REQUIREMENTS FOR THE DEGREE OF DOCTOR OF PHILOSOPHY

FACULTY OF ENGINEERING
UNIVERSITY OF MALAYA
KUALA LUMPUR

2016

UNIVERSITI MALAYA

ORIGINAL LITERARY WORK DECLARATION

Name of Candidate: Ali Karimi

Registration/Matric No: KHA100092

Name of Degree: Doctor of Philosophy (PhD)

Title of Project Paper/Research Report/Dissertation/Thesis ("this Work"):

FABRICATION OF NANO COMPOSITE HYDROGELS BASED ON POLYVINYL ALCOHOL FOR BIOMEDICAL APPLICATIONS

Field of Study: Chemical Engineering

I do solemnly and sincerely declare that:

(1) I am the sole author/writer of this Work;
(2) This Work is original;
(3) Any use of any work in which copyright exists was done by way of fair dealing and for permitted purposes and any excerpt or extract from, or reference to or reproduction of any copyright work has been disclosed expressly and sufficiently and the title of the Work and its authorship have been acknowledged in this Work;
(4) I do not have any actual knowledge nor ought I reasonably to know that the making of this work constitutes an infringement of any copyright work;
(5) I hereby assign all and every rights in the copyright to this Work to the University of Malaya ("UM"), who henceforth shall be owner of the copyright in this Work and that any reproduction or use in any form or by any means whatsoever is prohibited without the written consent of UM having been first had and obtained;
(6) I am fully aware that if in the course of making this Work I have infringed any copyright whether intentionally or otherwise, I may be subject to legal action or any other action as may be determined by UM.

Candidate's Signature **Date: 06. 09. 2016**

Subscribed and solemnly declared before,

Witness's Signature **Date:**

Name:
Designation: Chemical Engineering Department,
Faculty of Engineering, University of Malaya, Kuala Lumpur, 50603, Malaysia
Tel. /Fax: +60 379675206/ +60 379675313

ABSTRACT

In order to obtain nontoxic, tissue-compatible and efficient hydrogels for biomedical applications, Polyvinyl alcohol (PVA) / Na^+-montmorillonite (Na^+-MMT) nanocomposite hydrogels were prepared by a cyclic freeze-thaw process (physical method). Effect of nanoclay content and sonication mixing on the nanocomposite structure and morphology as well as its properties (mechanical, thermal), and also its swelling and deswelling kinetics were investigated.

Glutaraldehyde reacts with PVA to form covalently cross-linked networks. The acetal linkages were formed between hydroxyl groups of PVA and aldehyde groups of glutaraldehyde that was used for physicochemical synthesis of nanocomposites. A novel PVA nanocomposite hydrogel was synthesized by physicochemical method**.** Effect of physical and physicochemical cross linking on the structure, morphology, thermal, mechanical, swelling and deswelling properties of nanocomposite hydrogels were investigated and were compared together. The results were shown that physicochemical crosslinking of PVA nanocomposite leads to decreasing of crystallinity and melting temperature also increasing the Hardness and Water vapor transmission rate (WVTR) values than physical crosslinked. Swelling and deswelling measurements were done by gravimetric method and indicated that controlled crosslinking of PVA nanocomposite hydrogel caused to increase the swelling ratio and also decrease the cumulative amount of water loss. Sorption and desorption kinetics for both physical and physicochemical methods were based on diffusion mechanism and obey the Fickian model. As an important result using the controlled crosslinking can obtain the PVA nanocomposite hydrogel with higher swelling capacity than conventional PVA nanocomposite hydrogel. In order to find an optimum amount of nanoclay content for achieving the optimal Equilibrium water content (EWC) and WVTR properties of nanocomposite cryogels, my investigations were performed on the barrier and swelling properties of the

nanocomposites and it was shown that Na^+-MMT may act as a co-crosslinker. According to the results, the swelling characteristics of nanocomposite cryogels increases with the nanoclay content up to 1-2% nanoclay, after that they start to decrease uniformly. In contrast, the water removal from cryogels decreased and its time of removal prolonged on increasing the nanoclay content. Based on the results of WVTR measurements, the barrier properties of the nanocomposites can be improved by increasing the nanoclay content and it is concluded that the optimum range of nanoclay for having optimum WVTR at 37 °C is up to 1% nanoclay. It was found that the EWC of PVA nanocomposite cryogel containing 1% nanoclay, having 74% water content compared to the other nanocomposites at 37 °C. Results of EWC (above 60%) and WVTR (at about 8.5 $g/m^2/h$) are within the acceptable range for biomedical applications such as skin treatment and wound dressing.

With the aim of investigation on the antibacterial properties of PVA/Na^+-MMT nanocomposite hydrogels against two types of bacteria**,** Escherichia coli (E-Coli); as a gram negative bacteria and Staphylococcus aureus (S-Aureus); as a gram positive bacteria, polyvinyl pyrrolidone – Iodine (PVP-Iodine) has been used in the hydrogel network. The effect of nanoclay content on release of antibacterial agent for loaded hydrogels was also investigated in vitro and found to be dependent on crosslinking amount due to interaction between PVA and nanoclay.

ABSTRAK

Dalam usaha untuk mendapatkan hidrogel tanpa toksik, tidak berbahaya, tisu yang bersesuaian dan berkesan bagi aplikasi bioperubatan, Polivinil alkohol (PVA) / Na^+-montmorillonite (Na^+-MMT) Hidrogel nanokomposit telah disediakan mengunakan satu proses kitaran beku-cair kitaran (kaedah fizikal). Kesan kandungan tanah liat nano dan campuran sonikast pada struktur nanokomposit dan morfologi serta sifat-sifatnya (mekanikal, haba), dan juga kinetic swelling dan deswelling yang telah dikaji.

Glutaraldehyde bertindak balas dengan PVA untuk membentuk rangkaian kovalen balas berkaitan. Hubungan asetal telah dibentuk antara kumpulan hidroksil PVA dan aldehid kumpulan glutaraldehyde yang digunakan untuk sintesis fizikokimia nanocomposites. PVA nanokomposit hidrogel telah disintesis melalui kaedah fizikokimia. Kesan sambung- silang fizikal dan fizikokimia kepada struktur, morfologi, haba, mekanikal, sifat swelling dan deswelling Hidrogel nanokomposit telah disiasat dan dibandingkan. Keputusan telah menunjukkan bahawa Sambung-silang fizikokimia PVA nanokomposit membawa kepada pengurangan penghabluran dan suhu lebur juga meningkatkan kekerasan dan kadar penghantaran wap air (WVTR) berbanding sambyng-silang fizikal. ukuran swelling dan deswelling telah dilakukan dengan kaedah gravimetrik dan ia menunjukkan Sambung-silang terkawal PVA nanokomposit hidrogel disebabkan untuk meningkatkan nisbah swelling dan juga mengurangkan jumlah kerugian air terkumpul. Kinetic Erapan dan penyaherapan kinetik bagi kaedah kedua-dua kaedah fizikal dan fizikokimia adalah berdasarkan mekanisme penyebaran dan mengikut model Fickian. Sebagai hasil penggunaan Sambung-silang terkawal boleh mendapatkan hidrogel PVA nanokomposit dengan kapasiti swelling yang lebih tinggi daripada konvensional PVA nanokomposit hidrogel. Dalam usaha untuk mencari jumlah optimum kandungan tanah liat nano bagi mencapai kandungan optimum Keseimbangan air (EWC) dan ciri-ciri WVTR daripada cryogel nanokomposit, kajian telah dilakukan ke atas halangan dan

sifat swelling nanokomposit dan ia menunjukkan bahawa Na^+ -MMT boleh bertindak sebagai penyambung-silang. Berdasarkan hasil kajian, ciri-ciri swelling nanokomposit cryogel meningkat dengan 1-2% kandungan tanah liat nano, dan selepas itu mula berkurangan secara seragam. Sebaliknya, penyingkiran air dari cryogel menurun dan masa penyingkiran berpanjangan mengikut peningkatan kandungan tangah liat nano itu. Berdasarkan hasil pengukuran WVTR, halangan nanokomposit boleh diperbaiki dengan meningkatkan kandungan tanah liat nano dan julat optimum tanah liat nano bagt mendapatkan suhu optimum WVTR pada 37° C adalah sehingga 1% tanah liat nano. Selain itu EWC PVA cryogel nanokomposit yang mengandungi 1% tanah liat nano, mempunyai 74% kandungan air berbanding dengan nanokomposit lain pada suhu 37° C. Keputusan EWC (melebihi 60%) dan WVTR (kira-kira 8.5 g / m^2 / h) adalah dalam julat yang boleh diterima bagi aplikasi bioperubatan seperti rawatan kulit dan pembalut luka.

bagt tujuan kajlan terhadap sifat antibakteria PVA / Na^+ -MMT Hidrogel nanokomposit terhadap dua jenis bakteria, Escherichia coli (E-Coli); sebagai bakteria gram negatif dan Staphylococcus aureus (S-Aureus); sebagai bakteria gram positif, Polivinil pyrrolidone - Iodin (PVP-Iodin) telah digunakan dalam rangkaian hidrogel. Kesan kandungan tanah liat nano terhadap pembebasan agen anti-bakteria untuk Hidrogel juga dikaji secara in-vitro dan didapati bergantung kepada jumlah sambung-silang berikutan interaksi antara PVA dan tanah liat nano.

ACKNOWLEDGEMENTS

First and foremost, I am very thankful to Allah for his unparalleled grace and guidance throughout of my life. This research project was not possible without help and kindness of the Almighty God.

I would like to express my sincere gratitude to my supervisor Professor Dr. Wan Mohd Ashri Wan Daud, for his guidance, insight and support throughout this research work.

I would like to express my special appreciation and thanks to the Chemical Engineering Department staff in university of Malaya, for their collaborations during the entire period of my study. I appreciate to Chemical Engineering Department in the University of Tehran, especially professor Navid Mostoufi and Dr. Babak Kaffashi, for their valuable time and collaboration provided in this research project.

I also would like to thank my dear colleague and old friend, Dr. Ahmad Nalbandi for his help throughout this thesis.

I dedicate this thesis to my father and my brother, for their love and support throughout my life, although they are not alive anymore. I also grant the dissertation to my dear mother, my dear wife, Fatemeh and my dear sons Amir Mohammad and Erfan for their devotion, love and patience.

And finally, I dedicate this thesis to those researchers who generously spend their life to serve the humanity.

Ali Karimi

Department of Chemical Engineering,

University of Malaya, Kuala Lumpur, Malaysia

TABLE OF CONTENTS

LIST OF FIGURES

LIST OF TABLES

LIST OF ABBREVIATIONS

AA	Acrylic acid
AFM	Atomic Force Microscopy
AIBN	2, 2'-Azobis-Isobutyronitrile
C12MMT	Dodecylammonium-modified MMT
C12OOHMMT	12-Aminolauric-modified MMT
DMA	Dynamic Mechanical Analysis
DMAc	N, N-dimethylacetamide
DMTA	Dynamic Mechanical Thermal Analysis
DSC	Differential Scanning Calorimetry
DW	Deionized Water
E’	Elastic (storage) modulus
E”	Viscous (loss) modulus
E-Coli	Escherichia Coli
EWC	Equilibrium Water Content
FESEM	Field Emission Scanning Electron Microscopy
FT	Freeze-Thaw
FT & GA	Freeze-Thaw & Glutaraldehyde
FTIR	Fourier Transform Infrared
GA	Glutaraldehyde
HDPE	High-Density Poly Ethylene
HPMC	Hydroxy Propyl Methyl Cellulose
MDSC	Modulated Differential Scanning Calorimetry
MMT	Montmorillonite
Na^{+}-MMT	Sodium Montmorillonite
NIPA	Poly (N-Iso Propyl Acrylamide)

NIPAAm	N-Iso Propyl Acrylamide
NIPAM	N-Iso Propyl Acrylamide
NMR	Nuclear magnetic resonance
OMLS	Organically Modified Layered Silicate
OMMT	Organically Modified Montmorillonite clay
PAA	Poly (Acrylic acid)
PAN	Poly Acrylonitrile
PANI	Poly Aniline
PCL	Poly Caprolactone
PDDA	Poly (Diallyl Dimethyl Ammonium Chloride)
PEO	Poly Eethylene Oxid
PES	Poly Ether Sulfone
PET	Poly Ethylene Terephthalate
PLA	Polyl Actic acid
PLS	Polymer Layered Silicate
PP	Poly Propylene
PS	Poly Styrene
PU	Poly Urethane
PVA	Poly Vinyl Alcohol
PVA/Na^{+}-MMT	Poly (vinyl alcohol) / Sodium Montmorillonite
PVOH	Poly Vinyl Alcohol
PVP	Poly Vinyl Pyrrolidone
PVP- Iodine	poly Vinyl Pyrrolidone – Iodine
SANS	Small-Angle Neutron Scattering
S.Aureus	Staphylococcus Aureus
SAXS	Small Angle X-ray Scattering

SEM	Scanning Electron Microscope
SPS	Smart polymers
SR	Swelling Ratio
TEM	Transmission Electron Microscopy
Tg	Glass Transition Temperature
TGA	Thermogravimetric Analysis
Tm	Melting temperature
UV	Ultraviolet
WAXD	Wide Angle X-ray Diffraction
WVTR	Water Vapor Transmission Rate
XRD	X-ray Diffraction
ΔHm	Enthalpy of melting
χ_C	Degree of crystallinity
M_∞	Initial amount of water inside the nanocomposite hydrogel
M_t	Water desorbed at any time t
Ws	Weight of the swollen gel
W_∞	Equilibrium water sorption.
W_d	Weight of the dry gel
W_t	Amount of absorbed water at any time t
$m(0)$	Weight of hydrogel at the initial time zero
$m(\infty)$	Weight of hydrogel at drying time
$m(t)$	Weight of hydrogel at time t

LIST OF APPENDICES

CHAPTER 1: GENERAL INTRODUCTION

1.1 Background

In the past years, several attempts have been made to the preparation and characterization of nano composite hydrogels, the elasticity and permeability of gels with the reinforcing ability of clays embedded into the hydrogels are combined in these hydrogels (Bignotti et al., 2004; Ekici et al., 2006; Haraguchi et al., 2003). Also using nanoclay in nanocomposite hydrogel structures leads to enhanced chemical, physical and mechanical properties (Haraguchi & Takehisa, 2002; Schexnailder & Schmidt, 2009; Haraguchi, 2007).

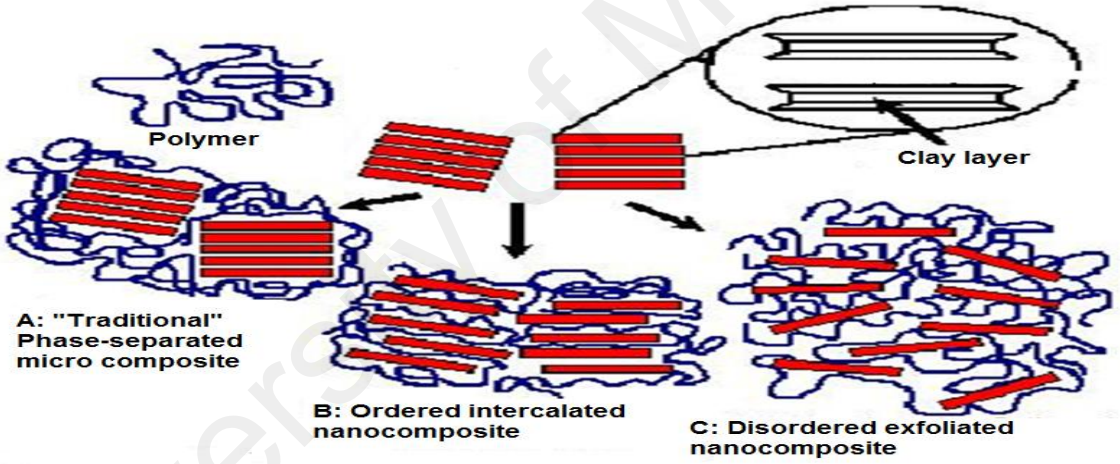

Figure 1.1: Schematic diagram showing structures of polymeric composites: A) Conventional (traditional) B, C) Nanotechnology

Among the natural mineral clays such as bentonite (Lee & Chen, 2004; Huang et al., 2009), laponite (Abdurrahmanoglu et al., 2008; Liu et al., 2007; Song et al., 2008; Nie & Oppermann, 2005), hydrotalcite (Lee & Lee, 2006, Zhang et al., 2009) and montmorillonite (Kasgoz & Durmus, 2008, Lee & Fu, 2003, Sur et al., 2003, Al et al., 2003), the main natural mineral clay that widely used to prepare nanocomposite hydrogels, is montmorillonite (MMT). This is due to its good water absorption, extensive swelling in water and cation exchange capacity (Gao et al., 1999, Gamiz et

al., 1992, Gao et al., 2001). Due to the presence of silanol groups on the MMT and ability to hydrogen bonding, montmorillonite can interact with hydrophilic polymers to participate in ensuring the stability of the nanocomposite systems (Mirzan et al., 2001, Velazco-Diaz et al., 2005). Thus, MMT can act as a co-crosslinker for hydrophilic polymers in solution (Mc Gann et al., 2009).

Polyvinyl alcohol (PVA) is produced commercially via hydrolysis of polyvinyl acetate being polymerized from vinyl acetate monomer (Fig.1.2). PVA has exceptional properties such as; hydrophilic, water soluble, biodegradable, biocompatible, non- toxic, non carcinogenic and non expensive, that capable to form gel by chemical or physical methods (Giusti et al., 1993, Valenta & Anver, 2004, Patachia, 2003, Hennink & van Nostrum, 2002, Peppas et al., 2000, Ratner et al., 2004, Hassan & Peppas, 2000, Hoffman, 2001).

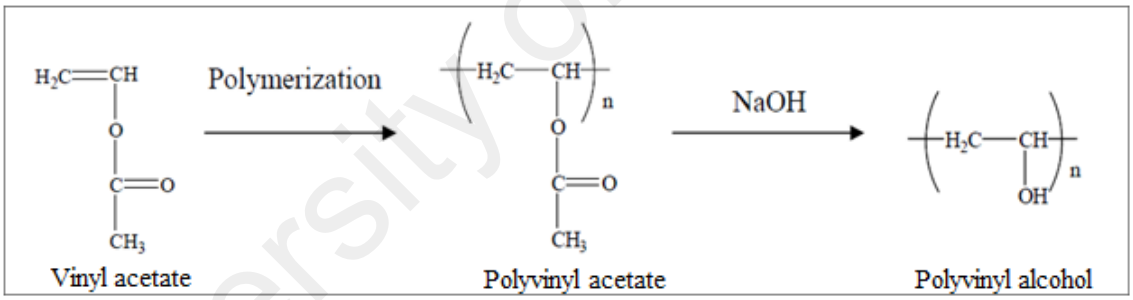

Figure 1.2: Vinyl acetate polymerization and its hydrolysis to polyvinyl alcohol

It has been used in various bio medical applications, for instance as drug delivery devices (Li et al., 1998), artificial organs (Chen et al., 1994), wound dressing (Razzak et al., 2001, Yoshii et al., 1999, Yoshii et al., 1995), contact lenses (Hyon et al., 1994), skin treatment systems (Cha et al., 1993), protein adsorption, protein controlled release and delivery by chemical and physical methods (Elizabeth & Fabia, 2006, Christie et al., 2000, Peppas & Simmons, 2004). PVA hydrogels can be prepared in several cross-linking methods. Chemical crosslinked PVA such as covalent cross-linking by glutaraldehyde (Fig.1.3).

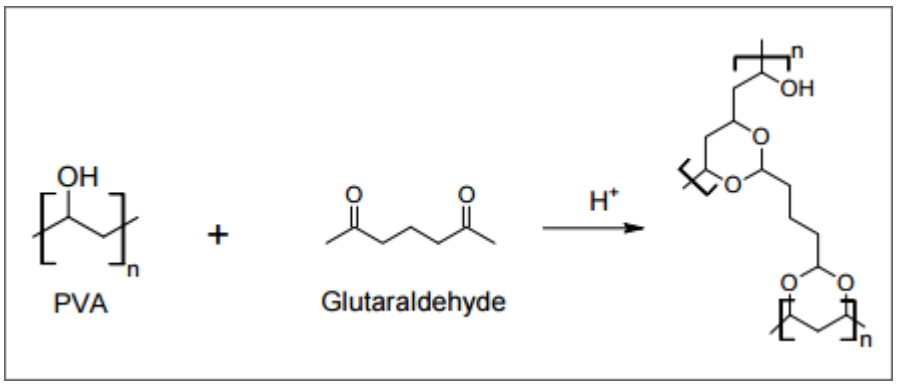

Figure 1.3: Chemical crosslinking of PVA using glutaraldehyde

In general, the hydroxyl groups of PVA can react with all multi-functional compounds to obtain three-dimensional PVA networks (Caro et al., 1976, Korsmeye & Peppas, 1981, Gimenez et al., 1997). Physical cross linked PVA prepared by gamma irradiation (Varshney, 2007, Mirzan et al. 2001), and freezing–thawing process have reported by some of the researchers, (Velazco-Diaz et al., 2005, Mc Gann et al., 2009, Sirousazar & Yari, 2010, (Watase & Nishinari, 1988, Nagura et al., 1989, Yamura et al., 1989) For example, Varshney (2007), reported the synthesis of PVA-based hydrogel by gamma-irradiation technique and Mirzan et al. (2001) reported the synthesis of gamma-irradiated polyvinyl alcohol-polyvinyl pyrrolidone (PVA-PVP) hydrogel. In other studies some of the researchers have used the freeze-thaw method for the synthesis of PVA-based hydrogels (Velazco-Diaz et al., 2005, Mc Gann et al., 2009, Sirousazar & Yari, 2010). For instance, Kim et al. (2008) have used the freeze-thaw method for development of polyvinyl alcohol-alginate gel-matrix-based wound dressing containing nitro furazone. Also in order to synthesis of PVA/PVP/glycerin/antibacterial agent hydrogel for wound dressing use of the gamma-irradiation followed by freeze-thaw method have reported by Nho et al. (2009). PVA solutions have formed gels during freeze-thaw process. Changing in regional concentration of polymer molecules, form the intermolecular forces and leads to the formation of micro crystals (Okazaki et al.

1995). The crystalline domains play the role of cross-linking sites in the hydrogel networks (Takeshita et al. 1999).

PVA gels have physical linkage without any chemical cross-linkers, they are suitable to design nontoxic and biocompatible, biomedical devices for microorganisms (Okazaki et al. 1995, Wilcox et al. 1999, Lozinsky et al. 2000, Hassan et al. 2000). Polyvinyl alcohol nanocomposites have been studied by several authors (Velazco-Diaz et al., 2005, Mc Gann et al., 2009, Sirousazar & Yari, 2010). The first fabrication of PVA/MMT composites reported by Greenland (1963) used solvent casting method with water as a co-solvent. After that Ogata et al., (1997) using the same method have produced PVA/MMT composites. Also, Strawhecker and Manias have used solvent casting method in attempts to fabrication of PVA/MMT nanocomposite films. They produced PVA/MMT nanocomposite films from a MMT/water suspension containing dissolved PVA by casting and they found a co-existence of silicate layers in the intercalated and exfoliated states. Also they reported that the properties of PVA nanocomposite such as the mechanical, thermal and water vapor transmission are beyond the pure PVA and its conventionally composites (Strawhecker & Manias, 2000). Preparation of the nanocomposites based on PVA with three different types of clays-pristine MMT and organically modified MMT, reported by Chang et al. (2003). In order to prepar nanocomposites they used Na ion exchanged clays (i.e. Na^+-saponite and Na^+-montmorllonite) and alkyl ammonium ion-exchanged clays by the solution intercalation method. They concluded that the hydrophilic character of clay promotes dispersion of inorganic crystalline layers in water soluble polymers (Blumstein, 1965, Zhao et al., 1989). Synthesis of a series of PVA/MMT nanocomposites through in situ intercalative polymerization method using AIBN as initiator has been reported by Yu et al. (2003). Kokabi et al. (2007) have reported the nanocomposite hydrogels based on PVA and organically modified montmorillonite clay were introduced as wound dressings, which

prepared by the cyclic freezing–thawing method. Investigation of the PVA hydrogels'behavior in contact with physiological liquids or at designing electrolyte sensor shows an intelligent behavior in the presence of electrolyte solutions (Patachia et al., 2007).

1.2 Problem Statement

Nanocomposite hydrogels are 3- dimentional polymer networks with hydrophilic groups containing nanoclay that have high affinity of water absorption. Because of their properties like the natural soft tissue they are biocompatible and suitable for biological applications. They are able to absorb water or physiological fluids up to hundreds, even thousands times of their dry weights. When fully swollen, they are soft and smooth, having physical properties similar to natural and living tissues.

Polyvinyl alcohol is a synthetic and hydrophilic polymer with a simple chemical structure, high hydroxyl group contents provide PVA and PVA-based materials many desired properties (biocompatible, nontoxic, non-carcinogenic and inert in body fluids) suitable for biomedical applications. PVA can form hydrogels of high water content with several different methods such as chemical crosslinking, freeze/thawing, gamma irradiation and photopolymerisation. PVA hydrogels have desirable mechanical, swelling and optical properties which make them suitable for tissue engineering.

Due to the presence of silanol groups on the montmorillonite (MMT) and ability to hydrogen bonding, MMT can interact with hydrophilic polymers such as PVA (Fig. 1.4). It has good water absorption, extensive swelling in water and cation exchange capacity to participate in ensuring the stability of the nanocomposite systems.

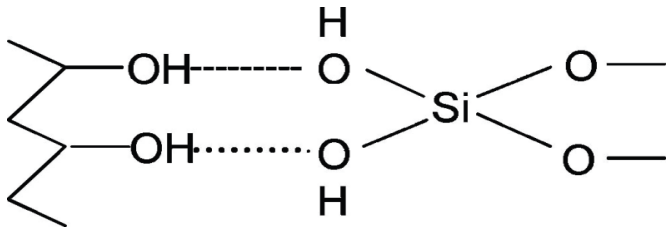

Figure 1.4: Hydrogen bonded polyvinyl alcohol organic –inorganic hybrid structures

Despite the widespread use of hydrogels in biological and biomedical applications, due to the chemical reactions, organical modifications and chemical crossliking most hydrogels do not provide all of the desired requirements to interact with biological systems. The hydrogels have some disadvantages such as; presence of chemicals and residual cross-linking agents in the hydrogel that are toxic and even carcinogenic for the tissues and organisms. Residuals elimination are expensive that include the increasing of production costs. Therefore a need was felt to redesign a new non toxic nanocomposite hydrogel in order to overcome limitations related to fulfilling the above-mentioned requirements.

Cryogelation is one of the methods of physical hydrogel formation. These gels are formed through processes which force formation of non-covalent bonds such as hydrogen bonds, ionic bonds or by basic entanglement of the polymeric chains and crystallites after freezing and thawing cycles. The gels are very beneficial in the sense that there is no need for addition of any chemical crosslinker. Cryogels form under moderate freezing conditions in which frozen solvent causes phase separation and acts as a porogen, leading to a gel with high water content. Gelation can occur in each of the three steps of the freeze-thawing process; freezing, storage in frozen state or during thawing. For PVA the most important step is thawing, since this is where most of the gel formation occurs. One of the main aspects of cryogelation is that not all of the solvent freezes under these conditions and there is always a portion of the solvent in the

liquid phase. The surface tension between the thawed solvent and the gel phase causes round pores. The freeze/thaw or cryogelation method has an important advantage over chemical methods. Due to its purely physical nature there is no risk of remnant chemicals that might compromise the biocompatibility of the final hydrogel. Also, gels formed with this method are highly elastic and durable, which is quite important for soft tissue engineering.

The swelling behavior of hydrogels and their swelling kinetics in different media based on their applications are important. The presence of osmotically active mobile ions affects the swelling behavior of hydrogels. In vitro studies of biocompatibility preliminary in simulated physiological fluids have a great importance on the application of biomaterials. The resemblance of PVA hydrogels to living tissues in their physical properties because of their relatively high water content as well as soft and rubbery consistency shows that PVA hydrogels have potential applications in this field and are excellent candidates for biomedical applications.

Skin is the important body external defense system serving as a mechanical barrier to prevent bacterial and microorganisms to enter the body. Skin treatment and wound dressing are examples of hydrogel applications in the biomedical field. Dressings the wounds with the hydrogels are usually accomplished by directly applying the hydrogels to the injured skin and wounds. Wound dressings must ideally have characteristics like maintenance of moisture, permeability of gases, protection against secondary infection, thermal insulation, elastic, biodegradable and biocompatible, thus the non-toxicity, biocompatibility and antibacterial properties of the hydrogel must be considered.

1.3 Objectives

The main objective of this thesis is focused on fabricate and characterize the non toxic nanocomposite cryogels based on polyvinyl alcohol and Na^{+}- montmorillonite via

physical and physicochemical crosslinking as a novelty and deeply understand their properties, relating to biomedical applications. For the first time the critical concentration of nanoclay has been optimized to achieve the required both EWC and WVTR characteristics in an acceptable range for biomedical applications such as; skin treatment and wound dressing. The main objectives of this research are:

1- To fabricate of physical PVA/Na^+-MMT nanocomposite hydrogels (Cryogels), and physicochemical PVA/Na^+-MMT nanocomposite hydrogels.

2- To compare the properties of PVA/Na^+-MMT nanocomposite hydrogels prepared by physical and physicochemical cross linking.

3- To fabricate and characterize of non toxic hydrogels based on PVA/Na^+-MMT nanocomposites for biomedical applications.

4- To optimize the nanoclay content in acceptable range of Equilibrium water content (EWC) and Water vapor transmission rate (WVTR) for biomedical applications.

5- To investigate and finding the water sorption and desorption kinetics model of prepared PVA/Na^+-MMT nanocomposite hydrogels.

6- To investigate the effect of nanoclay content on release of antibacterial agent for loaded PVA/Na^+-MMT nanocomposite hydrogels.

1.4 Outline of the thesis

This thesis comprises the following main chapters:

1. Chapter One – GENERAL INTRODUCTION

This chapter includes a brief introduction to the research and objectives of the study.

2. Chapter Two - LITERATURE REVIEW

This chapter gives a comprehensive literature survey for the Materials, preparation, and characterization of PVA/MMT nanocomposite hydrogels

3. Chapter Three – METHODOLOGY

This chapter describes the experimental procedure which includes nanocomposite hydrogels preparation, swelling cxperiments, structural charactrizations and morphology, thermal and mechanical analysis, Hardness measurements, permeation analysis and water sorption and desorption kinetics.

4. Chapter Four - RESULTS AND DISCUSSION

The structural characterization and morphology of nanocomposite hydrogels, thermal and mechanical analysis, Hardness measurements , barrier properties and Permeation analysis, the swelling behavior of hydrogels which include equilibriurn swelling results, swelling ratio, swelling rate, water sorption and desorption kinetics, finding the diffusion kinetics model, are presented in this chapter.

5. Chapter Five – CONCLUSIONS AND RECOMENDATIONS

In the last chapter, the results and findings of this study have summarized and recommendations for future works have been suggested.

CHAPTER 2: REVIEW OF RELATED LITERATURE

2.1 Introduction

In the past years, several research groups have studied the preparation and characterization of nanocomposite hydrogel materials. These kinds of hydrogels are able to combine the elasticity and permeability of gels with the reinforcing ability of clays embedded in the hydrogels, providing a wide range of application in different fields for the hydrogels (Haraguchi et al., 2003, Bigotti et al., 2004, Ekici et al., 2006).

Montmorillonite (MMT) is a naturally occurring mineral clay that is widely used to prepare nanocomposite hydrogels, and this is mainly due to its good water absorption, extensive swelling in water and cation exchange capacity. Because of its intrinsic chemical composition, such as; presence of silanol groups (–Si–OH) on the layer surface of MMT and its ability to form hydrogen bonding (Fig.2.1), the montmorillonite is able to interact with hydrophilic polymers (Gamiz et al., 1992, Gao et al., 1999, Chiellini et al., 2000, Gao et al., 2001, Backfolk et al., 2006). Therefore, MMT and other phyllosilicates can act as co-crosslinkers of hydrophilic polymers in solution (Lin et al., 2001, Karimi & Wan Daud, 2014).

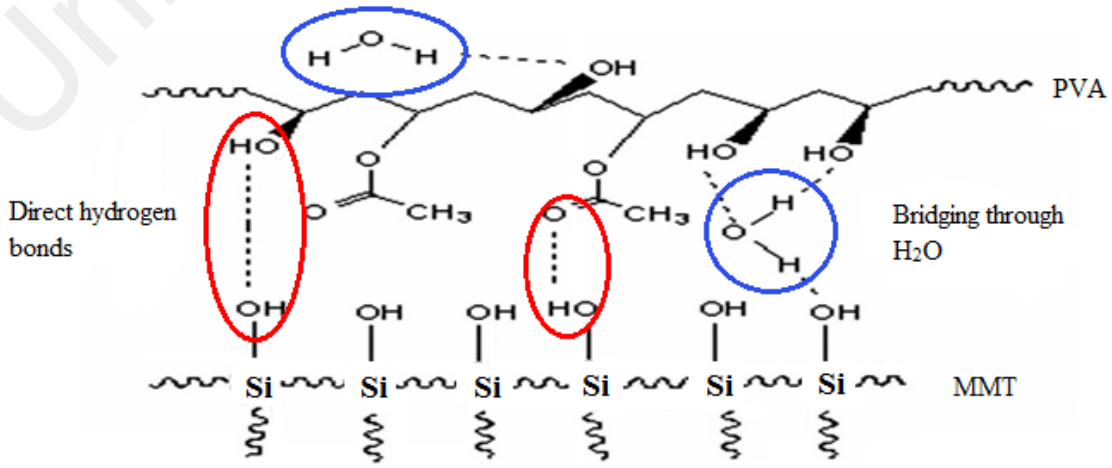

Figure 2.1: Interactions among PVA, water, and MMT

These features of MMT were thoroughly studied by Lee and Jou who investigated the effect of intercalated montmorillonite on the swelling and drug release behaviors of a nanocomposite constituted by N-isopropylacrylamide (NIPAAm) /acrylic acid (Lee & Jou, 2004). Liu and co-authors also observed a significant improvement in the tensile properties of NIPAAm-based nanocomposite hydrogels containing a modified hectorite-laponite mineral (Liu et al., 2006). An improvement of mechanical and thermal properties was also reported by Zheng and collaborators (Zheng et al., 2002) and by Lee and Lee for gelatin hydrogels containing montmorillonite (Lee & Lee, 2006). Churochkina et al., (1998) have shown that the mechanical properties of the Neutral and Slightly Charged Poly (acrylamide) Gels are modified with the addition of Na-montmorillonite (Churochkina et al., 1998). On the other hand, several authors have studied polyvinyl alcohol (PVA) nanocomposites (Carrado et al., 1996, Yu et al., 2003, De Bussetti et al., 2004).

PVA has exceptional and interesting properties such as being: hydrophilic, water-soluble, gas barrier, good chemical resistance, processability, non-toxic, non-carcinogenic biocompatibile, biodegradabe and inexpensive, and is capable of forming gel networks by chemical or physical methods (Mahdavi et al., 2013, Valenta & Anver, 2004, Patachia, S., 2003, Hennink & van Nostrum, 2002, Peppas et al., 2000, Ratner et al., 2004, Hassan & Peppas, 2000, Hoffman, A.S., 2001, Coviello et al., 2007, Silva et al., 2013). These properties play important roles in the design of pharmaceutical and biomedical devices. It has been used in various biomedical applications, for instance as drug delivery devices, artificial organs, wound dressings, contact lenses, antibacterial, skin treatment systems, protein adsorption, protein controlled release and for delivery by chemical and physical methods (Mirzan et al., 2001, Paradossi et al., 2003, Chen et al., 1994, Nacer Khodja et al., 2013, Gonzalez et al., 2012, Kokabi et al., 2007, Abd El-Mohdy, H.L., 2013, Vicentini et al., 2010, Shalumon et al., 2011, Gonzalez et al., 2011,

Li et al., 2013, Kenawy et al., 2014, Zhao et al., 2003, Hyon et al., 1994, Cha et al., 1993, Elizabeth & Fabia, 2006, Christie et al., 2000, Peppas & Simmons, 2004).

In the polymer nanocomposites of PVA and MMT as novel materials, the hydrogen bonding between the silanol groups and negatively charged on the surface of the MMT and hydroxyl groups of the PVA has the most important role to the surface interactions of MMT with the PVA chains (Grunlan et al., 2004, Hernandez et al., 2008). In addition, because of the existence of metal ions in the MMT lattice, interactions of the MMT layers with the acetoxy groups in the PVA chains will be increased causing strong PVA-MMT interactions that lead to enhancement of the MMT layers dispersion into the PVA matrix (Stathi et al., 2009). These interactions consequently lead to the intercalated or exfoliated composite structures and their overall performance (Sapalidis et al., 2011). Due to the presence of MMT the PVA crystallinity is decreased and nanocomposite biodegradation occurs faster than pure PVA (Lee et al., 2003, Shina. Ray et al., 2002).

It has been recognized that semi-diluted PVA solutions can form gels under cooling at low temperatures. Pines & Prins (1973) showed that PVA hydrogels can be formed via crystallization of PVA chains and or by liquid–liquid phase separation. PVA crystalline domains can act as crosslinking sites for the network (Takeshita et al., 1999). The interesting characteristic of PVA solutions has been used to produce PVA hydrogels without using any chemical crosslinkers that is important to make non-toxic, biocompatible and biomedical devices (Willcox et al., 1999, Hassan et al., 2000, Lozinsky & Damshkaln, 2000). PVA gels prepared by the sequential freezing-thawing process have physical linkages, so they are non toxic for organisms; changes in regional concentration of polymer molecules form intermolecular forces, leading to the formation of microcrystals (Okazaki et al., 1995).

In a number of articles, some PVA cryogels characteristics, their properties and the cryostructuring conditions have been discussed (Hajizadeh, et al., 2013, Tretinnikov, et al., 2015). Lozinskii and coworkers investigated changes in the mechanical properties of these polymeric gels with an increase in temperature from 295°K (normal temp.) to 350-390°K (lyogel melt) range (Lozinsky et al., 2003). Kobayachi et al., (1992) have prepared the PVA hydrogel with excellent mechanical properties, high clarity and high water content through crystallization at low temperatures. Also, Won-Ill et al., (1993) have prepared the PVA hydrogel with elasticity properties below 0°C, as well as good adhesion and excellent water holding properties, using water and organic solvents. They prepared the hydrogel from concentrated PVA solutions by a crystallization technique at low temperatures as a biomaterial for skin treatment systems.

Synthesis and characterization of PVA hydrogels and their hybrids by chemical and physical methods for protein adsorption, protein controlled release and delivery have been investigated by some researchers (Christie et al., 2000, Peppas & Simmons, 2004, Elizabeth & Fabia, 2006). They have also prepared the semi-crystalline PVA films and their blends with poly (acrylic acid) and poly (ethylene glycol) by freeze-thawing for drug delivery application. Moreover, the structure and morphology of PVA hydrogels were investigated **(**Hassan & Peppas, 2000 a, Hassan & Peppas, (2000) b, Hassan et al., 2000, Peppas & Tennenhous, 2004)

The conventional hydrogels have some disadvantages such as; presence of chemicals and residual cross-linking agents in the hydrogel that are toxic and even carcinogenic for living tissues and organisms. Residuals elimination are expensive that include the increasing of production costs.

PVA/MMT nanocomposite hydrogels have some advantages compared to the other conventional and similar systems. They are made of PVA which is a biodegradable,

biocompatible, non-toxic, non-carcinogenic and inexpensive polymer, as well as montmorillonite (MMT) which is a low cost, high surface area, hydrophilic and environmentally friendly and naturally abundant clay, being prepared by physical methods such as freezing - thawing cycles contains important advantage over chemical methods. These physical gels have a common benefit that is no need to add any chemical crosslinker to the hydrogels. Due to its pure physical structure there is no risk of remnant chemicals that might compromise the biocompatibility of the final hydrogel. Also, gels formed with this method are non-toxic and highly elastic and durable, which is quite important for biomedical applications.

2.2 Structure and properties of nanoclay (phyllosilicates)

2.2.1 Structure and properties of layered silicate

The most commonly used layered silicates are Montmorillonite (MMT), hectorite, and saponite. There are two types of structure for layered silicates: tetrahedral-substituted and octahedral-substituted moieties. The polymer matrices can interact more readily with tetrahedrally-substituted layered silicates than with octahedrally-substituted material due to the negative charges being located on the surface of silicate layers in the case of tetrahedrally-substituted silicates. The structure and chemical formula of these layered silicates are shown in Figure 2.2 and Table 2.1.

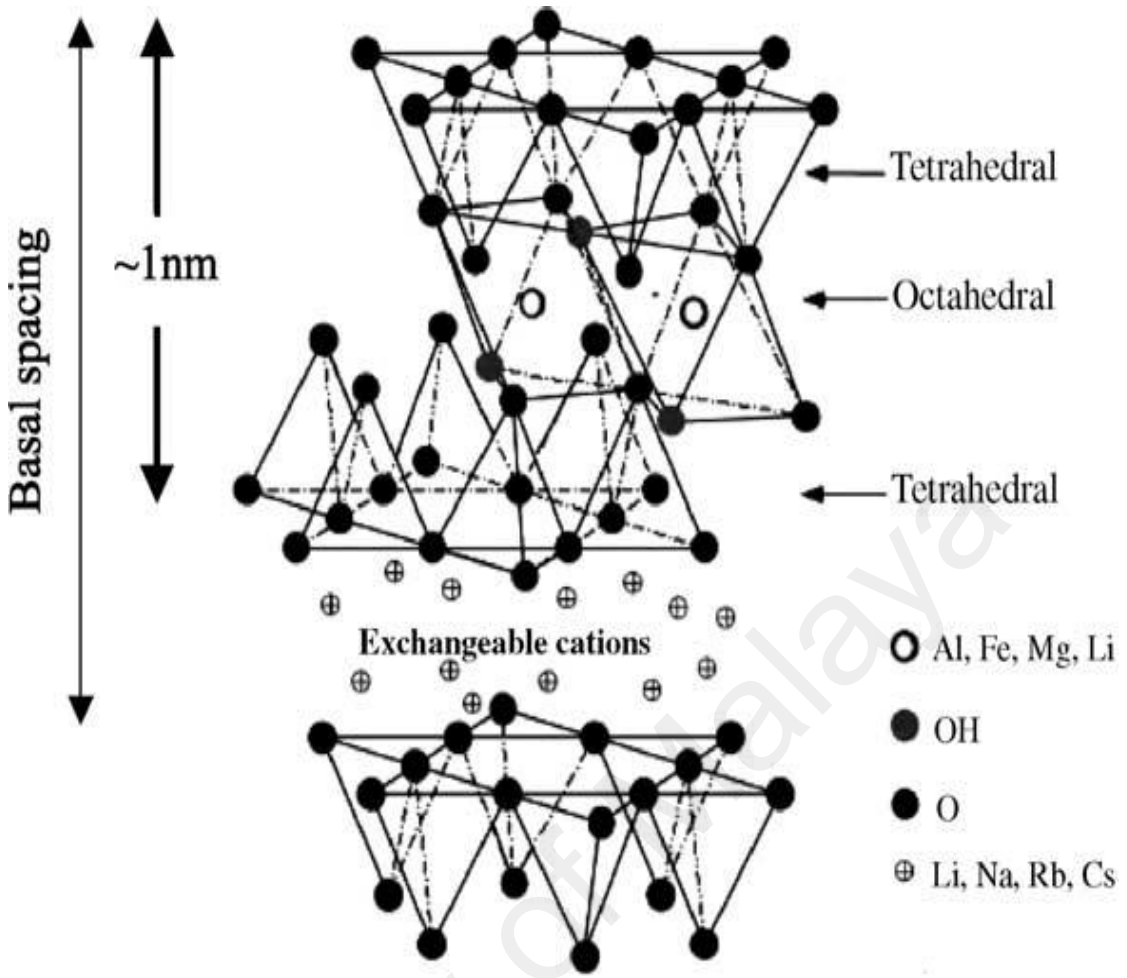

Figure 2.2: Structure of 2:1 phyllosilicates

The layered silicates have two particular characteristics for Polymer Layered Silicate (PLS) nanocomposites. The first characteristic is the dispersal ability of the silicate particles into individual layers, while the second ability is ion exchange reactions with organic and inorganic cations to fine-tune their surface chemistry. Of course, these two characteristics are related to the degree of dispersion of layered silicate in a particular polymer matrix depending on the interlayer cation.

Table 2.1: Chemical formula and characterization parameters of commonly used 2:1 phylosilicates.

2:1 phylosilicates	Chemical formula	CEC(mequiv/100g)	Particle length(nm)
Montmorillonite	$M^*_x(Al_{4-x}Mg_x)Si_8O_{20}(OH)_4$	110	100-150
Hectorite	$M_x(Mg_{6-x}Li_x)Si_8O_{20}(OH)_4$	120	200-300
Saponite	$M_x\ Mg_6\ (Si_{8-x}Al_x)Si_8O_{20}(OH)_4$	86.6	50-60

*__M__, monovalent cation; **x,** degree of isomorphous substitution (between 0.5 and 1.3).

2.2.2 Structure and properties of organically modified layered silicate (OMLS)

The physical mixture of a polymer with the layered silicate may not form a nanocomposite. This situation is similar to polymer blends, and in most cases, separation into discrete phases may take place. In immiscible systems, which typically correspond to the more conventionally-filled polymers, the poor physical interaction between the organic and inorganic components leads to poor mechanical and thermal properties. In contrast, strong interactions between the polymer and layered silicate in PLS nanocomposites lead to the organic and inorganic phases being dispersed at the nanometer level. As a result, the nanocomposite systems can show unique properties that are not shared by their micro conventionally-filled polymers (Okada et al., 1990, Giannelis 1996, Giannelis et al., 1999, LeBaron et al., 1999, Vaia et al., 1999, Biswas & Sinha Ray, 2001).

Montmorillonite is an inorganic material which is hydrophilic and usually contains hydrated Na^+ or K^+ ions (Blumstein, 1965). The layered silicates in a pristine state are only miscible with hydrophilic polymers, such as polyethylene oxide (PEO), and PVA (Vaia et al., 1999, Vaia et al., 1993). For miscibility, the silicates layered with other polymers must convert the hydrophilic silicate surface to an organophilic surface; this can be achieved via ion-exchange reactions using cationic surfactants such as primary, secondary, tertiary, and quaternary alkyl ammonium or alkyl phosphonium cations**.**

Alkyl ammonium or alkyl phosphonium cations in organosilicates are responsible for lowering the surface energy of the inorganic host and improving the wetting properties of the polymer matrix and the resulting larger interlayer spacing. Also, functional groups in these cations can react with the polymer matrix to increase the strength of the interface between the polymer matrix and the inorganic host (Blumstein, 1965, Aranda & Ruiz-Hitzky, 1992). Wide angle X-ray diffraction (WAXD) has been used to determine and perform arrangement and orientation of the alkyl chain for traditional structural characterization. According to the alkyl chain length, packing density and temperature, the polymer chains were thought to lie either parallel to the silicate layers forming mono- or bi-layers, or radiate away from the silicate layers forming mono- or bi-molecular arrangements (see Figure 2.3) (Greenland, 1963).

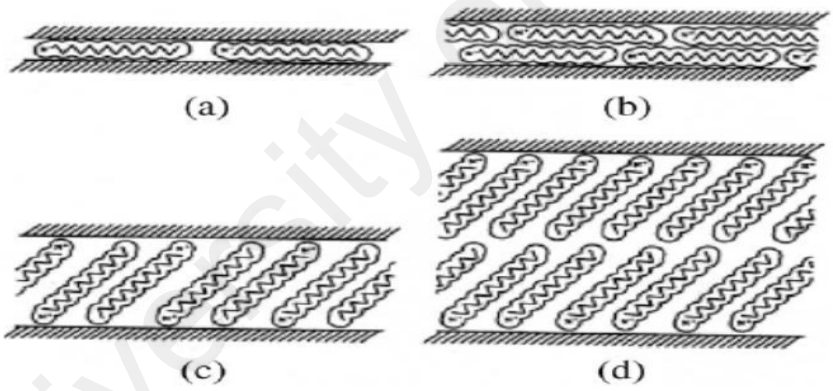

Figure 2.3: Arrangements of alkyl ammonium ions in mica-type layered silicates with different layer charges. Hatched areas are silicate layers (Greenland, 1963).

Krishnamoorti et al., (1996) have used FTIR experiments and showed an unrealistic structure. They found that alkyl chains can vary from liquid-like to solid-like, with the liquid-like structure dominating as the temperature increases, or as the interlayer density or chain length decreases (see Figure 2.4). This can be done due to the relatively small energy differences between the gauche and trans conformers; the earlier idealized models are described to assume all trans conformations. Also, the surfactants in the

layered silicate for longer chain length surfactants can show thermal transition caused by heat, like melting or liquid-crystalline to liquid-like transitions.

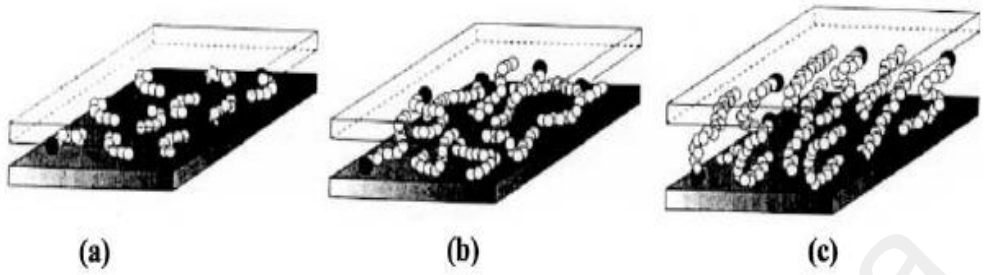

Figure 2.4: Alkyl chain aggregation models: (a) in short length chains, the molecules are effectively isolated from each other; (b) in medium length chains, quasi-discrete layers form with various degrees of in-plane disorder and inter-digitation between the layers; and (c) in long length chains, interlayer order increases leading to a liquid-crystalline polymer environment. Open circles represent the CH_2 segments, while cationic head groups are represented by filled circles (Krishnamoorti et al., 1996).

2.3 Types of polymeric nanocomposites and their preparative techniques

2.3.1 Types of polymeric nanocomposites

Generally, layer thickness in the layered silicates is in the order of 1 nm and a very high aspect ratio (e.g. 10–1000). Thus, polymer matrix provides much higher surface area for polymer/filler interaction than conventional composites. There are three different types of modified or unmodified PLS nanocomposites regarding thermodynamics, depending on the strength of interfacial interactions between the layered silicate and polymer matrix (see Figure 2.5):

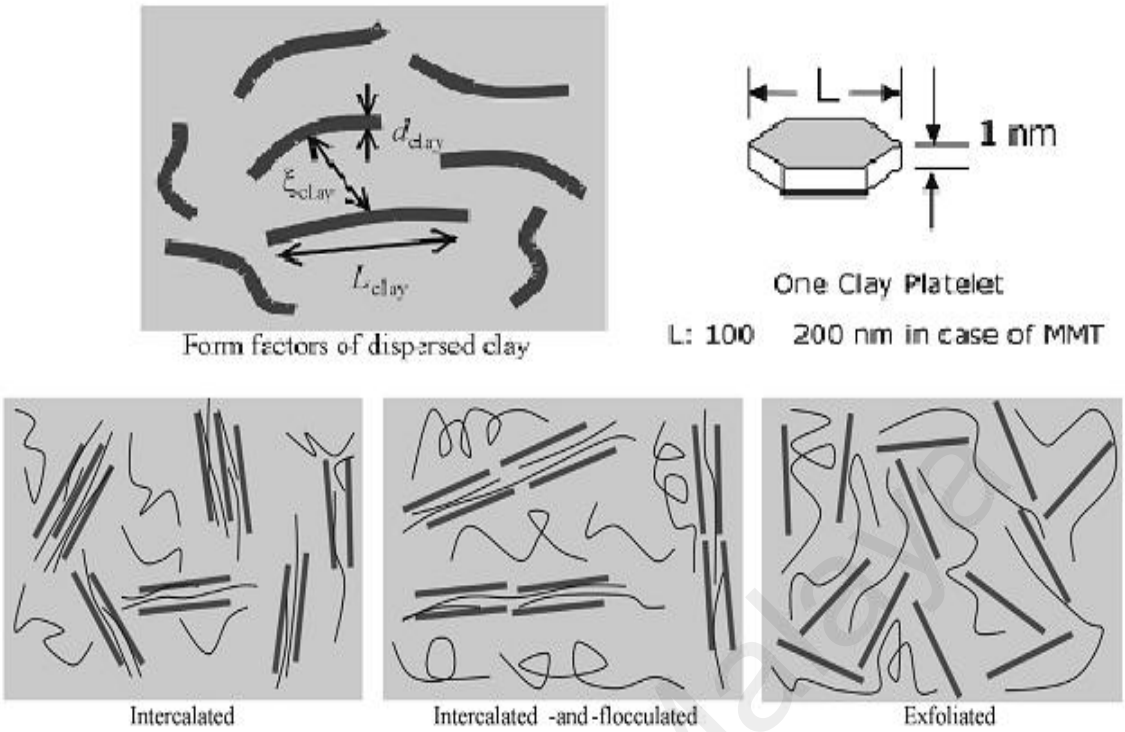

Figure 2.5: Schematic illustration of three different types of thermodynamically achievable polymer/layered silicate nanocomposites (Lagaly, 1986).

a. Intercalated nanocomposites:

Regardless of the clay to polymer ratio, in intercalated nanocomposites, insertion of the layered silicate structure into a polymer matrix occurs in a crystallographically regular manner. Normally, intercalated nanocomposites are formed into an interlayer via a few molecular layers of polymer. Typically, properties of the composites are similar to those of ceramic materials.

b. Flocculated nanocomposites:

Flocculated nanocomposites are conceptually the same as intercalated nanocomposites. However, silicate layers are sometimes flocculated due to hydroxylated edge to edge interactions of the silicate layers.

c. Exfoliated nanocomposites:

Exfoliated nanocomposites have individual clay layers that depend on clay loading which are separated in a continuous polymer matrix by average distances. Normally, the clay content of an intercalated nanocomposite is much higher than that of an exfoliated nanocomposite.

2.3.2 Polymer/layered silicate (PLS) nanocomposite technology

In the past, in order to improve the polymer performance, the application of inorganic nanoparticles as additives has been considered. Currently, various nano-reinforcement materials have been developed such as nanoclay (layered silicates) (Giannelis, 1996,

Giannelis et al., 1999, Vaia et al., 1994, Sinha Ray & Okamoto, 2003, Sinha Ray et al., 2003), ultrafine layered titanate (LeBaron et al., 1999), cellulose nano-whiskers (Biswas & Sinha Ray, 2001), and carbon nanotubes (Mitchell et al., 2002, Mohanty et al., 2003, Hiroi et al., 2004). However, carbon nanotubes-based polymer composites are a relatively clear case of new nanomaterials that show exceptional thermal, electrical and mechanical properties (Mitchell et al., 2002). There is a particular interest in organically-modified polymeric layered silicate (OMLS) nanocomposites, than the unmodified polymer resin, because OMLS nanocomposites have demonstrated significant enhancements including a large number of physical properties, such as thermal and environmental stability, barrier, solvent uptake, flammability resistance and biodegradability rate of biodegradable polymers (Vaia et al., 1994). Generally, these improvements are attained at lower silicate contents (65 wt %) than conventional filler-filled systems. Therefore, the polymer/OMLS nanocomposites are much lighter than conventional composites, and for specific applications, they are competitive with other materials. The conventional bulk characterization techniques such as NMR, thermally-stimulated current, DSC, rheology, and various kinds of spectroscopy are used to study

the structure and dynamics of confined and tethered chains (Hackett et al., 1998, Hackett et al., 2000, Potschke et al., 2003, Andrews & Wisenberger, 2004).

Improved properties of polymer/layered silicate nanocomposites are due to the strong interfacial interactions between the matrix and OMLS (Vander Hart et al., 2001).
A few weight percent of suitable dispersed OMLS in the polymeric matrix creates a much higher surface area for interactions between the polymer and the filler than in conventional composites. Based on the interaction strength between the polymer and OMLS, two different types of structure for nanocomposites are thermodynamically possible.

a) Intercalated nanocomposites, in which, regardless of the polymer/OMLS ratio and a repeat distance of a few nanometers, polymer chains attach to the silicate structure in a crystallographically regular fashion, and **(b)** exfoliated nanocomposites, where, according to OMLS loading, the individual silicate layers are separated in the polymer matrix by average distances.

In general, there are two procedures for the intercalation of polymer chains into silicate galleries: putting monomers in silicate galleries and then performing polymerization (Usuki et al., 1993, Chen et al., 2002, Loo & Gleason, 2003) or direct placement of polymer chains into the silicate galleries through melting (Vaia et al., 1993) or solution (Aranda & Ruiz-Hitzky, 1992).

2.3.3 Preparative techniques

According to the starting materials and processing techniques, there are three methods for the intercalation of polymers in layered hosts:

Table 2.2: Preparative techniques for polymer-based composite and nanocomposite systems.

Systems	Method	Ref.
PVA/MMT composite	Solvent casting, using water	(Kojima et al., 1993, Gaboune et al., 2006, Ogata et al., 1997)
PVA/MMT nanocomposite	Solvent casting using low viscosity	(Strawhecker & Manias, 2000)
PVA/MMT and modified MMT	Solvent casting, using (DMAc)	(Chang et al., 2003)
PVA/MMT nanocomposite	In situ intercalative polymerization with AIBN	(Yu et al., 2003)
PVA/Clay nanocomposite	Solution dispersion technique	(Carrado et al., 1996, Strawhecker & Manias, 2000, Chang et al., 2003, Yu et al., 2003)
PVA/MMT nanocomposite	Solution intercalation method	(Tomasko et al., 2003)
(PVA)/Ag; PMMA/Pd	Mixing and in situ polymerization	(Watkins & Mccarthy, 1995 b, Watkins &Mccarthy,1995 c, Carrado & Xu, 1998, Mbhele et al., 2003 Aymonier et al., 2003 Evora &Shukla, 2003)
Clay with PCL, PLA, HDPE, PEO,PVA,PVP Polyester/TiO_2 PVA)/Ag; PMMA/Pd Polyester/TiO_2 PET/$CaCO_3$ Epoxy vinyl ester/Fe_3O_4 Epoxy vinyl ester/γ-Fe_2O_3 Poly(acrylic acid)(PAA)/Ag PAA/Ni and PAA/Cu AgNO3, NiSO4 and $CuSO_4$	Intercalation / Pre-polymer from Solution	Liu et al., 2002, Jackson et al., 1996, Avadhani & Chujo, 1997, Kamigaito, 1991)
MMT with N6/PCL/PMMA/PU/Epoxy	In situ intercalative polymerization	(Alexandre & Dubois, 2000, Jimenez et al., 1997, Zhao et al., 1989, Usuki et al., 1993 a, Usuki et al., 1993 b, Messersmith & Giannelis, 1993, Okamoto et al., 2000,

Table 2.2, continued

Systems	Method	Ref.
Polyimide/SiO_2	Sol-gel process	(Watkins & Mccarthy, 1994), Di Lorenzo et al., 2002, Park et al., 2003, Xu et al., 1998)
2-hydroxyethylacrylate (HEA)/SiO_2 polyimide/silica; PMMA/SiO_2 polyethylacrylate/SiO_2 polycarbonate/SiO_2 and poly(amide-imide)/TiO_2		
Montmorillonite with	Melt Intercalation	(Vaia & Giannelis, 1997 a, Vaia & Giannelis, 1997 b)
PS/PEO/PP/ PVP ,Clay-PVPH Hectorite with PVPR, HPMC, PAN, PDDA, PANI	Template Synthesis	(Watkins & Mccarthy, 1995 a, Watkins & Mccarthy, 1995 b, Watkins & Mccarthy, 1995c, Carrado & Xu 1998, Mbhele et al., 2003, Aymonier et al., 2003, Evora &Shukla 2003, Di Lorenzo et al., 2002, Park et al., 2003, Xu et al., 1998, Liu et al., 2002, Jackson et al., 1996, Avadhani & Chujo1997)

2.3.3.1 Intercalation of polymer and pre-polymer from solution

In this method, polymer or pre-polymer is soluble and the silicate layers can be swelled in solvent. In the first stage, the layered silicate is swollen in a solvent, such as water, chloroform, or toluene, and then the polymer chains intercalate and displace the solvent within the interlayer of the silicate during mixing of the polymer and layered silicate solutions. After solvent removal, the intercalated structure remains and the result is a PLS-nanocomposite.

In terms of thermodynamics, a negative variation in the Gibbs free energy is required for the overall process, in which the polymer is exchanged with the previously intercalated solvent in the gallery. The entropy obtained by desorption of solvent molecules is the driving force for the polymer intercalation into layered silicate from a solution, which compensates for the decreased entropy of the confined, intercalated chains (Vaia & Giannelis, 1997 b). This method is suitable for the intercalation of polymers with no or low polarity into layered structures, and easily produces thin films with polymer-oriented clay intercalated layers. However, this method involves the abundant use of organic solvents, which, from an industrial point of view, are environmentally unfriendly and economically expensive.

2.3.3.2 In situ intercalative polymerization

In this method, the layered silicate can swell in the liquid monomer or a monomer solution and the polymer can be formed between the intercalated sheets. Polymerization reactions can be initiated by radiation or heat, through the diffusion of a suitable initiator, an organic initiator or catalyst that is fixed inside the interlayer before the swelling step via cation exchange.

2.3.3.3 Melt intercalation technique

Due to compatibility with recent industrial techniques, the melt intercalation technique has become a primary choice for the preparation of polymer/OMLS nanocomposites, and involves annealing the mixture of the polymer and OMLS above the softening point of the polymer either statically or under shearing. During the annealing, the polymer chains diffuse into the silicate layer galleries from the mass of melted polymer (Vaia & Giannelis, 1997a). On the other hand, during polymer intercalation from solution to replace the imported polymer chains, a relatively large number of solvent molecules have to be repelled from the host. From a waste view, the absence the solvent makes

direct melt intercalation an environmentally friendly and economically favorable method for industries. In addition, direct melt intercalation is highly specific for the polymer, leading to new hybrids that were previously inaccessible. Therefore, there are many advantages to direct melt intercalation than solution intercalation. Depending on the amount of penetration of the polymer chains into the silicate galleries, a range of nanocomposites can be obtained with intercalated or exfoliated structures. Experimental results indicate that silicate functionalization and constituent interactions have a critical influence on the outcome of polymer intercalation.

The researchers have found that (a) an optimal interlayer structure on the OMLS, with respect to the number per unit area and size of surfactant chains, is the most favorable for nanocomposite formation, and (b) polymer intercalation depends on the existence of polar interactions between the OMLS and the polymer matrix.

To understand the thermodynamics of nanocomposite formation, (Vaia & Giannelis, 1997 a & b) used a mean-field statistical lattice model and reported experimental results and calculations based on the mean field theory that agreed well.

While confinement of the molten polymer with the formation of nanocomposite is associated with a loss of entropy, this process is allowed because entropy is gained with the layer separation and results in a net entropy change close to zero. Therefore, according to the theoretical model, energetic factors, which may be determined from the surface energies of the polymer and OMLS are the most important for nanocomposite formation via polymer melt intercalation.

According to the report of (Vaia & Giannelis, 1997 a & b), in order to maximize the configurational freedom of the functionalizing chains upon layer separation, and to maximize potential interaction sites at the interlayer surface, the interlayer structure of the OMLS should first be optimized. In these systems, the desirable structures have a

chain arrangement that is slightly more extended than that of pseudo-bilayer polar groups in the polymers which are capable of hydrogen bonding formation or interactions, such as Lewis-acid/base interactions. Thus to minimize unfavorable interactions between the aliphatic chains and the polymer, some short functional groups in the OMLS and the great polarizability or hydrophilicity of the polymer should existed.

Table 2.3: Advantages and disadvantages for three main groups of Intercalation methods.

Process	Advantages	Disadvantages	Ref.
Intercalation/Pre-polymer from Solution	Synthesis of intercalated nanocomposites based on polymers with low or even no polarity. Preparation of homogeneous dispersions of the filler.	Industrial use of large amounts of solvents.	Gao et al., 2002, Jackson et al., 1996, Avadhani, & Chujo, 1997, Kamigaito, O.J. 1991)
In situ Intercalative Polymerization	Easy procedure, based on the dispersion of the filler in the polymer precursors.	Difficult control of intra-gallery polymerization. Limited applications.	(Alexandre & Dubois,2000, Jimenez et al., 1997, Zhao et al., 1989, Usuki, et al., 1993a, Usuki et al., 1993b, Messersmith. & Giannelis, 1993, Okamoto et al., 2000)
Melt Intercalation	Environmentally benign; use of polymers is not suited to other processes; compatible with industrial polymer processes.	Limited applications to polyolefins, which represent the majority of used polymers.	(Vaia & Giannelis, 1997a, Vaia & Giannelis, 1997b)

2.4 Techniques used for the preparation of PVA hydrogels and PVA nanocomposite hydrogels and their characterization.

Hydrogels can be prepared by different methods. The most widely employed methods are chemical cross-linking using glutaraldehyde as the cross-linking agent (Kawasumi et al., 1997, Ossipov & Hilborn, 2006), and physical cross-linking by UV radiation (Benamer et al., 2006), irradiation (Ajji, 2005, Benamer et al., 2006, Martens & Anseth, 2000), and by the use of repeated freeze-thawing cycles (Martens & Anseth, 2000, Peppas & Mongia, 1997). Hassan & Peppas (2000) and Hassan et al., (2000), have reported the preparation of hydrogels using physical methods such as freezing and thawing, chemical methods using a covalent cross-linking agent including boric acid, glutaraldehyde and formaldehyde and radiation methods using electron beams known as irradiation. Polyvinyl alcohol hydrogel prepared by freezing and thawing is not toxic, not carcinogenic and has good biocompatibility. PVA hydrogels were studied by Stauffer and Peppas for biomedical and pharmaceutical applications (Stauffer & Peppas, 1992). Intermolecular bonds (mostly hydrogen bonds) which form during the freeze-thawing process of PVA water solutions, act as efficient cross-links. Jolanta Stasko et al. have reported the influence of PVA molecular weight on the water absorption, gel formation and the density of gels prepared by the freeze-thawing method (Stasko et al., 2009). A schematic illustration of crosslinking methods used in hydrogel preparation is shown below (Hamidi et al., 2008):

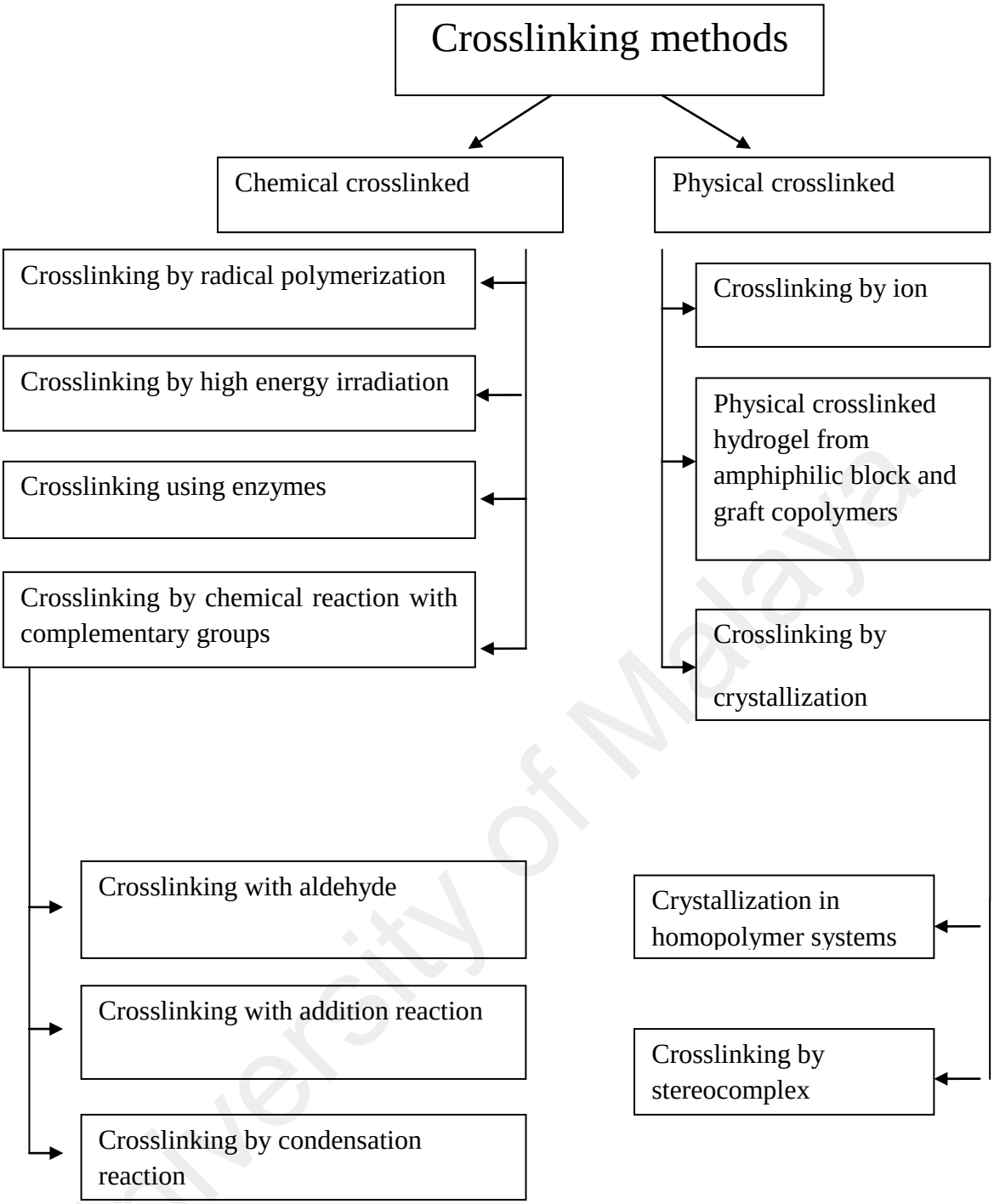

Figure 2.6: Novel crosslinking methods used in hydrogels (Hamidi.et al. 2008)

2.4.1 Covalently crosslinked and cryogels

Most research in smart polymers (SPS) has focused on hydrogels that swell in aqueous solutions. The smart gels can be synthesized by conventional methods at room temperature; these prepared hydrogels have small pore sizes. Also, smart macroporous hydrogels reviewed in several papers (Kopecek, 2003, Rosiak & Ulan ski 1999, Roy & Gupta 2003), have been synthesized by different methods and with various applications.

Cryogels are large pore size hydrogels which have been synthesized in moderately frozen conditions with interesting properties (Lozinsky et al., 2003). These gels can be prepared at temperatures lower than the melting temperature of the solvent. Karimi et al. have recently reported preparation of a novel physicochemical crosslinked nanocomposite hydrogel based on PVA and natural Na-montmorillonite (Na^+-MMT) using chemical crosslinking followed by a Freezing-Thawing process (Karimi & Wan Daud, 2014).

Table 2.4: Crosslinking methods for the preparation of nanocomposite hydrogels

Preparation methods	**Ref.**
Chemica crosslinking by glutaraldehyde	(Valentın et al., 2009)
Irradiation by gammaradiation	(Takeshita et al., 1999, Morgan & Gilman, 2003)
Irradiation by UV radiation	(Sinha Ray et al., 2003)
Freezing/ thawing	(Peppas &.Mongia, 1997, Davis et al., 2002, Lee et al., 1998, Kokabi et al., 2007)
physicochemical crosslinking	(Karimi & Wan Daud, 2014)

A short discribtion for the freez-thaw process is presented here. Most of the solvents are frozen at subzero temperatures, while the dissolved substances are concentrated in small non-frozen regions known as the “liquid microphase”. The volume of the non-frozen liquid microphase is much lower than that of the solid phase; the concentration of local monomer is much higher than the concentration of monomer in the initial reaction mixture, meaning that gel formation occurs in the liquid microphase and the crystals of frozen solvents perform in a manner that is similar to porogen. After melting of the ice crystals, a network of large interconnected pores is formed, meaning that an attractive system is obtained for surface grafting with large interconnected pores and a high

surface area that is available for grafting and the efficient mass transport of monomers (Fig 2.7).

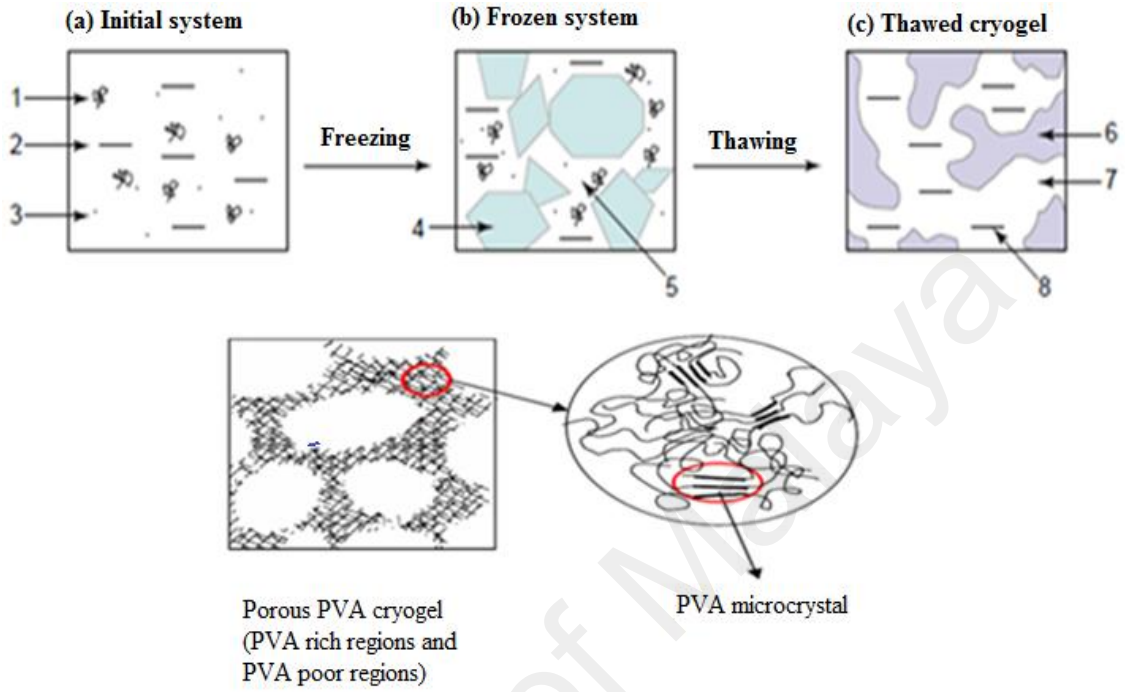

Figure 2.7: Schematic diagram showing, PVA hydrogels prepared by freeze-thawing cycles with a PVA-rich region and a PVA-poor region.
1, macromolecules in a solution; 2, solvent; 3, low-molecular solutes; 4, polycrystals of frozen solvent; 5, unfrozen liquid microphase; 6, polymeric framework of a cryogel; 7, macropores; 8, solvent.

Now, most research is focused on hydrogels that are sensitive to small changes in pH or temperature (Lozinsky et al., 2003, Karimi, 2008), has reported synthesis of two types of ionic hydrogels consisting of pH sensitive (copolymer of acrylamide and sodium acrylate) and temperature and pH sensitive (copolymer of N-isopropylacrylamide and sodium acrylate) (Karimi, 2008). Moreover the response to changes in solvents, ionic strength, electric or magnetic fields, and light intensity have been investigated in other gels. Some gels have also been designed to respond to specific biomolecules such as glucose or chemical triggers (Traitel et al., 2000, Miyataa et al., 2002). Response to stimulation makes them useful as smart materials and they have been established in numerous applications.

Table 2.5: Response to changes in smart hydrogels

Changes for response	System	Ref.
Temperature	Different Hydrogels	(Lozinsky et al., 2003, Karimi, 2008)
pH	Different Hydrogels	(Lozinsky et al., 2003,Karimi, 2008)
Temp and pH	NIPAM and sodium acrylate	(Karimi, 2008)
Electric field	Poly(dimethyl siloxane) gels containing randomly distributed TiO_2 particles	(Zhao et al., 1989)
Magnetic field	NIPA and PVA	(Zhao et al., 1989)
Solvent		(Zhao et al., 1989, Schuetz & Gurny, 2008)
Light intensity	(NIPAM) in D_2O	(Zhao et al., 1989, Schuetz & Gurny, 2008)
Glucose and protein drug delivery	Self-regulated	(Litvinov & De, 2002, Simon & Schneider, 1991)

2.4.2 Polyvinyl alcohol nanocomposites and their characterizations

The first fabrication of PVA/MMT composites was reported by Greenland (1963); who used the solvent casting method with water as co-solvent. After that, Ogata et al. (1997) used the same method to produce PVA/MMT composites. Also, Strawhecker and Manias have used the solvent casting method in an attempt to make the PVA/MMT nanocomposite films (Strawhecker & Manias, 2000). PVA/MMT nanocomposite films were produced by film casting from an MMT/water suspension containing dissolved PVA. In this research a suspension of Na^+-MMT in water was stirred and sonicated. Then, fully hydrolyzed atactic PVA with low viscosity was added to the stirring suspension. The casted films were characterized using WAXD and TEM.

Figure 2.8 shows the WAXD scans of 20, 40, 60, 80 and 100 wt% MMT concentrations; (the corresponding d-spacing distributions for the same concentrations can be seen inset). The XRD patterns show that the d-spacing and their distribution systematically decreased with increasing MMT wt% in the nanocomposites.

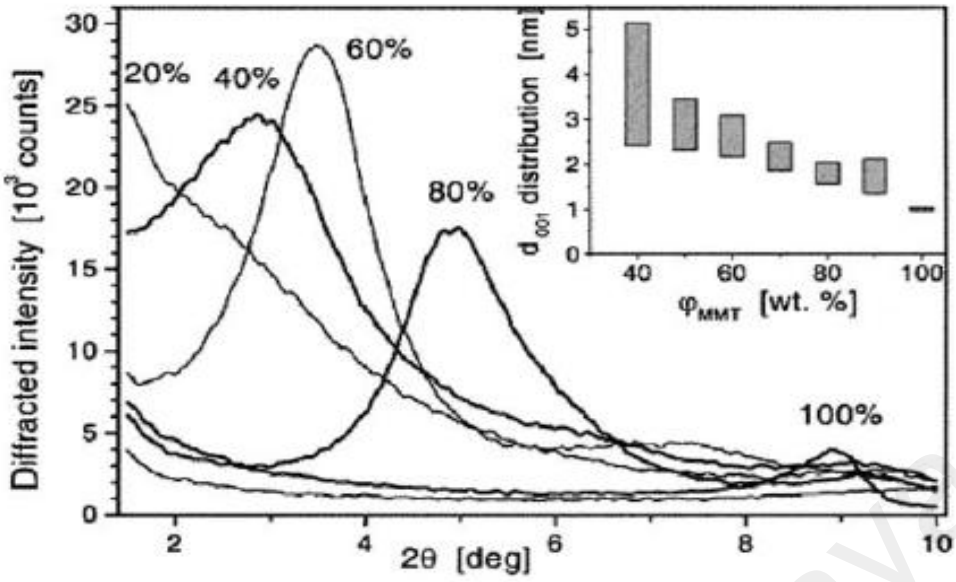

Figure 2.8: XRD patterns of the PVA/MMT hybrids as a function of MMT. The inset shows the distribution of the MMT intercalated d-spacings for the respective hybrids (Strawhecker & Manias, 2000).

In the TEM (Figure 2.9) image of 20 wt% filled clay nanocomposite, (it can be seen the existence of silicate layers in the intercalated and exfoliated structures).

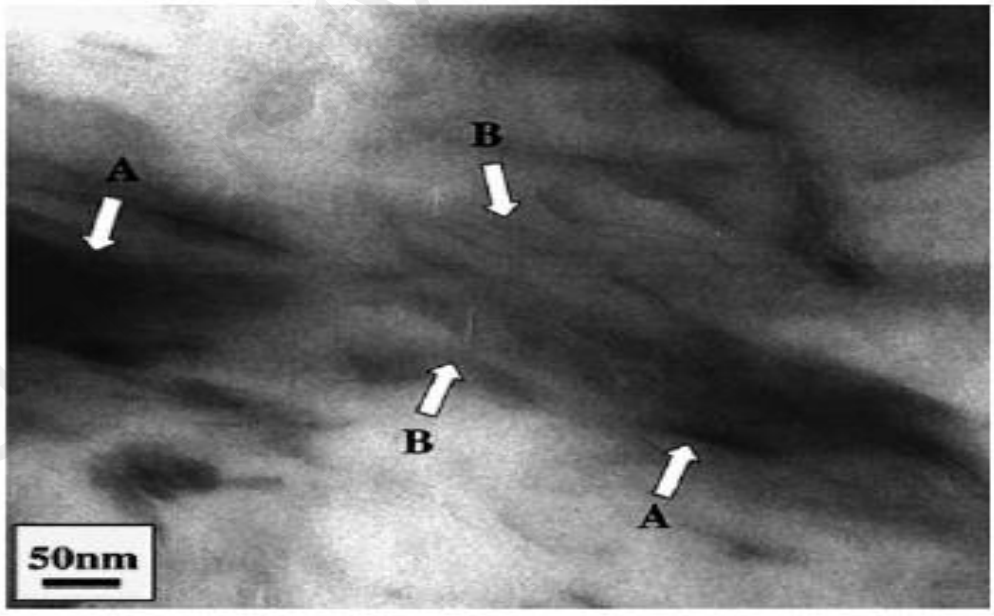

Figure 2.9: Bright field TEM image of 20 wt% PVA/MMT nanocomposite, revealing the coexistence of intercalated (A) and exfoliated (B) MMT layers (Strawhecker & Manias, 2000).

At first glance, the d-spacing on the polymer/silicate mass ratio and dependence of the intercalated structure seems to be in contrast with the theoretical expectations (Carrado et al., 1996, Doppers et al., 2004, Fornes et al., 2001, Sinha Ray et al., 2002). The equilibrium nanocomposite structure forecasted from the thermodynamics is related to the intercalated periodic nanocomposite with d-spacing of around 1.8 nm, which is expected to be independent of the polymer-to-silicate composition (Hassan & Peppas, 2000). However, thermodynamics is only able to forecast the equilibrium structure. Actually, in this research, the structure of the nanocomposite is dictated by kinetics; the layers remain in colloidal suspension in the water solution of PVA and MMT. The suspension must be dried slowly and the silicate layers remain distributed and embedded in the polymer gel. All of the water is removed by further drying, although according to thermodynamics, the MMT layers re-aggregate in an intercalated fashion; the slow polymer dynamics is a trap for some of the layers and they therefore remain dispersed in the polymer matrix. Clearly, the kinetic restrictions imposed by the polymer become less important as the polymer-to-silicate fraction decreases, and intercalated structures are formed for higher amounts of MMT. For these periodic structures, the d-spacing changes, with the wt% of MMT representing the different weight ratios for polymer–silicate, and with an increase in the amount of MMT.

Preparation of PVA-based nanocomposites with three different types of clay-pristine MMT and organically modified MMT was reported by Chang et al. (2003). In this work, they used the same solvent casting method for the nanocomposite preparation; however, in addition to water, N, N-dimethylacetamide (DMAc) was also used as co-solvent. Dodecylammonium-modified MMT (C12MMT) and 12-aminolauric-modified MMT (C12OOHMMT) were used as OMLS. XRD patterns of different types of clay and TEM images of their nanocomposites with PVA are shown in Figure 2.10 and Figure 2.11 respectively (Chang et al., 2003). These figures show the formation of

exfoliated nanocomposites when pristine clays were used for the fabrication of nanocomposites. Because intercalated nanocomposites were produced with OMLS, it can be concluded that the hydrophilic character of clay promotes the dispersion of inorganic crystalline layers in water-soluble polymers (LeBaron et al., 1999, Vaia et al., 1996).

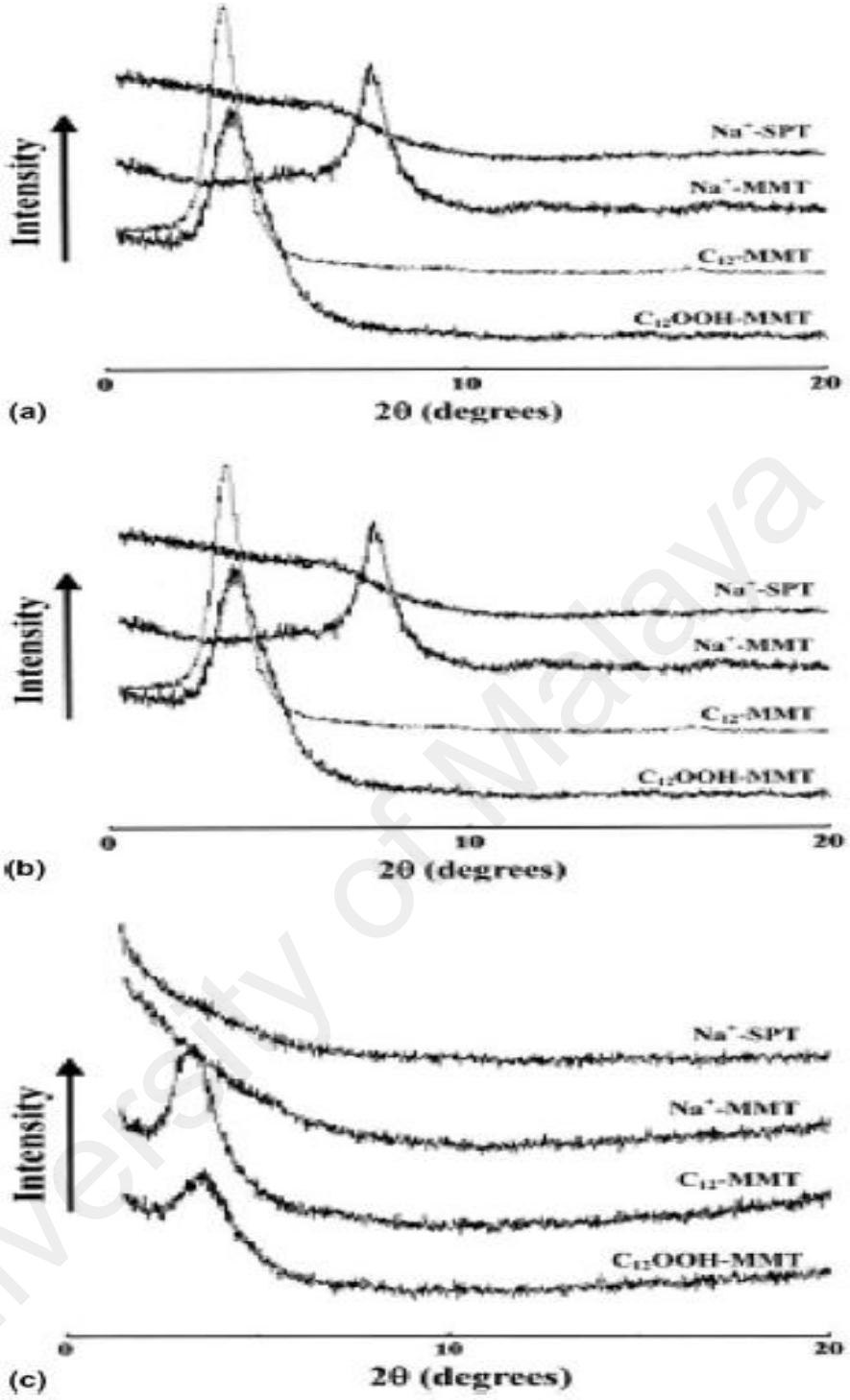

Figure 2.10: XRD patterns of: (a) clays, (b) 4 wt% clays/PVA hybrid films, and (c) 8 wt% clays/PVA hybrids (Chang et al., 2003).

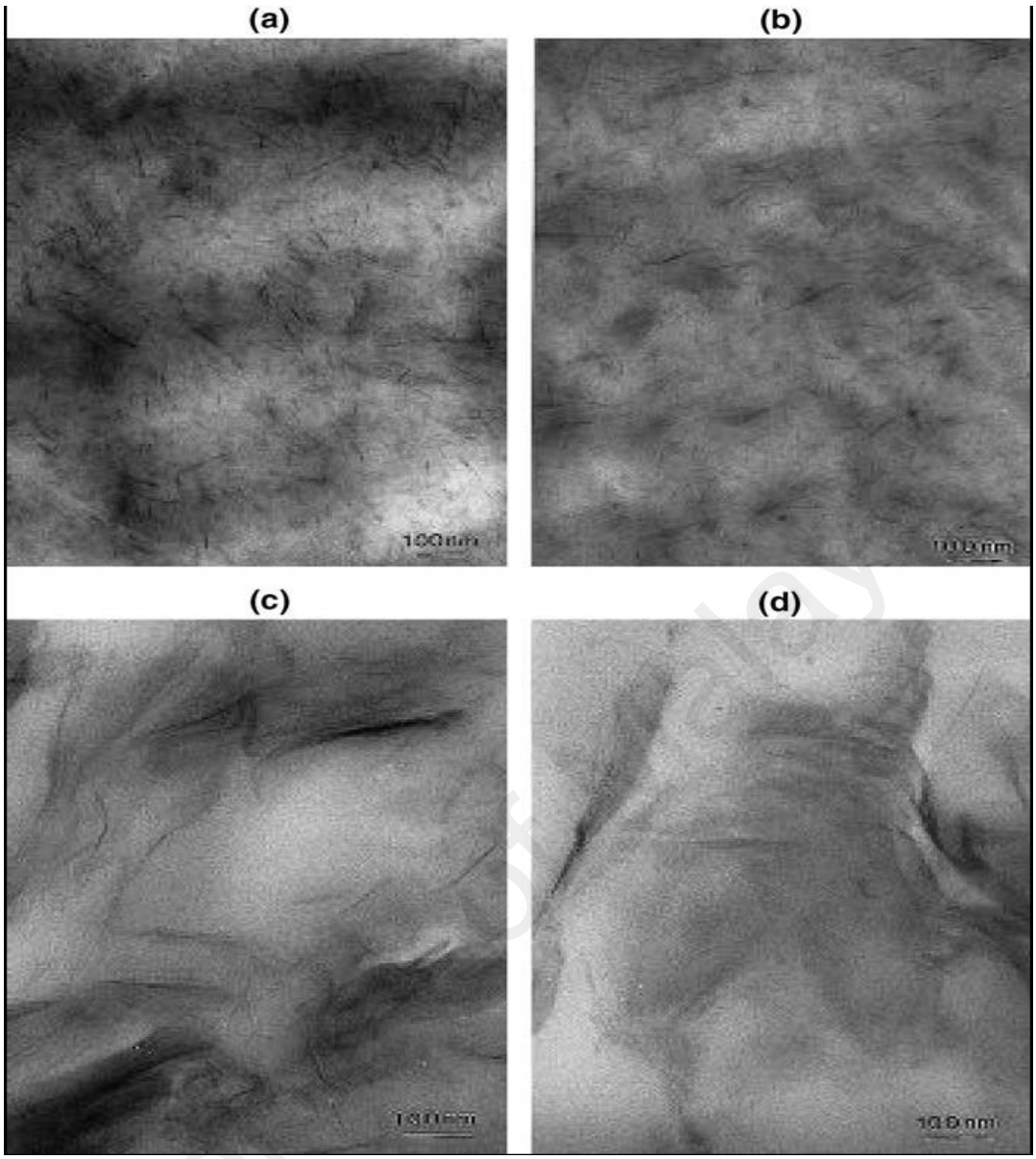

Figure 2.11: TEM photographs of PVA hybrids containing 4 wt% clay: (a) Na^+-SPT; (b) Na^+-MMT; (c) C12-MMT; (d) C12OOH-MMT (Chang et al., 2003).

Synthesis of a series of PVA/MMT nanocomposites by in situ intercalative polymerization using AIBN as initiator has been reported by Yu et al. (2003). At first, vinyl acetate monomers were intercalated into the organically modified MMT galleries and then a one-step free radical polymerization was performed.

Most important techniques for characterization of nanocomposites are shown in Table 2.6.

Table 2.6: Most important techniques for characterization of nanocomposites.

Property	Techniques	Ref.
Thermal analyses	**DSC**	(Potschke et al., 2003, Andrews & Wisenberger, 2004, VanderHart et al., 2001, Usuki et al., 1993 b, Hassan & Peppas, 2000)
Thermal analyses	**MDSC**	(Cohen et al., 1992) **(**Potschke et al., 2003, Andrews & Wisenberger, 2004, VanderHart et al., 2001**)**
Rheology	**Rheology**	**(**Shaffer & Windle, 1999, Vaia et al., 1994)
Molecular structure	**NMR**	(VanderHart et al., 2001, Usuki et al., 1993 b, Chen et al., 2002, Loo & Gleason2003)
Micro structure	**Cryo-TEM**	Lepoittevin et al., 2002)
Micro structure	**TEM**	(Zhu et al., 2001, Sur et al., 2001, Lepoittevin et al., 2002, Lim et al., 2002, Mallam et al., 1989, Kim et al., 1992, Becker et al., 2002, Strawhecker & Manias, 2001, Paranhos et al., 2007a, Paranhos et al., 2007b, Mathias et al., 1999, Churochkina et al., 1998)
Phase analyses	**XRD**	(Sinha Ray et al., 2003 a, Morgan & Gilman, 2003, Sinha Ray et al., 2003b)
Phase analyses	**SAXS**	(Bafna et al., 2003, Bafna et al., 2002, Yu & Xiao, 2008, Pal et al., 2008, Mallam et al., 1989, Cohen et al., 1992, Schosseler et al., 1994)
Nano Structure	**SANS**	(Mallam et al., 1989, Cohen et al., 1992, Schosseler et al., 1994 Shibayama et al., 1992)
Thermomechanical	**DMA**	**(**Liu et al., 2002, Morgan & Gilman, 2003)
Structure	**FTIR**	**(**Loo & Gleason2003)
Micro structure	**SEM**	**(**Yu et al., 2003, Patachia et al., 2009)

Table 2.6, continued

Property	Techniques	Ref.
Micro structure	**OPM**	**(**Yu et al., 2003)
Thermal analyses	**TGA**	(Paul et al., 2003, Pantoustier et al., 2002, Lepoittevin et al.,2002a, Zhu et al., 2001, Sur et al., 2001, Lepoittevin et al., 2002b)
Types of Analyses	**Various kinds of spectroscopy**	(Potschke et al., 2003, Andrews & Wisenberger, 2004, VanderHart et al., 2001)
Particle size	**Light scattering**	(Mallam et al., 1989, Cohen et al., 1992, Schosseler et al., 1994 Shibayama et al., 1992)
Swelling	**Swelling**	(Yu & Xiao, 2008)
Micro structure	**AFM**	**(** Patachia et al., 2009)
Phase analyses	**WAXD**	(Sinha Ray et al., 2002)

Then, for the synthesis of PVA/MMT nanocomposites, the prepared polyvinyl acetate/OMLS solution was saponified through direct hydrolysis with NaOH solution. The formation of a mixed intercalated/exfoliated structure of the PVA/MMT nanocomposites was proven with XRD patterns and TEM images.

Paranhos et al. have studied control of the degree of crystallinity for PVA by changing clay and sulfonated polyester (PES) contents (Paranhos C.M., et al., (2007 a).

In Figure 2.12, the FTIR spectra of the hydrogels containing 0 (N0), 10% (N10) nanoclay, bulk PVA and pure MMT (MOM) are shown. It can be seen that the typical bands of PVA (3273 cm^{-1}, –OH stretching; 2914 cm^{-1}, –CH2 stretching; 1087 cm^{-1}, C–O stretching) and MMT (1006 cm^{-1} and 671 cm^{-1}; Si–O stretching) are confirmed. A strong interaction is shown between –OH of PVA and silanol groups of MMT.

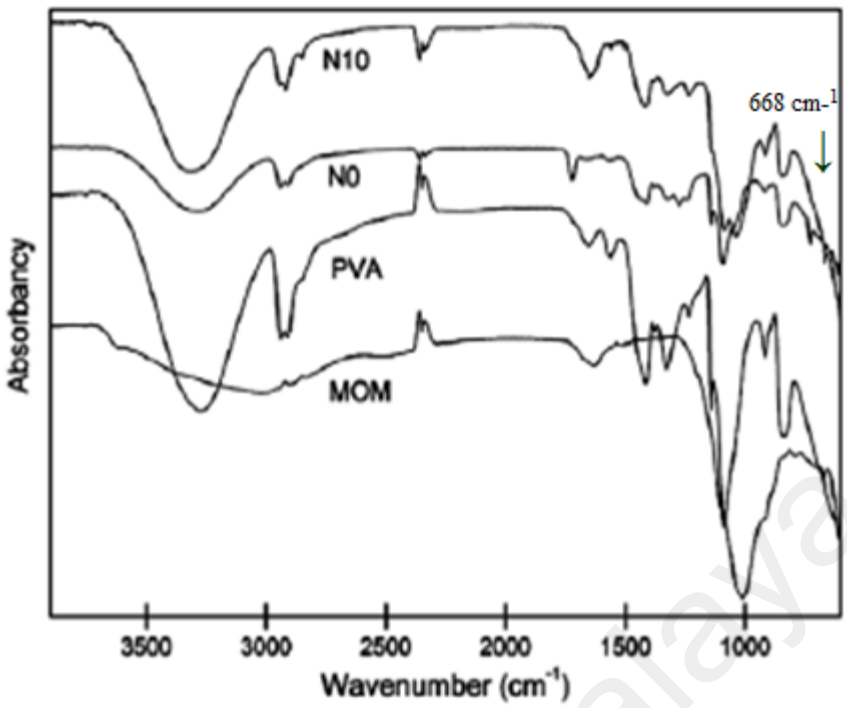

Figure 2.12: FTIR spectra of PVA, PVA/PES and nanocomposite hydrogels (Paranhos C.M., et al., 2007 a).

The absorption peaks at 1034 cm^{-1} and 668 cm^{-1} in N10 hydrogel is clearly attributed to the presence of MMT. It should be noted that these peaks are shifted in comparison with those of pure MMT. There is another important peak associated with the crystalline domains of PVA (1142 cm^{-1}) for evaluation of the interactions between PVA and MMT. This peak indicates that the interactions between PVA and MMT do not occur on the crystalline domains of PVA because there is no shift in the presence of clay. In the case of N0 hydrogels, with the presence of MMT, the carbonyl peak at 1720 cm^{-1} and the aromatic C–H peak at 726 cm^{-1} are completely suppressed. Also, depression of the 1087cm^{-1} peak of PVA in the presence of PES can confirm the strong interactions between PVA and PES. These characteristics suggest that the PVA/PES matrix and MMT are not blended and that a complex interaction exists. Evaluation of the WAXS patterns of bulk PVA, pure MMT (MOM) and nanocomposite hydrogels in Figure 2.13 indicates that presence of PES causes a strong disorder on the

PVA matrix. A shift in the diffraction peak of PVA towards higher values of 2θ is due to strong interactions between PVA and PES that indicates small crystalline PVA domains are formed compared to pure PVA.

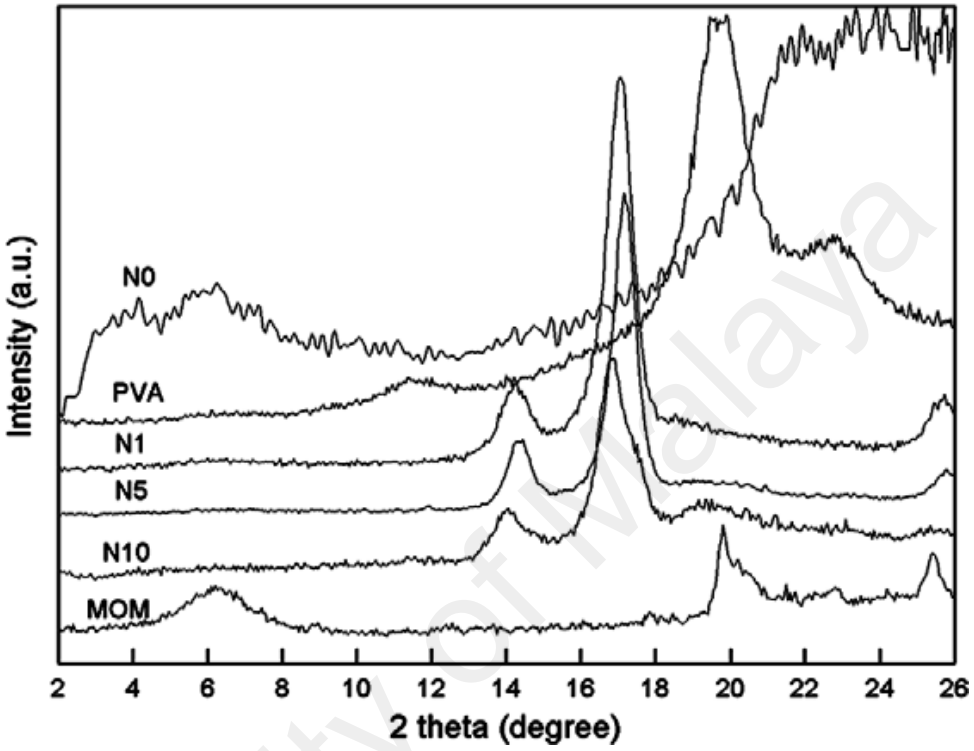

Figure 2.13: WAXS patterns of PVA, PVA/PES and nanocomposite hydrogels (Paranhos C.M., et al., 2007a).

It can be seen that the WAXS patterns of nanocomposite hydrogels do not have any diffraction peak in 2θ = 2–10° which is opposed to the diffraction peak at 2θ = 6.25° (d spacing = 14.13) for pure MMT. These characteristics indicate the possibility of extensively intercalated silicate layers of MMT that are dispersed in the PVA matrix. PVA has its 101, 101 and 200 crystalline reflections in the 2θ = 10–25° range, which corresponds to 9.4°, 19.9°and 22.7°, respectively. There is a significant change in the WAXS patterns of the hydrogels due to the presence of MMT and PES compared with pure PVA. It can be seen that the 101 and 101 peaks are depressed into a single peak shifted to lower 2θ angles with increasing MMT content and moreover, a new crystalline peak appears around 2θ = 14.5°. According to the other report of the

Paranhos et al., increasing MMT content in PVA/MMT hydrogels does not lead to any significant changes in the (101) crystalline level of PVA (Paranhos et al., 2007 a). These results suggest the important presence of PES and its role in the crystalline features of the nanocomposite hydrogels.

The authors have shown that MMT acts as a crystalline nucleation agent for PVA chains (Bandi & Schiraldi, 2006, Van Krevelen, 1997, Tager, 1978, Kokabi et al., 2007). However, growing up of the PVA crystallites from PVA/MMT interface are directly affected by PES. Thus, the crystalline domains of PVA undergo a disarrangement process and as the result in the WAXS pattern, a constricted crystalline structure can be seen. A significant change in the crystalline reflections of PVA with sodium MMT nanocomposite was observed by Strawhecker and Manias (2001); also, Bandi and Schiraldi reported the same effect in composites of clay/PVA and clay aerogel/PVA (Bandi & Schiraldi, 2006). They attributed this new crystalline phase to strong specific interactions between the inorganic surface and the polymer at an interfacial level. However, the presence and role of PES on the crystallinity of PVA have been investigated by Paranhos et al. (2007 a).

The addition of MMT into the PVA matrix favors the crystallization of PVA and the further addition of MMT causes an increase in the tactoid number; consequently, the mobility and alignment of PVA chains are decreased. This delay mechanism reduces the crystallite size of PVA.

In the case of PVA/MMT hydrogels, the crystallite size of PVA is independent of the MMT content (Paranhos et al., 2007 b). These results confirm that the presence of PES is the main factor causing changes in the crystalline domains of PVA.

According to this research (Paranhos et al., 2007 a), in order to better understand the changes to the crystalline structure of nanocomposite hydrogels in the presence of PES,

DSC was employed to quantify the degree of crystallinity of the samples. Table 2.7 summarizes the DSC results obtained from the nanocomposite hydrogels. The presence of PES in the PVA matrix causes a shift in the melting endotherm peak of PVA to lower temperatures. This fact is in accordance with the disordered aspect observed in the WAXS pattern. These features are attributed to interactions between PVA and PES. In fact, PVA hydroxyls are strongly bonded with PES carbonyls via hydrogen bonding, as can be seen in FTIR spectra. These interactions cause disruption of the lamellar arrangement during the formation of PVA crystallites, resulting in a diminution of the average crystallite size and consequently in a lowering of the PVA melting point, confirming the WAXS results obtained. From the DSC curves, the enthalpy of melting (ΔH_m) determined from the area of the DSC endothermic peak varied from 37 J g^{-1} for pure PVA to 102 J g^{-1} in presence of PES. Since the degree of crystallization of PVA/PES is higher than that of pure PVA, and since the average crystallite size is lower, this indicates that the number of crystallites is higher in PVA/PES than in PVA. The DSC curves correspond to nanocomposite hydrogels with several MMT contents also exhibit a lower average melting temperature of crystallites compared to that of pure PVA. Furthermore, an increase in T_m is apparent in DSC curves, this trend being more pronounced with increasing MMT contents. This feature reveals an increase in the average size of the crystalline PVA domains and a decrease in the crystallite size dispersion following the addition of larger amounts of MMT in PVA/PES. In addition, it is possible to note that the addition of 1 wt% MMT causes an increase in ΔHm from 102 to 110 J g^{-1}. For higher MMT amounts, the melting enthalpies decrease. The degree of crystallinity of the samples were calculated from the ratio between the ΔH_m of the sample and the ΔH_m of 100% crystalline PVA (ΔH_m = 150.0 J g^{-1})

Table 2.7: DSC parameters obtained from the nanocomposite hydrogels (Paranhos et al. 2007a).

Sample (°C)	ΔH_m (Jg^{-1})	χ_C (%)	T_m
PVA	37	24.6	227.8
N0	102	68.0	138.7
N1	110	73.3	162.9
N5	94.7	63.1	165.1
N10	84.5	56.6	189.4

(The experimental errors associated to the thermal analysis experiment are ±1 Jg^{-1}, ±1.5% and ±1.8°C for ΔH_m, χ_C and T_m, respectively).

Paranhos et al. (2007a) have reported that a small amount of MMT favors the heterogeneous nucleation of the PVA chains. Table 2.8 shows the crystalline parameters of the PVA matrix as a function of MMT content in nanocomposite hydrogels. Nevertheless, it seems that increasing the content of MMT induces steric hindrance on the PVA matrix; thus, the degree of crystallinity of the composites is decreased. The WAXS analysis is consistent with these results.

Table 2.8: Crystalline parameters of PVA matrix as a function of MMT content in a nanocomposite Hydrogel (Paranhos et al., 2007 a).

Sample	Average d-spacing (A°)	Average crystallite dimension (A°)
PVA	4.4 ±0.3	45.6 ±1.2
N1	5.2 ±0.3	93.4 ±1.2
N5	5.2 ±0.3	109.6 ±1.2
N10	5.3 ±0.3	72.2 ±1.2

The WAXS patterns show that the MMT platelets are randomly dispersed in the PVA/PES matrix and are significantly separated. As in the past reported by other groups (Takeshita et al., 1999, Strawhecker & Manias, 2000), the strong interaction between MMTand PVA leads to the formation of an interfacial layer. According to this research (Paranhos et al., 2007 a), the glass transition temperature, T_g of samples was evaluated to confirm the formation of an interfacial layer between PVA and MMT; the results are

summarized in Table 2.9. T_g is reported as the temperature for the maximum loss modulus peak in DMA curves. According to the free volume theory, glass transition is related to the start of a liquid-like motion of much longer segments of molecules. This motion directly corresponds to the increase in free volume due to the thermal expansion of the system (Van Krevelen, 1997, Tager, 1978). The loss modulus of the samples as a function of temperature is shown in Figure 2.14. The incorporation of MMT into the PVA matrix strongly reduces the glass transition temperature of PVA. The thermal mobility of MMT causes an increase in the local free volume at the PVA–MMT interface. A similar decrease of T_g in nanocomposites based on PVA and clay aerogels has been reported by Bandi and Schiraldi (2006). This behavior can be explained by the following mechanisms:

(i) adsorption of polymer chains to the inorganic surface (leads to an increase in T_g); (ii) extent of alignment of polymer chains between the MMT platelets due the intercalation process (leads to a decrease in T_g); (iii) an increase in the chain dynamics due to an increase in the local free volume at the clay-PVA interface (leads to a decrease in T_g) (Bandi & Schiraldi, 2006).

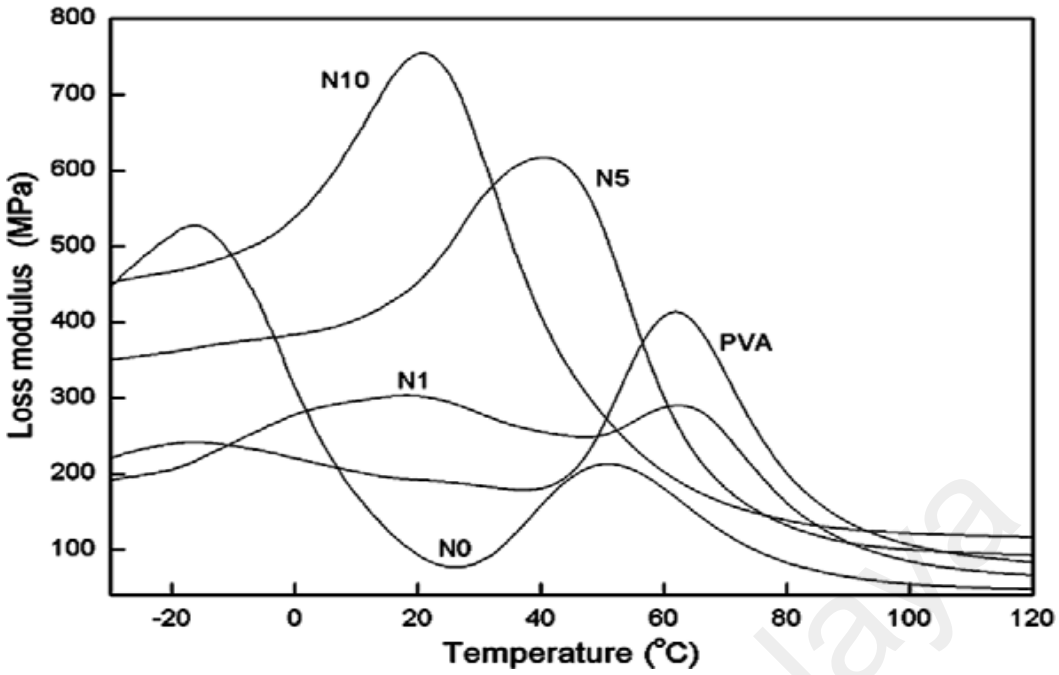

Figure 2.14: Loss modulus of PVA, PVA/PES and nanocomposite hydrogels (Paranhos et al., 2007 a).

Table 2.9: Glass transition temperature (T_g) of PVA, PVA/PES and nanocomposite hydrogels (Paranhos et al., 2007a).

Sample	**Tg (°C)**
PVA	61.8±0.9
N0	50.96±0.9
N1	62.15±0.9
N5	40.39±0.9
N10	20.96±0.9

Figure 2.15shows SEM images of the nanocomposite hydrogels. It can be seen that the matrix is filamentous, with interconnecting pores. Also, increasing the clay content leads to a dense morphology, indicating a more packed structure. This change in morphology is attributed to the re-ordered crystalline phase of the PVA matrix.

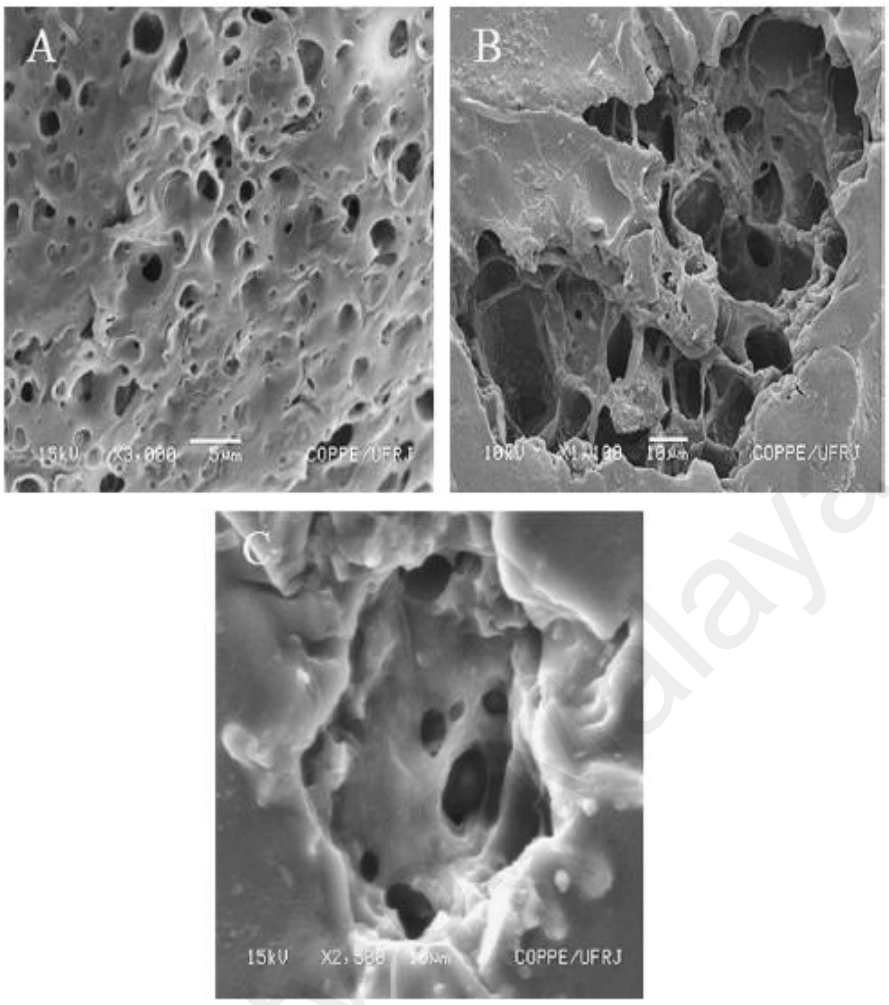

Figure 2.15: SEM micrographs of the nanocomposite hydrogels: (A) N1, (B) N5 and (C) N10 (Paranhos et al., 2007 a).

Kokabi et al. (2007) prepared nanocomposite hydrogels from the raw materials of PVA and organically modified montmorillonite clay (OMMT) using the cyclic freeze-thawing method. It was proposed the nanocomposites can be used as novel wound dressings. According to their report, the structure of MMT and OMMT and the nanocomposite wound dressings were determined using XRD. As shown in Figure 2.16**,** the X-ray diffraction for MMT has a characteristic peak at 6.9°, while the corresponding peak for OMMT is observed at 4.1°. The diffraction peak for OMMT showed a decrease of 2θ in comparison with MMT, which suggests the d-spacing of MMT increased due to the organic modification process. Also, a characteristic diffraction peak at 4.1° can be seen for OMMT, while the peaks of PVA nanocomposites are seen at

around 2.8°. An increase in the d-spacing of OMMT in the presence of PVA implies that PVA intercalates between individual silicate layers during the freeze-thawing process without any serious dependency on OMMT loading.

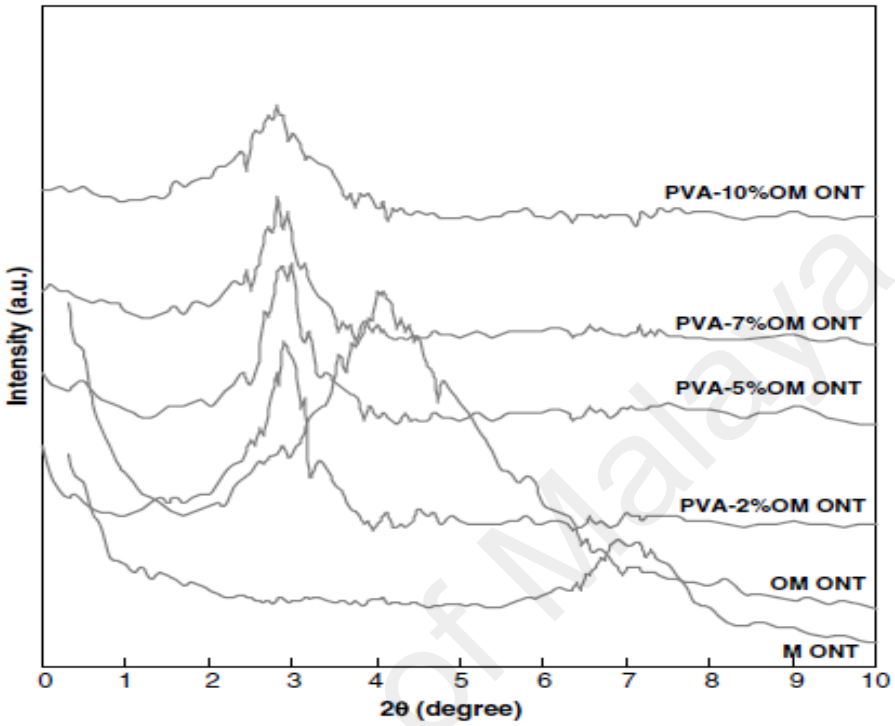

Figure 2.16: XRD of MMT (MONT), OMMT(OMONT) and PVA nanocomposite hydrogels (Kokabi et al., 2007).

TEM is a convenient method for observation of the dispersion of OMMT in the PVA matrix. A TEM micrograph of PVA containing 5% OMMT is shown in Figure 2.17. The dark lines in the picture are the layers of OMMT. According to XRD patterns, it can be seen that the intercalation of PVA chains caused the interlayer spacing to increase and that most OMMT in the PVA-5% OMMT system was still parallel to each other.

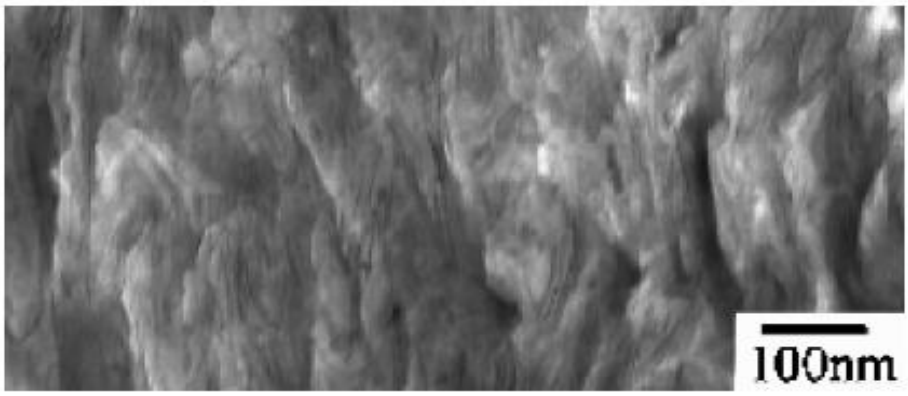

Figure 2.17: TEM of PVA-5% OMMT nanocomposite hydrogels (Kokabi et al., 2007).

2.5 Summary

The structure and properties of nanoclays (phyllosilicates) being classified in modified and unmodified montmorillonite were reviewed. The existence of montmorillonite nanolayers in the PVA hydrogel network has shown to cause significant changes in crystallinity, mechanical and thermal properties of PVA nanocomposite hydrogels compared to pure PVA hydrogels. This is due to two particular characteristics of MMT nanoclays. The first is the dispersal ability of the MMT particles into individual layers and the second is the use of ion exchange reactions with organic and inorganic cations to improve their surface chemistry. It is found that the unmodified MMT is more efficient than modified moiety, because it is hydrophilic and compatible with PVA. The crosslinking methods used in fabrication of PVA nanocomposite hydrogels and the resulting intercalation and exfoliation structures have been discussed. Among different chemical and physical crosslinking methods studied, the freeze-thawing method is found to be non toxic, so it can be used in biological and medicinal applications. This method is based on crystallization of polymers during the freeze-thawing cycles and formation of intermolecular bonds (mostly hydrogen bonds) between PVA and nanoparticles during the freeze-thawing process.

A group of analyzing techniques, such as XRD, SEM, TEM, FTIR, DMA and DSC, which are used for the characterization of PVA nanocomposite hydrogels, have been reviewed. The XRD patterns and TEM images have proven the intercalated and exfoliated structures in PVA nanocomposite hydrogels. Investigation of FT-IR spectra shows the bond formation between OH in PVA chains and silanol groups of MMT. Also, DSC and DMA showed a decrease in crystallinity and the glass transition temperature of PVA due to the incorporation of nanoclay, while the loss modulus is increased compared to pure PVA.

CHAPTER 3: RESEARCH METHODOLOGY

3.1 PART 1: Non toxic hydrogels based on polyvinyl alcohol/Na^+-Montmorillonite nanocomposites for biomedical applications: Fabrication & Characterization

3.1.1. Materials

Polyvinyl alcohol (PVA) having the chemical structure presented in Fig. 3.1, with a molecular weight 89000–98000 and degree of hydrolysis more than 99%. was purchased from Sigma-Aldrich Sdn. Bhd. (Malaysia). Montmorillonite[1] (Na^+-MMT) Cloisite Na^+ was supplied by Connell Bros Company (Malaysia). Deionized water (DI water) was utilized to prepare all aqueous solutions in this research. All materials were used as received without any purification.

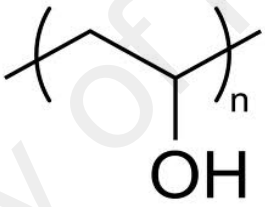

Figure 3.1: Polyvinyl alcohol, PVA

3.1.2. Fabrication of nanocomposite hydrogels (cryogels)

The setup for fabrication of nanocomposite hydrogels was consisted of a one liter two-walled glass reactor connected to a circolator bath , a mechanical stirrer and a sonication system (Fig. 3.2 , 3.3).

Aqueous solutions of Na^+-MMT with different concentrations, containing 0, 0.5, 1, 3, 5, 7 and 10 wt.% by weight based on PVA were prepared in deionized water. At first these solutions were mixed mechanically for 1 h and then were sonicated for 30 min to

[1]- Montmoeillonite is not available as nanoparticle in the nature but it can be easily delaminated or exfoliated to nano platelets with a thickness of about 1nm. This Nanoclay has high surface area of 700 – 800 meter square per gram [Goettler et al. (2007)]. According to Southetn Clay Products data sheet Cloisite Na^+, has S.g. 2.86 gm/cc, Moisture content <= 2%, particle Size: <=2µ about 10%, <=6 µ about 50%, and <=13µ about 90%. (Appendix B)

achieve complete dissolution. Then gradually 15 wt. % by weight PVA powder was added to each solution at the temperature of 90 °C while stirring, and continued stirring for 1 h to achieve complete dissolution. These solutions were sonicated for 30 min at 60 °C, then poured into plastic molds and exposed to 1–3 cycles of freezing (at -20 °C for 24 h), and thawing (at 23 °C for 24 h) in constant humidity. The thickness of nanocomposite hydrogel films was about 1 mm.

Figure 3.2: Setup for synthesis of PVA/ Na^{+}-MMT nanocomposite hydrogels

Figure 3.3: Sonication of nanoclay and PVA aqueous solution

3.1.3. Structure and morphology

Structure and morphology of nanocomposites were investigated by FTIR, XRD, FESEM, TEM and AFM. The IR spectra of the samples were prepared with a Perkin Elmer FTIR spectrophotometer (Perkin Elmer Spectrum 400) in the region 500–4000 cm^{-1} using the KBr pellet technique (Fig.3.4). XRD was performed using a Philips PW-1840 X-Ray diffractometer with Cu lamp and wavelength: λ (kα) = 1.54 Å (Fig.3.5). The nanostructures of all PVA/ Na^{+}-MMT nanocomposite hydrogels, their cross-sectional view and top surface morphologies were examined using FESEM (Genesis Apex 4 Zeiss Edax).

Transmission electron microscopy (TEM) was performed with a Transmission Electron Microscope at KeV 100, Model: EM 208 Philips, and atomic force microscopy (AFM) was conducted by an AFM (Ambios Technology, USA) instrument.

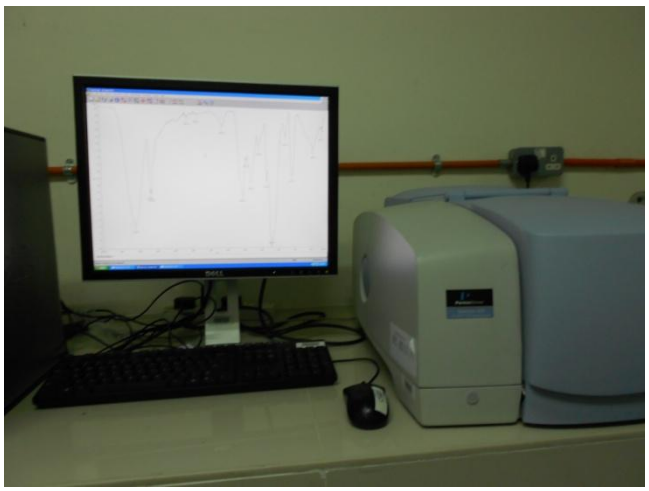

Figure 3.4: FT-IR spectrophotometer used for structural analysis

Figure 3.5: X-Ray diffractometer for morphology analysis

3.1.4. Thermal and mechanical analysis

The thermal properties of the PVA/ Na^{+}-MMT nanocomposites were evaluated using thermo gravimetric analysis (TGA) and differential scanning calorimetry (DSC). A TA Instrument Q 500 TGA and a Mettler Toledo STARe DSC1 were used, respectively, for these analyses. TGA experiments were carried out with the sample weight of 5 mg, under the flow of nitrogen gas, while heating the sample from 25 to 800 °C with a heat rate of 10 °C min^{-1}.

DSC measurements were carried out in a dry nitrogen atmosphere by heating the samples from -50 to 300 °C with a heat rate of 10 °Cmin^{-1}.

Dynamic mechanical experiments were performed using a DMA instrument (DMA, Q 800 TA Instruments) with a frequency of 1 Hz and oscillation amplitude of 0.15 mm. DMA measurements were conducted under nitrogen atmosphere, while heating the sample from -50 to 200 °C with a heat rate of 5 °C min^{-1}.

Hardness measurements were carried out on PVA/ Na^{+}-MMT nanocomposite films having thicknesses of 5–6 mm at 25 °C, according to ASTM D-2240-95 in shore A, using a digital hardness tester (Instron, Wilson Instruments, and Series B 2000). The hardness value of each sample was recorded as an average of five measured data values.

For the water vapor transmission rate (WVTR) analysis of the PVA/ Na^{+}-MMT nanocomposite hydrogels, monograph of the European pharmacopeia was used. A circular sample of nanocomposite hydrogel with a diameter of 3.5 cm was cut and mounted on the mouth of a cup containing 25 ml of deionized water. The cup was then placed in a constant temperature and humidity chamber for 24 h (Figs. 3.6 and 3.7). The water vapor transmission rate (WVTR) was determined as follows:

$$\textbf{WVTR (g/m2/h)} = \frac{w_i - w_f}{24 * A} * 10^6 \qquad \textbf{(3-1)}$$

Where, W_i and W_f are the total weight of the cup and its nanocomposite hydrogel membrane before and after placing in a constant temperature and humidity chamber, respectively. A(mm^2) is the surface area of the cup mouth.

Figure 3.6: Constant temperature and humidity chamber for WVTR analysis

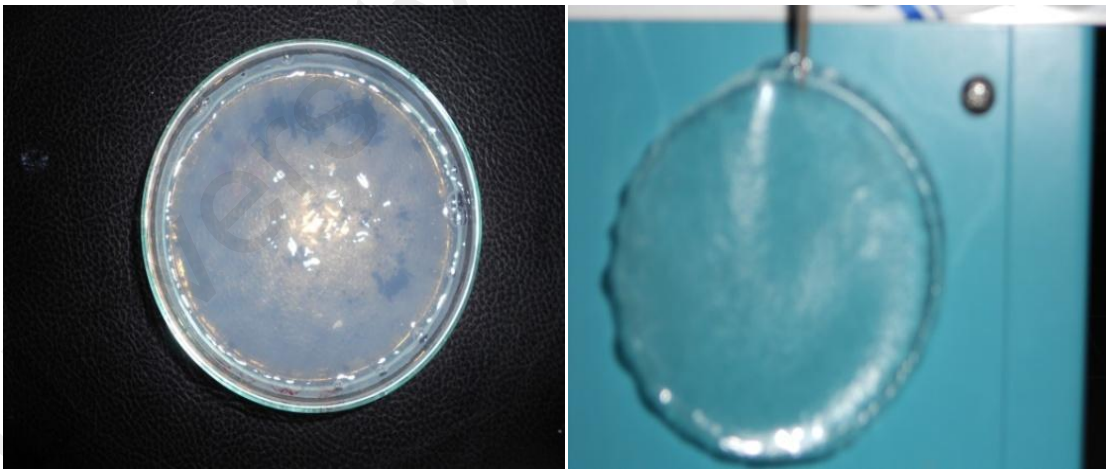

Figure 3.7: PVA/ Na^{+}-MMT nanocomposite cryogel membranes prepared for WVTR analysis

3.2 PART 2: Nanocomposite cryogels based on poly (vinyl alcohol)/ unmodified Na^+-montmorillonite suitable for wound dressing application: optimizing nanoclay content

3.2.1. Materials

Materials were used similar to what mentioned in section 3.1.1.

3.2.2. Fabrication of nanocomposite cryogels

Fabrication of nanocomposite cryogels were done similar to what described in section 3.1.2.

3.2.3. Morphology and thermomechanical properties

Morphology and thermomechanical properties of nanocomposites were investigated by XRD, FESEM and DMA, based on sections 3.1.3, and 3.1.4.

3.2.4. Barrier properties

The water vapor transmission rate (WVTR) of the PVA/ Na^+-MMT nanocomposite cryogel membranes were estimated according to section 3.1.4.

3.2.5. Kinetics

3.2.5.1. Water sorption kinetics in deionized water

The PVA/Na^+-MMT nanocomposite cryogels were cut in a square shape with the dimensions of 5×5×1 mm, and dried at 25 °C until a constant weight was achieved. The dried samples were weighed by an analytical balance having an accuracy of 0.0001 g, then immersed separately in a deionized water bath at pH =7 and temperature of 37 °C. The swollen nanocomposite cryogels were removed from the bath at predetermined intervals, wiping off the excess surface water with filter paper, and then weighed precisely. Then, the samples were again immersed in a fresh deionized water bath and

this process continued until equilibrium swelling was reached. The weight change was recorded as a function of time. The measures were made in triplicate.

Equilibrium swelling ratio, the swelling ratio, and the swelling fraction were calculated by equations 3-2 to 3-4**,**

Equilibrium swelling ratio = $\frac{W_s - W_d}{W_d}$ **(3-2)**

where W_d is weight of the dry gel and Ws is weight of the swollen gel in the equilibrium conditions.

Swelling ratio (SR)= $\frac{W_s}{W_d}$ **(3-3)**

where W_s is weight of the swollen gel and W_d is weight of the dry gel, respectively.

Swelling fraction = $\frac{W_t}{W_\infty}$ **(3-4)**

where, W_t is the amount of absorbed water that was obtained as a function of time, and W_∞ is the equilibrium water sorption.

and the Equilibrium water content was determined as follows:

EWC (%) = $\frac{W_s - W_d}{W_S}$ **(3-5)**

where, W_d is weight of the dry gel, W_s is weight of the swollen gel at equilibrium state, W_t is the amount of absorbed water that was obtained as a function of time and W_∞ is the equilibrium sorption respectively.

3.2.5.2. Water desorption kinetics for swelled gels

Each sample that had reached the swelling equilibrium was removed from the deionized water bath. Its excess surface water was removed by a filter paper and the gel was weighed using an analytical balance with an accuracy of 0.0001 g as the swollen weight (Ws). Then, the gels were placed separately in an atmosphere at 25 °C with constant humidity for predetermined interval times. This process continued until the gels were

completely dried and reached a constant weight. The amount of water desorption was recorded as a function of time. The measurements were made in triplicate.

The water desorption was calculated as follows:

$$\frac{\boldsymbol{M_t}}{\boldsymbol{M_\infty}} = \frac{\boldsymbol{m(t) - m(0)}}{\boldsymbol{m(\infty) - m(0)}} \qquad \textbf{(3-6)}$$

where, M_t is the water desorbed at any time t, M_∞ is the initial amount of water inside the nanocomposite hydrogel, $m(t), m(0)$ and $m(\infty)$ are the weights of hydrogel at the time of t, the initial time zero and at the time of complete drying of samples, respectively.

3.3 PART 3: Comparison the Properties of PVA/Na^+-MMT Nanocomposite Hydrogels Prepared by Physical and Physicochemical Crosslinking

3.3.1. Materials

Materials were used similar to what mentioned in section 3.1.1 except for glutaraldehyde.

3.3.2 Fabrication of Physical Nanocomposite Hydrogels (Cryogels)

Fabrication of nanocomposite hydrogels were done similar to that in section 3.1.2.

3.3.3 Fabrication of Physicochemical Nanocomposite Hydrogels

The physical nanocomposite hydrogels were immersed in 0.04% aqueous solution of glutaraldehyde (hydrogel weight to glutaraldehyde solution volume, 1 g/100 cc) for 12 h at 5 °C, and then kept in an acidic solution (Fig. 3.8) for 1 h at 40°C. The gels were rinsed in deionized water and neutralized to pH 7.

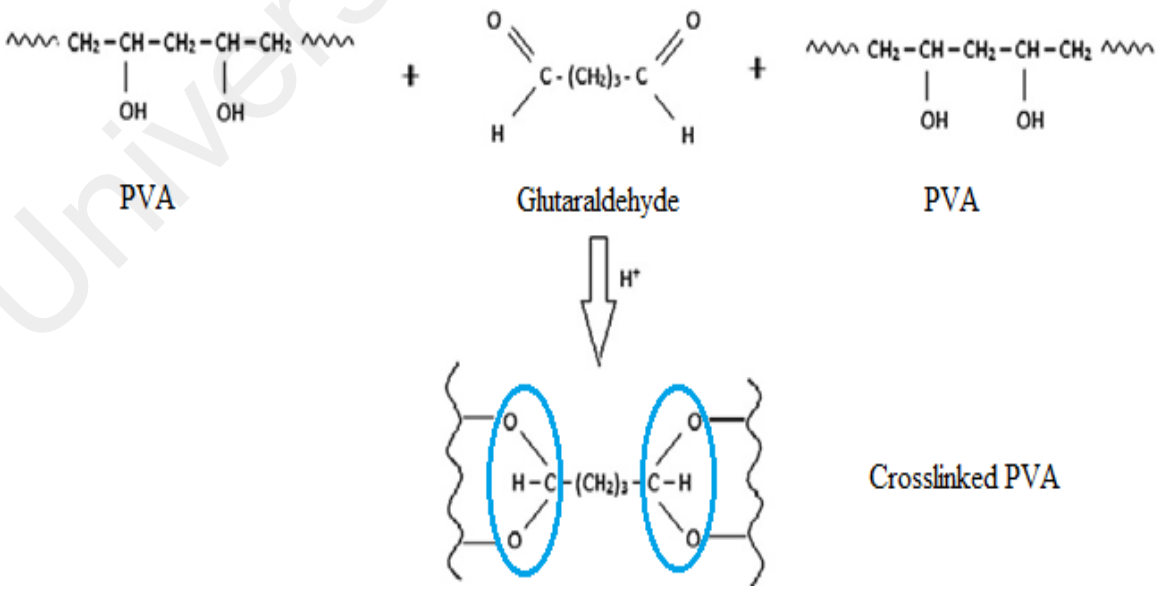

Figure 3.8: Chemical crosslinking of PVA with glutaraldehyde

3.3.4. Structure and morphology

Structure and morphology of nanocomposites were investigated according to section 3.1.3.

3.3.5. Thermal and mechanical analysis

Thermal and mechanical properties of nanocomposites were investigated according to section 3.1.4. The water vapor transmission rate (WVTR) was determined base on equation 3-1.

3.3.6 Kinetics

3.3.6.1 Water sorption kinetics in deionized water

Water sorption kinetics in deionized water for pure PVA cryogel and The PVA/Na^+-MMT nanocomposite cryogels at pH =7 and temperature of 25 °C were determined according to section 3.2.5.1.

3.3.6.2. Water desorption kinetics for swelled gels

Water desorption kinetics for swelled gels at 25 °C were determined based on section 3.2.5.2. The water desorption was calculated according to the equation 3-6.

3.4 PART 4: Fabrication of (PVA/Na^+-MMT/ PVP-Iodine) nanocomposite hydrogel system and study of in vitro its antibacterial properties for wound dressing application

3.4.1. Materials

Materials were used similar to what mentioned in section 3.1.1 except for Polyvinyl pyrrolidone- Iodin (10% aqueous solution PVP- I) that was taken as antiseptic solution and physiological saline solution.

3.4.2. Preparation of nanocomposite hydrogels

Fabrication of nanocomposite hydrogels were done similar to that in section 3.1.2.

3.4.3. Swelling studies

The dried samples with the size 5*5*1 mm, were weighed by an analytical balance with an accuracy of 0.0001g, and were immersed in pH 7 physiological solution bath at 37°C, the swollen nanocomposite hydrogels were removed of the bath at determined interval times, wiping off the excess surface water with filter paper and weighed carefully. The samples were then immersed again in the fresh physiological solution bath and this process continued until equilibrium swelling. The weight change was recorded as a function of time. The measurements were made in triplicate.

Equilibrium swelling ratio was obtained by the equation 3-2.

3.4.4. Loading of antibacterial agent into hydrogels

The PVA/MMT nanocomposite hydrogels were cut in square of size 5*5*1mm, and dried at 25°C until constant weight. A 10% aqueous solution of polyvinyl pyrrolidone-Iodin (Povidone-Iodine) as an antibacterial agent was loaded into the nanocomposite hydrogels (Fig. 3.9) by immersion the dry hydrogels in the solution until equilibrium

swelling. The swollen hydrogels were taken and dried at room temperature until they were reached to constant weights.

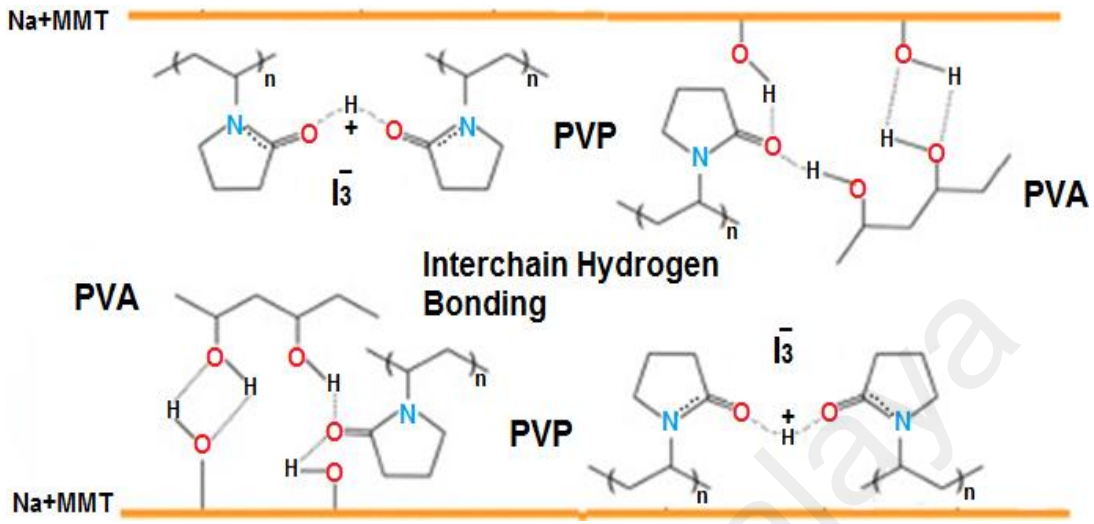

Figure 3.9: Inter chain Hydrogen bonding within a PVA-Na+MMT/PVP–I blend occurs between carbonyl groups on PVP and hydroxyl groups on PVA and silanol groups on Na+MMT

3.4.5. In vitro release experiment and Evaluation of antibacterial activity

According to Kirby-Bauer test, using the agar diffusion method, halos of poor bacterial growth surround some wafers indicating susceptibility to the antimicrobial agent. The zone of inhibition on agar media was used for determination of the antibacterial effects of Povidone-iodine nanocomposite hydrogels against Escherichia coli (E-coli); as a gram negative bacteria and Staphylococcus aureus (S-aureus); as geram positive bacteria respectively.

Povidone-iodine nanocomposite hydrogels were placed on Mueller-Hinton agar plates of bacteria with 4 mm deep, 60 mm diameter and the pH between 7.2 to 7.4. Inoculation is made with a broth culture diluted to match a 0.5 Mc Farland turbidity standard, which is roughly equivalent to 150 million Cells per ml. Then the plats were incubated at 37°C for 24hours. After that the zone of inhibition on the agar plates were examined and the diameters of inhibition zone surrounding the nanocomposite hydrogels were measured. Each assay was made in triplicate on two separate experimental runs.

CHAPTER 4: RESULTS AND DISCUSSIONS

4.1. Introduction

Nanocomposite hydrogels are polymer networks containing nanoclay that have high affinity of absorption the water or physiological fluids up to hundreds, even thousands times of their dry weights. Polyvinyl alcohol (PVA) nanocomposites have been studied by several researchers (Velazco-Diaz et al., 2005, Mc Gann et al., 2009, Sirousazar & Yari, 2010).

The first fabrication of PVA/MMT composites was reported by Greenland (1963). He used a solvent casting method and utilized water as a co-solvent. After that Ogata et al., (1997), used the same method to produce PVA/MMT composites. In the past, Strawhecker and Manias have used the solvent casting method, in an attempt to fabricate PVA/MMT nanocomposite films. They reported the properties of PVA nanocomposite films such as the mechanical, thermal and water vapor transmission rate, and found that the properties are far beyond those of pure PVA and its conventional composites (Strawhecker & Manias, 2000). Preparation of nanocomposites of PVA with two different types of clays, consisting of pristine-MMT and organically-modified MMT, were reported by Chang et al. (2003). They concluded that the hydrophilic character of the clays promotes dispersion of inorganic crystalline layers in water-soluble polymers. A solvent casting method for synthesis of PVA-based mixed uncrosslinked membranes containing Na-montmorillonite has reported (Nho Aet al., 2009). Moreover, Doppers et al. (2004) have investigated the solution intercalation method and in situ diffusion of acetone and water into nanocomposites for synthesis of PVA/MMT nanocomposite. They found that the acetone diffusion rate reduced significantly with clay loading while it had little influence on the water uptake.

PVA polymer has exceptional properties, including hydrophilic, water soluble, biodegradable, biocompatible, nontoxic, noncarcinogenic, nonexpensive, and able to form the gel via chemical and physical methods (Giusti et al., 1993, Valenta & Anver, 2004, Patachia, 2003, Hennink & van Nostrum, 2002, Peppas et al., 2000, Ratner et al., 2004, Hassan & Peppas, 2000, Hoffman, 2001). PVA has been used in various biomedical applications such as drug delivery devices (Li et al., 1998), artificial organs (Chen et al., 1994), wound dressing (Razzak et al., 2001, Yoshii et al., 1999, Yoshii et al., 1995), contact lenses (Hyon et al., 1994), skin treatment systems (Cha et al., 1993), protein adsorption, protein controlled release, and delivery devices, using one of the chemical or physical methods of crosslinking (Elizabeth & Fabia, 2006, Christie et al., 2000, Peppas & Simmons, 2004). PVA hydrogels can be prepared by several crosslinking methods. Chemical crosslinking of PVA includes covalent crosslinking using crosslinking agents such as formaldehyde, glutaraldehyde, terephthalaldehyde, and hexamethylenediamine to increase the gel strength (Varshney, 2007, Mirzan et al., 2001, Kenawy et al., 2013). In general, the hydroxyl groups in PVA can react with a number of multifunctional compounds creating three dimensional PVA networks (Caro et al., 1976, Korsmeye & Peppas, 1981, Gimenez et al., 1997). Physical cross linked PVA prepared by gamma irradiation and freezing thawing processes has been reported by many researchers (Velazco-Diaz et al., 2005, Mc Gann et al., 2009, Sirousazar & Yari, 2010, Watase & Nishinari, 1988, Nagura et al., 1989, Yamura et al., 1989). For example, Varshney (2007) reported the synthesis of PVA-based hydrogel and Mirzan et al., (2001), reported the preparation of the gamma-irradiated polyvinyl alcohol-polyvinyl pyrrolidone (PVA-PVP) hydrogel by gamma-irradiation technique. They determined the amount of gel fraction, mechanical properties, water content, and water absorption capacity of the hydrogel for wound dressing applications. In a number of studies, several researchers have used the freeze-thaw method for the synthesis of PVA-

based hydrogels (Velazco-Diaz et al., 2005, Mc Gann et al., 2009, Sirousazar & Yari, 2010). For instance, Kim et al. (2008) used the freeze-thaw method for the development of a polyvinyl alcohol-alginate gel-matrix based wound dressing containing nitro furazone. Also, Nho et al. (2009), used gamma-irradiation followed by the freeze-thaw method to synthesize a PVA/PVP/glycerin/ antibacterial agent hydrogel for wound dressing.

The freezing-thawing technique basically consists of freezing a homogeneous aqueous solution containing polymer at low temperatures and then thawing back to room temperature (Stauffer & Peppas, 1992). This process can be repeated for a few times. The freeze-thawing method for PVA results in a stable physical cross-linked PVA cryogel. During the freezing steps the formation of ice crystals within the aqueous PVA system leads to the macroporous structure that is mostly imprinted by formation of ice crystals. Due to drive out the amorphous polymer segments by the ice crystals, the PVA aqueous solution separate into polymer-rich parts and polymer-poor parts of a porous polymer network (Peppas, 1975, Lozinsky, 1998, Lozinsky et al., 2003, Lozinsky et al., 1984, Wu & Wisecarver, 1992). Changes in the regional concentration of polymer molecules generate intermolecular forces and leads to the formation of microcrystals (Ogata et al., 1997). Polymer chain folded microcrystallites that formed in polymer-rich phases, play the role of crosslinking sites in the hydrogel networks (Peppas, 1975, Lozinsky, 1998, Lozinsky et al., 2003, Lozinsky et al., 1984, Wu & Wisecarver, 1992, Strawhecker, K.E. & Manias, E. (2000).

Chemical crosslinked hydrogels have some disadvantages, including the existence of residual crosslinking agents in the hydrogel which can be toxic to the tissues and organs. Residual elimination of the crosslinkers is sometimes expensive, which has caused production costs to be increased.

PVA solutions can form gels during the freeze-thaw process. Changes in regional concentration of polymer molecules upon sublimation of solvent through freeze-thaw process create intermolecular forces, leading to the formation of micro crystals**.** The crystalline domains play the role of crosslinking sites in the hydrogel networks (Takeshita et al. 1999).

Incorporation of nanoclay in PVA hydrogel leads to enhancement of its chemical, physical and mechanical properties (Haraguchi & Takehisa, 2002; Schexnailder & Schmidt, 2009; Haraguchi, 2007). Montmorillonite (MMT) is the most widely used mineral in preparation of nanocomposite hydrogels. This is due to its good water absorption, extensive swelling and cation exchange ability in water (Gao et al., 1999, Gamiz et al., 1992, Gao et al., 2001). Due to the presence of silanol groups on the surface of MMT and their ability to form hydrogen bonds, MMT can interact with hydrophilic polymers, participating in stability improvement of the nanocomposite systems (Mirzan et al., 2001, Velazco-Diaz et al., 2005). Thus, MMT may act as a co-crosslinker for hydrophilic polymers (Mc Gann et al., 2009).

The swelling behavior of hydrogels and theirs swelling kinetics in different media based on their applications are important as well as in vitro studies of biocompatibility preliminary in simulated physiological fluids have a great importance on the application of biomaterials. The resemblance of PVA hydrogels to living tissues in their physical properties because of their relatively high water content as well as soft and rubbery consistency shows that PVA hydrogels have potential applications in this field and are excellent candidates for biomedical applications. Skin treatment and wound dressing are examples of hydrogel applications in the biomedical field. Dressings the wounds with the hydrogels are usually accomplished by directly applying the hydrogels to the injured skin and wounds, thus the non-toxicity, biocompatibility and antibacterial properties of the hydrogel must be considered.

Physical prepared PVA gels have physical linkages without any hazardous ingredients such as crosslinking agents, catalysts, organic solvents, emulsifiers, and others (Hickey & Peppas, 1995, Ostuka et al., 2011), which are usually used in chemical crosslinking. This makes them suitable to design nontoxic, biocompatible and biomedical devices for organisms (Okazaki et al. 1995, Wilcox et al. 1999, Lozinsky et al. 2000, Hassan et al. 2000). Several researchers have reported physical crosslinked PVA, prepared by gamma irradiation and freeze-thaw processes (Sur et al., 2003, Al et al., 2008, Gao et al., 1999, Lozinsky, 1998, Gonzalez et al., 2012, Lozinsky et al., 1984, Wu & Wisecarver, 1992, Elizabeth & Fabia, 2006). Moreover, Mirzan et al. (2001) reported the synthesis of gamma-irradiated polyvinyl alcohol-polyvinyl pyrrolidone copolymer (PVA-PVP) hydrogel.

The physicochemical crosslinking method used in this research consisted using a very small amount of glutaraldehyde followed by repeated freezing and thawing cycles. This method in addition to having the advantages of freezing-thawing method increases (improves) the structural strength and swelling properties of the gel. However, synthesis of PVA nanocomposite hydrogels by physicochemical methods has not been reported yet. In this research, for the first time we have synthesized PVA nanocomposite hydrogels using the unmodified Na^+-MMT nanoclay via a physicochemical method. Also, a new mixing technique (controlled sonication followed by mechanical mixing) was used for the preparation of nanocomposite hydrogels. In previous studies, there is not enough attention paid to hydrophilic and non toxic properties of unmodified MMT compared to modified MMT. Additionally, the role of ultrasonic mixing to disperse MMT nanoparticles has not been investigated. In this work we have investigated for the first time the use of unmodified Na^+-MMT nanoclay for fabrication of non toxic PVA nanocomposite hydrogels by freeze-thaw technique used for skin treatment and wound dressing applications.

However, there is not much interest to hydrophilic properties, swelling capacity, sorption and desorption kinetics of PVA nanocomposite hydrogels using the unmodified Na^+-MMT nanoclay. In previous studies, there was no report indicating the design and preparation of nanocomposites cryogel free from harmful components that its swelling and permeability characteristics were optimized for biomedical applications. In the present research PVA nanocomposite cryogels based on the unmodified Na^+-MMT nanoclay free from any toxic materials have been synthesized via ultrasonic mixing and freeze-thaw process. For the first time the critical concentration of nanoclay has been optimized to achieve the required both. In this research, non toxic and biocompatible antibacterial nanocomposite hydrogel systems based on PVA/ Na^+-MMT and PVP-Iodine were fabricated for wound dressing and skin treatment. Due to the hydrogen bonding ability of the PVP-Iodine with the PVA and its good biocompatibility, it was loaded in to PVA network as an antibacterial agent and investigated the antibacterial properties of (PVA/Na^+-MMT/ PVP-Iodine) system invitro against gram negative and gram positive bacteria.

4.2 PART 1: Non toxic hydrogels based on polyvinyl alcohol/Na^+-Montmorillonite nanocomposites for biomedical applications: Fabrication & Characterization

4.2.1 Structural characterization and morphology

FTIR spectra of the dry samples of the pure PVA hydrogel and the PVA/ Na^+-MMT nanocomposite hydrogels containing 1, 5 and 10% nanoclay are shown in Figure 4.1 Characteristic bands were seen for Na^+-MMT (Si-O stretching, 1000–1050cm^{-1}), and for PVA (-OH stretching, 3270–3300 cm^{-1}; -CH_2 stretching, 2900–2922 cm^{-1}; C-O stretching 1075–1087 cm^{-1}); C-H bending vibration was seen at 839 cm^{-1} and 1326 cm^{-1}. The peak that appeared at 1650 cm^{-1} is attributed to -OH deformation vibrations.

The stretching vibration of a C-C-C bond appeared at 1141–1142 cm^{-1} (Upadhyay & Bhat, 2005). This band corresponds to the crystalline domains of PVA and are present in all the spectra. Figure 4.1 indicates that there is no interaction between PVA and Na^+-MMT in the crystalline domains of PVA, because the band at 1142 cm^{-1} does not show any shift or any height changes caused by the effects of the clay. Increasing the content of Na^+-MMT caused a decrease in the intensity of the C-O stretching band of PVA within the range of 1075–1087 cm^{-1} , while the intensity of the Si-O stretching band at 1000–1050 cm^{-1} range increases, which indicated the presence of hydrogen bonding between the Si-O group of Na^+-MMT and -OH group of PVA due to interaction between PVA and Na^+-MMT (Gao et al., 2001). It can also be seen in Figure 4.13 that the intensities of the -OH stretching bands at 3000–3600 cm^{-1} decreased with an increase in the clay content. This is due to the hydrogen bonding of the hydroxyl groups among PVA and Na^+-MMT that they are weaker than interactions between -OH groups in PVA chains.

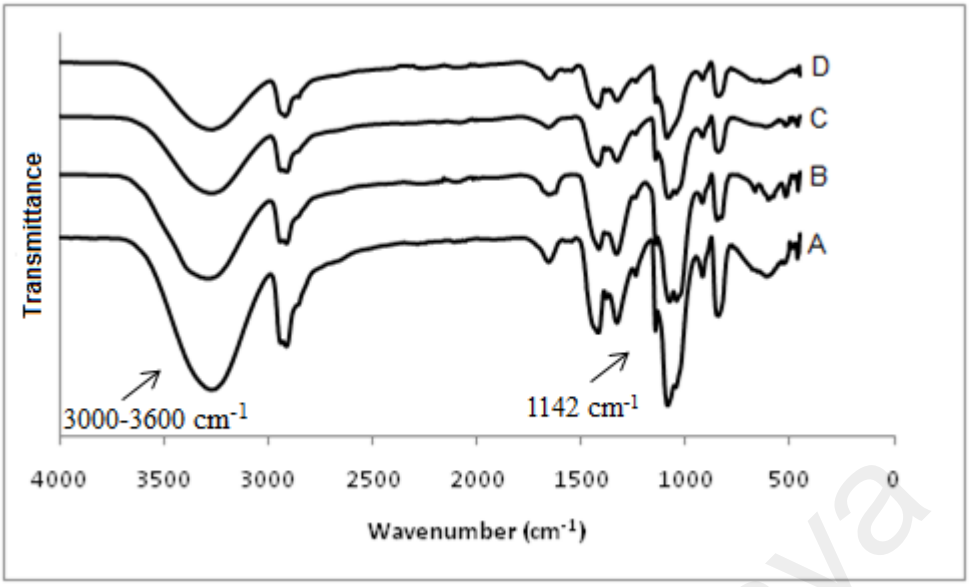

Figure 4.1: FTIR spectra of (A) the pure PVA hydrogel, PVA/ Na^+-MMT hydrogel containing (B) 1, (C) 5and (D)10% nanoclay

The morphological structure of nanocomposite hydrogels was studied by FESEM technique. Sample preparation was done and they were fractured and mounted to expose the bulk before examination. The FESEM images presented in Figure 4.2 show that the nanoclay Na^+-MMT is homogeneously incorporated in the PVA matrix and the morphology of nanocomposites becomes smoother than pure PVA. This was due to good dispersion of Na^+-MMT in the PVA matrix by sonication mixing and also due to the high degree of compatibility between PVA and Na^+-MMT.

It was found that by increasing the clay content, this leads to a decrease in the number and size of the pores that causes a dense morphology to be formed and so indicate a more packed network. It appears that the presence of Na^+-MMT between the PVA chains leads to destruction in the orientation of PVA crystalline regions, so its amorphous phase grows.

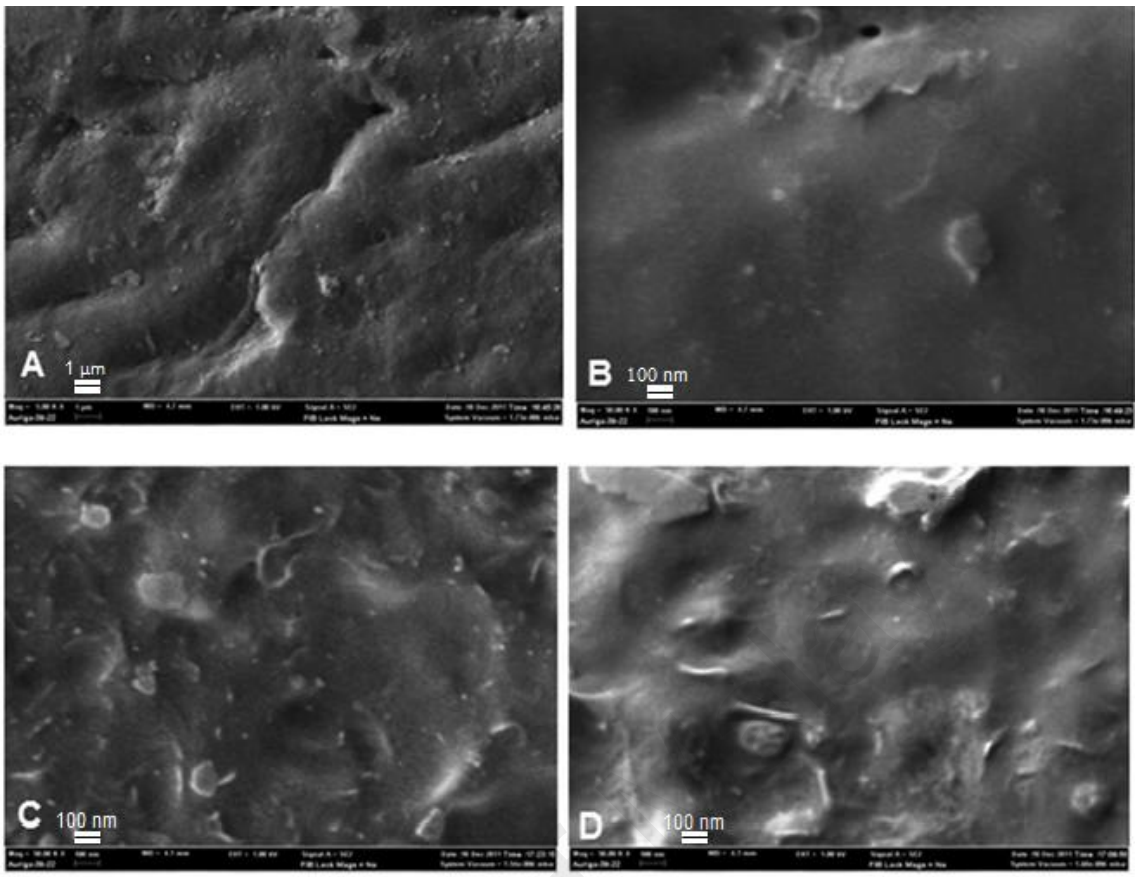

Figure 4.2: FESEM images of pure PVA hydrogel (A), PVA/Na1-MMT nanocomposite hydrogels containing 1 (B), 5 (C), and 10 wt% (D) nanoclay

Figure 4.3 shows the XRD patterns of Na^+-MMT, pure PVA hydrogel, and PVA/ Na^+-MMT nanocomposite hydrogels containing 1, 5 and 10% nanoclay. At first glance, the existence of nanoclay causes significant changes to the crystalline forms of the PVA. The XRD pattern of PVA hydrogel in the $2\theta = 2–25°$ showed a broad peak at about 20° that is attributed to the semi-crystalline nature of PVA (Nanda et al. 2010, Bhargav et al. 2009). The pure Na^+-MMT showed two peaks at 19.69° and 7.17° respectively, but the PVA did not indicate any peaks in the region of 2–10°.

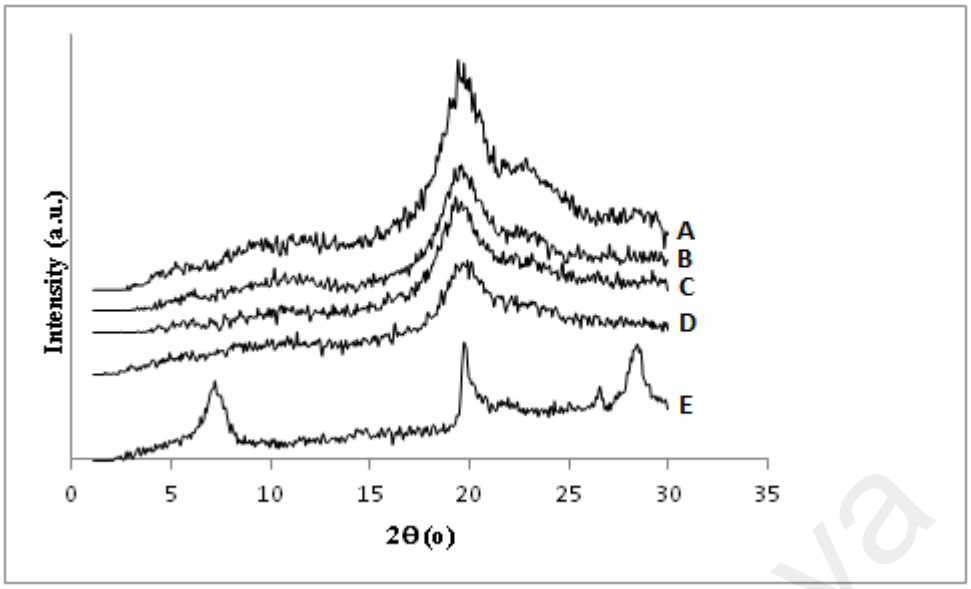

Figure 4.3: XRD patterns of the pure PVA hydrogel (A), PVA/ Na^+-MMT hydrogel containing 1(B), 5(C), 10% (D) nanoclay and pure Na^+-MMT (E)

The presence of 1, 5 and 10 wt.% of the Na^+-MMT resulted in a shift in the peak position at 19.69° (*d*-spacing = 4.57 Å) towards smaller angles of 19.54°, 19.41° and 19.35° (*d*-spacing = 4.60 Å, 4.63 Å and 4.65 Å), respectively. Also, the nanocomposite hydrogel patterns do not show any diffraction peak at 2ɵ = 2–10°. These results indicated that there was an increase in distance between the platelets due to the PVA chains being intercalated and exfoliated into the individual silicate layers of Na^+-MMT. This was likely due to well-dispersed Na^+-MMT into the PVA matrix by sonication and also because of the compatibility between PVA chains and Na^+-MMT. The chemical and physical interactions between the PVA and nanoclay layers' surfaces can occur through the hydrogen bonding between -OH and Si-O-Si groups in nanoclay with the -OH groups of PVA chains and their dipole-dipole bonding. Therefore, good interaction and compatibility, along with high dispersion of the components led to exfoliation. These results were confirmed by TEM analysis.

According to the XRD results, it can be seen that the presence of Na^+-MMT caused the new crystalline phase and changes on the crystalline domain of the PVA matrix

(Strawhecker & Manias, 2000, Jeong et al. 2005). From the literature, MMT has been found having a role as crystalline nucleating agent for PVA chains (Yu et al., 2003, Carrado et al., 1996, Bandi & Schiraldi, 2006, Paranhos et al., 2007). Also, it has been found that the crystallinity of PVA is decreased with increasing the clay content, while its amorphous phase is increased.

In order to analysis the morphology of nanocomposites, the TEM results were combined with those of the XRD's. A TEM image of the PVA/ Na^+-MMT nanocomposite hydrogel containing 5% nanoclay is shown in Figure 4.4 It can be observed that the clay nanoparticles are highly dispersed into the polymer matrix and the silicate layers are mostly in the exfoliated state.

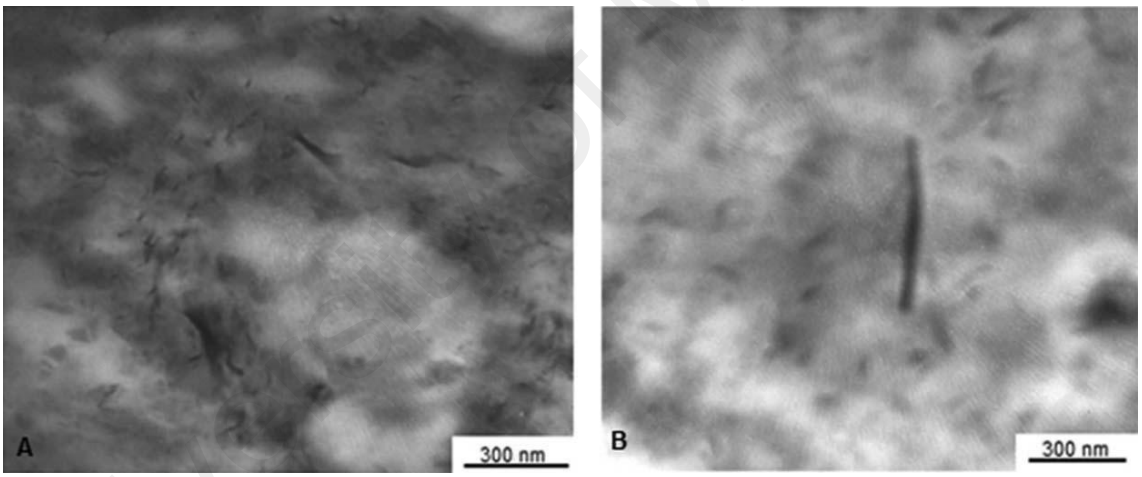

Figure 4.4: TEM of PVA/ Na1-MMT hydrogels containing (A) 5 wt% and (B) 10 wt% nanoclay

These results are obtained because of having high dispersion of nanoclay upon sonication, and achiveing good interactions and compatibility of nanoclay with PVA chains. The observations are in good agreement with the XRD results.

The three-dimensional and topographic images of the PVA/ Na^+-MMT nanocomposite hydrogels were studied by AFM technique. Figure 4.5 shows an AFM image of PVA/Na^+-MMT nanocomposite hydrogel containing 5% nanoclay. As shown in this

image the Na^+-MMT nanoparticles were uniformly dispersed in the PVA matrix. This was due to good distribution of nanoclay in the PVA matrix by high dispersion of nanoclay via sonication, and good interactions and compatibility of nanoclay with PVA chains. The results were in agreement with the TEM observations.

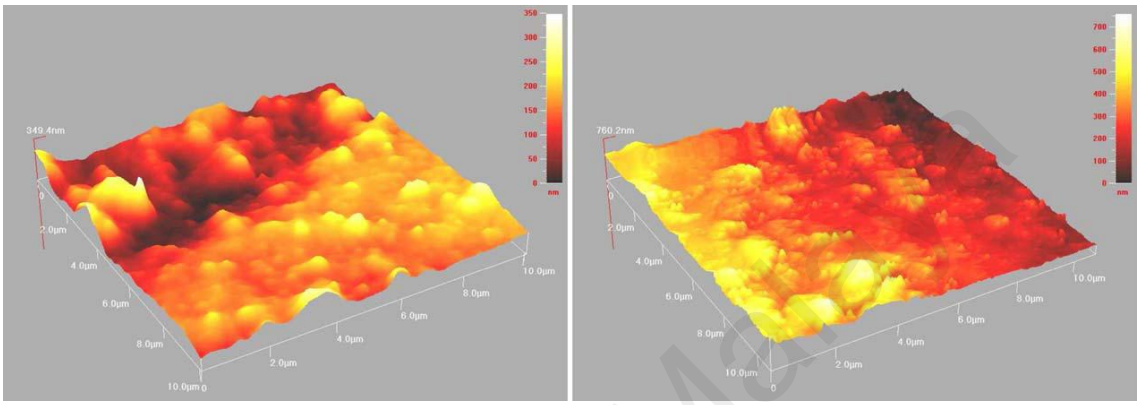

Figure 4.5: AFM images of PVA/ Na^+-MMT hydrogel containing 5% nanoclay

4.2.2 Thermal and mechanical analysis

TGA thermographs of the dry samples of th**e** pure PVA hydrogel and the PVA/Na^+-MMT nanocomposite hydrogels containing 1, 5 and 10% nanoclay are shown in Figure 4.6. At first glance, three main weight loss regions are seen in the TGA curves. The first region, at the temperature range of 80–150 °C, appeared due to the evaporation of H_2O molecules, showing that they are physical and chemical bounded; the weight loss of the nanocomposites in this area was about 2.9–3.55 wt.%.

The second region, at about 250–390 °C, was due to the side chain degradation of the polymer matrix in the PVA/Na^+-MMT nanocomposite; the weight loss calculated in this area was approximately 50–70 wt. %. The third region at about 440 °C, with a total weight loss of about 75–95 wt. % up to 500 °C and 77-100 wt. % up to 700 °C corresponds to the cleavage of the C-C bonds of PVA backbone existed in the PVA/Na^+-MMT nanocomposite as listed in Table 4.1:

Table 4.1: Weight loss results of TGA for pure PVA hydrogel and PVA/Na^+-MMT nanocomposite hydrogels at various temperatures

Types	Weight loss (%)			
	100°C	300°C	500°C	700°C
PVA hydrogel	0.82	48.03	95.30	99.84
PVA/1 wt% Na^+-MMT	0.86	48.12	94.18	95.39
PVA/5 wt% Na^+-MMT	0.43	50.74	87.27	88.81
PVA/7 wt% Na^+-MMT	0.83	49.94	82.91	83.95
PVA/10 wt% Na^+-MMT	0.81	59.21	74.25	77.0

In general, the structural decomposition of the PVA occurs in the range of about 200 to 500 °C, and after 600 °C the curve flattens due to the inorganic residue. These results indicate that the thermal decomposition region of the PVA/Na^+-MMT nanocomposites shifts toward the higher temperatures compared to the PVA. Therefore it could be concluded that an increase in nanoclay content may lead to an improvement in thermal stability of the PVA due to the existence of chemical and physical interactions between the PVA and nanoclay layers' surfaces that can occur through the hydrogen bonding of the -OH and Si-O-Si groups of nanoclay with the -OH groups of PVA chains and their dipole-dipole bonding. There is an opposite trend in the thermal stability of 10% nanoclay content. This behavior can be attributed to the insulating role and mass transfer barrier of the intercalated and agglomerated nanoclay in relation with the volatile products generated during decomposition. This heat barrier acts inversely after a certain degree of decomposition. It means that the accumulated heat of the nanoclay will be released and acts as a new heat source with the outside heat source simultaneously (Chang et al., 2003). Thus, after a certain temperature, the nanocomposite containing higher nanoclay shows lower thermal stability.

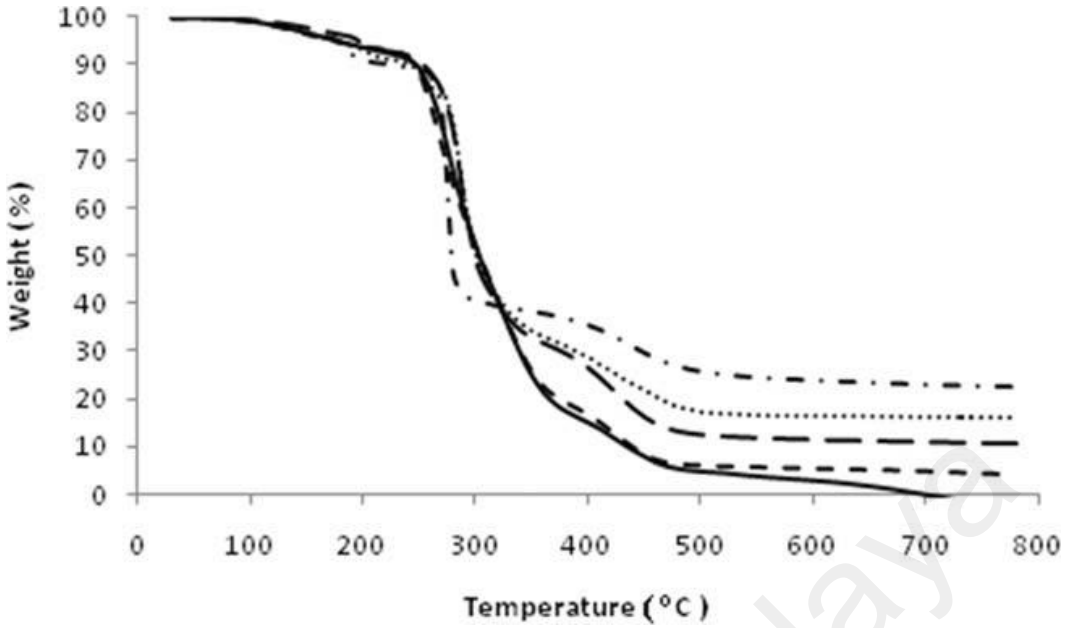

Figure 4.6: Weight loss from TGA scans for pure PVA hydrogel (——) and PVA/ Na^+-MMT nanocomposite hydrogels containing 1 (– – –), 5 (— —), 7 (·····), and 10 wt% nanoclay (– · –).

Figure 4.7 shows the DSC thermograms of the PVA/Na^+-MMT nanocomposite hydrogels containing 1, 5 and 10% nanoclay and the pure PVA hydrogel. In Figure 4.7 the pure PVA hydrogel exhibits an endothermic peak within 220-230°C, corresponding to the melting temperature of the pure PVA hydrogel. This peak is shifted toward a lower temperature as the amount of the nanoclay increases. It can be seen that a new melting peak appeared at a lower temperature for nanocomposite hydrogels containing 1, 5 and 10% nanoclay. This evidence suggests that nanoclay acts as a nucleating agent in crystallization of PVA chains. The peak broadening suggests a change in the amount of semi-crystalline and amorphous phases. It was found that an increase in the nanoclay content would lead to a decrease in the degree of crystallinity due to the change in relative fractions of semi-crystalline phase and amorphous phase.

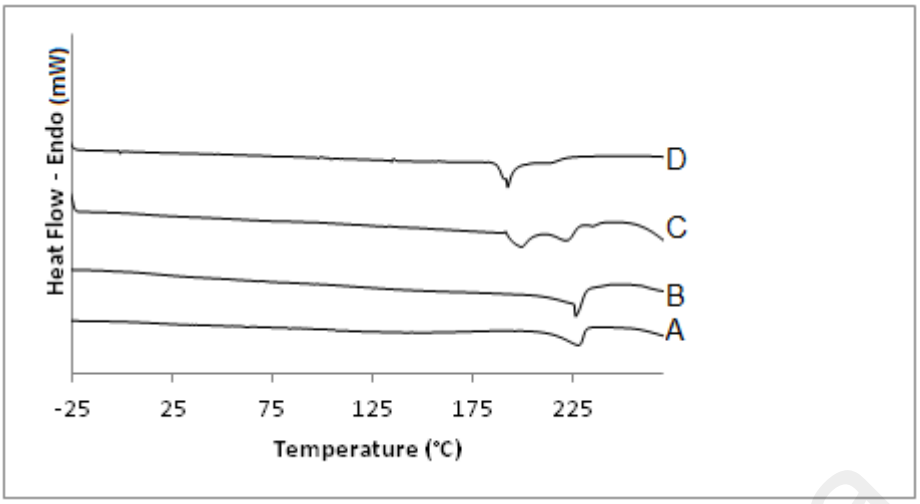

Figure 4.7: DSC curves for (A) the pure PVA hydrogel and PVA/ Na^+-MMT nanocomposite hydrogels containing (B) 1, (C) 5 and (D) 10% nanoclay

The presence of nanoclay in the PVA hydrogel structure causes two melting peaks to appear in the DSC thermogram. The peak corresponding to the higher melting point is related to pure PVA, and the peak corresponding to the lower melting point is attributed to the intercalated and exfoliated structures formed by PVA/nanoclay interactions. It can be said that the first melting region is related to the pure PVA crystalline phase and the second melting region is attributed to the newly formed crystalline phase of "PVA plus nanoclay". The newly formed crystalline phase is due to the interaction between PVA with the intercalated and exfoliated nanoclay structures that are formed during the freeze-thaw process.

The hydrogen bonding between pure PVA molecules is stronger than those between PVA chains and nanoclay. The presence of nanoclay causes the hydrogen bonding between PVA chains as well as van der Waals' forces to be weakened. Thus, the melting point would be shifted toward lower temperatures. In addition, the melting point decreases with increasing nanoclay content.

Dynamic mechanical analysis (DMA) is usually run on polymeric materials such as nanocomposites to measure their responses toward a cyclic deformation as a function of

temperature. The mode of deformation in DMA experiments can be tension, torsion and flexural (three-point bending). Three main parameters can be obtained from DMA: (1) the elastic (storage) modulus (E'), corresponding to the elastic response to the deformation; (2) the viscous (loss) modulus (E"), corresponding to the plastic response to the deformation; and (3) tan δ, that is the (E"/ E') ratio. The tan δ curve can be used to estimate the glass transition temperature (T_g) of the polymeric samples.

The DMA thermograms of pure PVA hydrogel and the PVA/Na^+-MMT nanocomposite hydrogels containing 1, 5 and 10% nanoclay are shown in Figure 4.8. The figure compares the values of tan δ within the temperature range of -50 to 200 °C for the pure PVA hydrogel and three samples of nanocomposite hydrogels containing 1, 5 and 10% nanoclay, respectively. At first glance, it can be seen that the tan δ is decreased as the nanoclay increased. Glass transition temperatures (T_g) can be obtained from the peak location in the tan δ curve. In Figure 4.8, the thermograms show the glass transition temperatures of the pure PVA hydrogel, and their nanocomposite hydrogels containing 1, 5 and 10% nanoclay, being 40, 42, 45 and 50 °C respectively. It was found that the tan δ peaks are shifted toward higher temperatures as the amount of nanoclay increases; this behavior is due to the hydrogen bonding of the -OH and Si-O-Si groups in nanoclay with the -OH groups in PVA chains and hence more chain stiffness being produced. The results indicated that the T_g values obtained by this method were lower than the values obtained by DSC, but a satisfactory agreement was observed between the Tg values from two different methods. It is known that the mechanical properties of polymer are related not only to its crystallinity but also to the molecular structure of its amorphous regions (Fukumori & Nakaoki, 2013). The Tg data obtained from DMA are always different from that of DSC, and DMA-based Tg is more accurate (Yang et al., 2009).

The height of the damping peak in the DMA curve shows the mobility of the polymer molecular chains that leads to damping of energy. The higher the peak, the less

restriction there is toward the polymer chain motions. The damping peak height decreases as the nanoclay content increases. This is due to the restriction for the polymer chain motions, created by nanoclay. Also, the peak is shifted toward higher temperatures as the amount of nanoclay increases. This behavior is due to the hydrogen bonding causing more chain stiffness and rigidity, leading to less flexibility in the polymer. This property was confirmed by the hardness test.

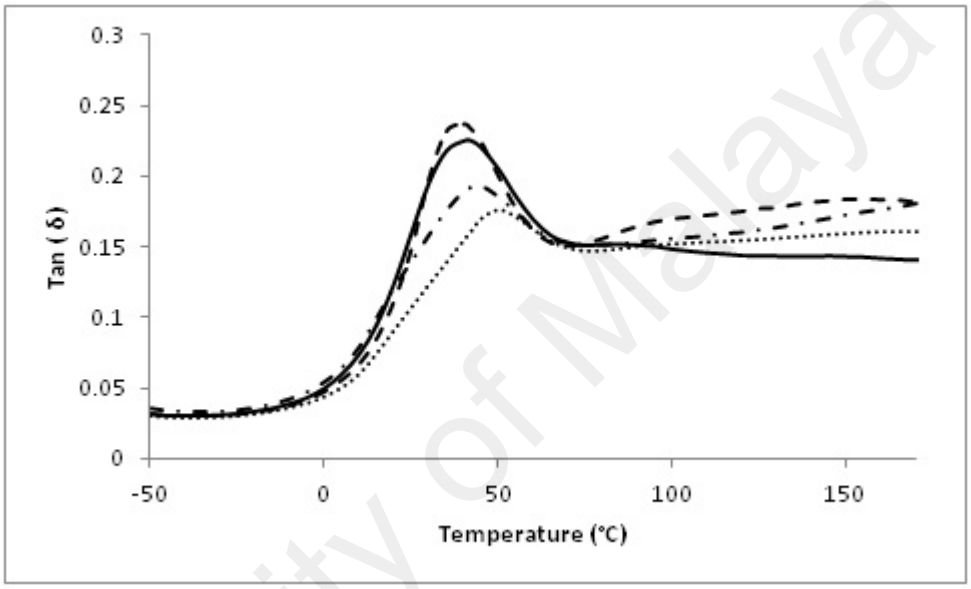

Figure 4.8: Temperature dependence of tan δ for the pure PVA hydrogel (- - - - -) and PVA/ Na^+-MMT nanocomposite hydrogels containing 1(——), 5 (– · –) and 10% nanoclay (·····)

Figure 4.9 shows the hardness values of pure PVA hydrogel and its nanocomposite hydrogels (PVA/Na^+-MMT) containing 1, 3, 5, 7 and 10% nanoclay. It can be seen that the increase in nanoclay content can lead to an increase in hardness. It was found that addition of 1, 3, 5, 7 and 10% by weight of Na^+-MMT increases the hardness of pure PVA hydrogel by 23.81, 40.48, 66.67, 92.86 and 109.52%, respectively. These results are due to the chemical and physical interactions between the PVA and nanoclay layers' surfaces that occurred through the hydrogen bonding of the -OH and Si-O-Si groups of nanoclay with the -OH groups in PVA chains and their dipole-dipole bonding.

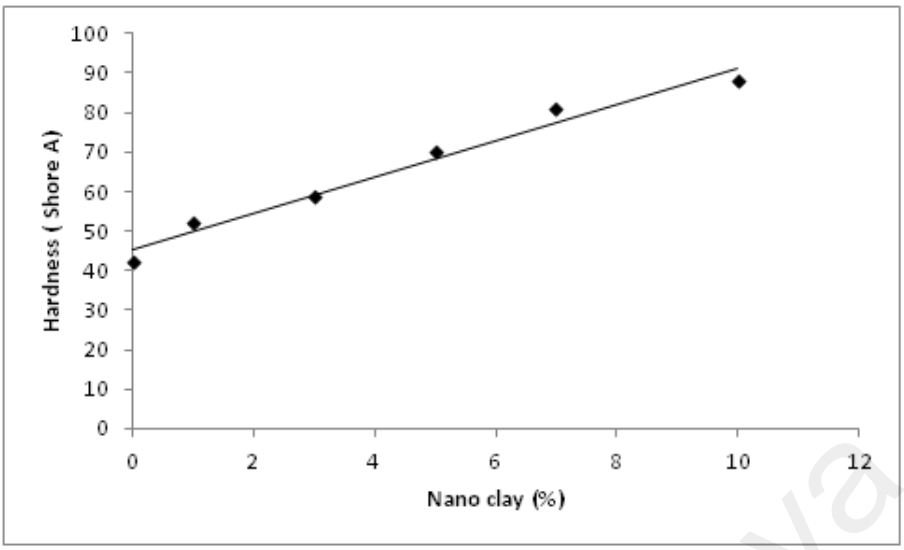

Figure 4.9: Hardness of PVA/ Na^+-MMT nanocomposite hydrogels containing 0, 1, 3, 5, 7 and 10% nanoclay

Figure 4.10 compares the values of the WVTR for pure PVA hydrogel and PVA/Na^+-MMT nanocomposite hydrogels containing 1, 3, 5, 7 and 10% nanoclay at 25 °C (43% RH), 37 °C (35% RH) and 50 °C (18% RH). It was observed that the WVTR decreased as the nanoclay content increases; this behavior is due to the increase of the path tortuosity for the penetrating molecules passing through the nanoclay layers. On the contrary, it was found that the WVTR is increased by increasing the temperature, because the kinetic energy of the molecules increases with increasing temperature. It is known that the WVTR for normal skin is 8.5g/m^2/h and that for injured skin is beyond 11.6 g/m^2/h (Mi et al., 2001). The results in Figure 10 indicate that the WVTR of PVA nanocomposite hydrogels containing 0–1% nanoclay at 37 °C are 8.52g/m^2/h to 11.22g/m^2/h. Thus, the nanocomposite hydrogels may be a suitable candidate for use as wound dressings.

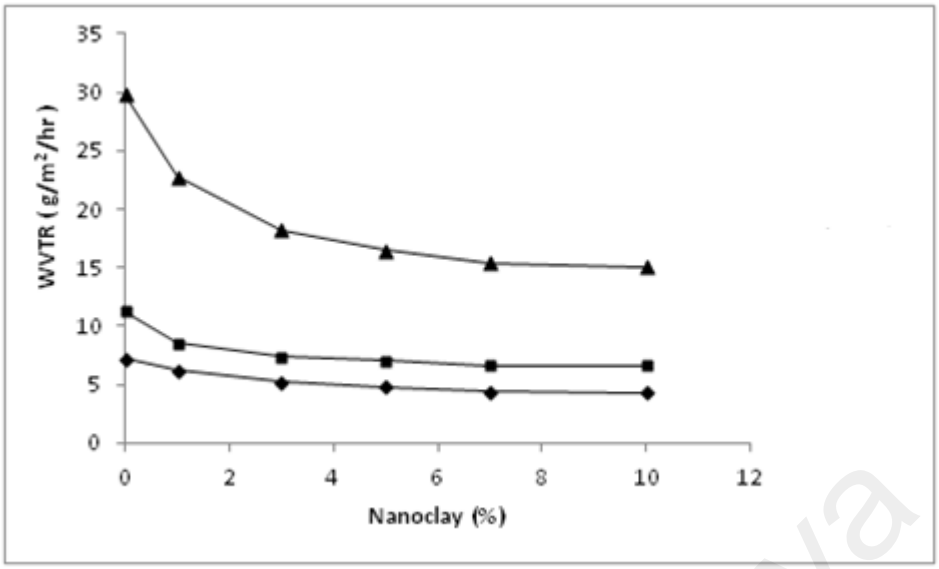

Figure 4.10: Comparison of WVTR for the PVA/ Na^+-MMT nanocomposite hydrogels containing 0, 1, 3, 5, 7 and 10% nanoclay at 25 (◆), 37(■) and 50 °C (▲).

4.3 PART 2: Nanocomposite cryogels based on poly (vinyl alcohol)/ unmodified Na^+-montmorillonite suitable for wound dressing application: optimizing nanoclay content

4.3.1 Effect of nanoclay content on morphology and thermomechanical properties

The morphological structure of nanocomposite cryogels was studied by FESEM technique. Sample preparation was done and they were fractured and mounted to expose the bulk before examination. The FESEM images presented in Figure 4.11 show that the nanoclay Na^+-MMT is homogeneously incorporated in the PVA matrix and the morphology of nanocomposites becomes smoother than pure PVA. This was due to good dispersion of Na^+-MMT in the PVA matrix by sonication mixing and also due to the high degree of compatibility between PVA and Na^+-MMT. It was found that by increasing clay content more than 1 wt. %, the number and size of pores in the nanocomposite were decreased causing a dense morphology and packed network to be formed. It appears that the presence of Na^+-MMT between the PVA chains leads to destruction in the orientation of PVA crystalline lattice, so its amorphous regions grows.

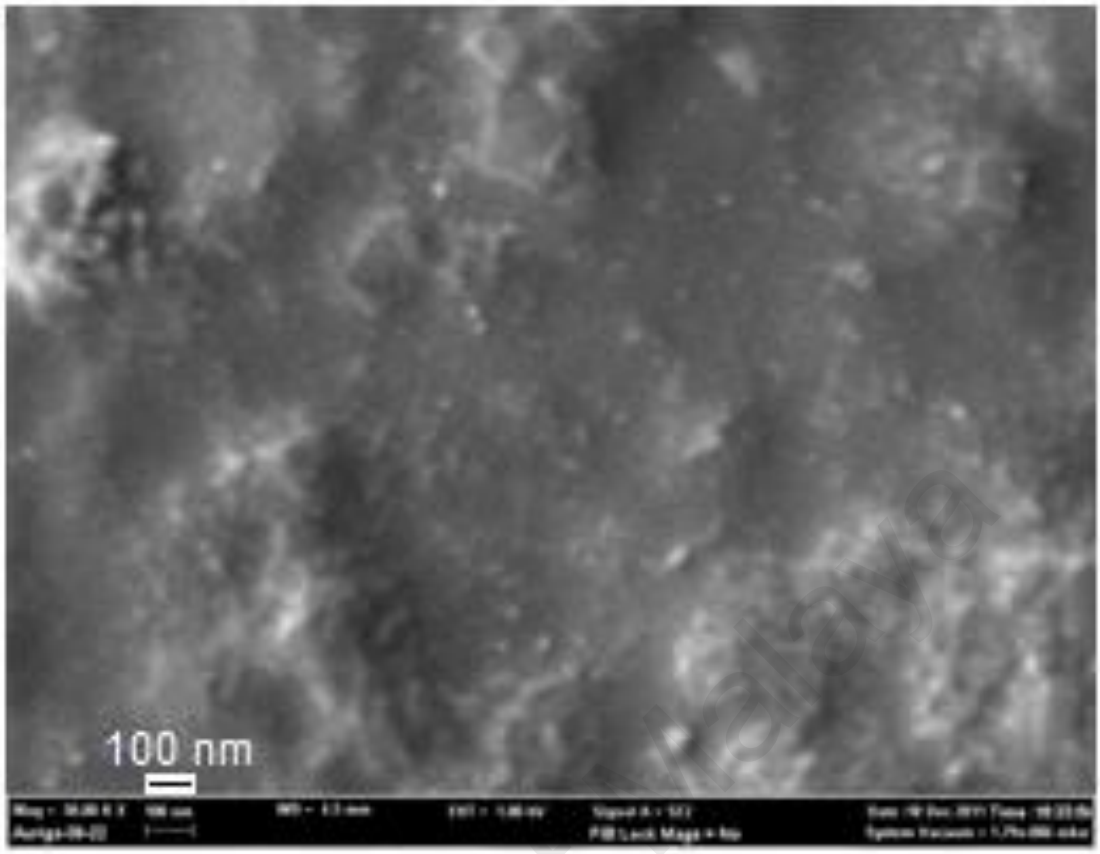

(a)

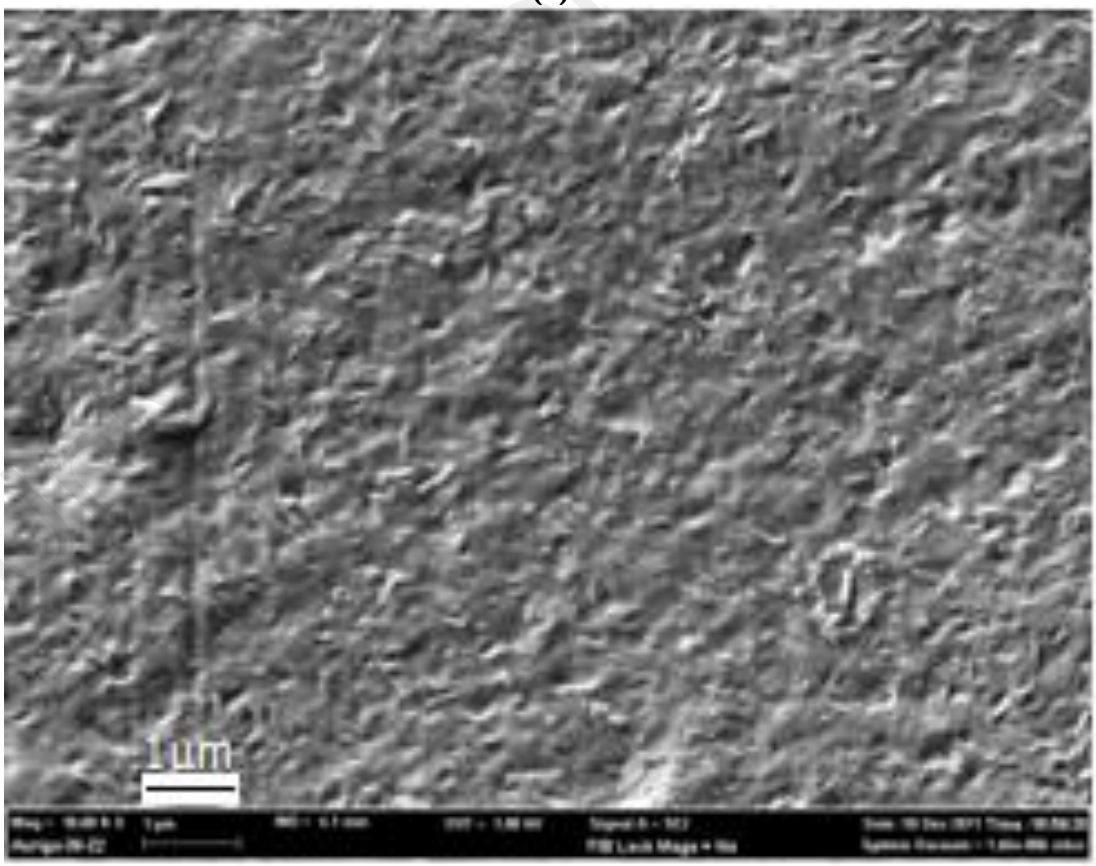

(b)

Figure 4.11: FESEM images of (a) pure PVA cryogel and PVA/ Na^{+}-MMT nanocomposite cryogel containing (b) 1wt. % nanoclay

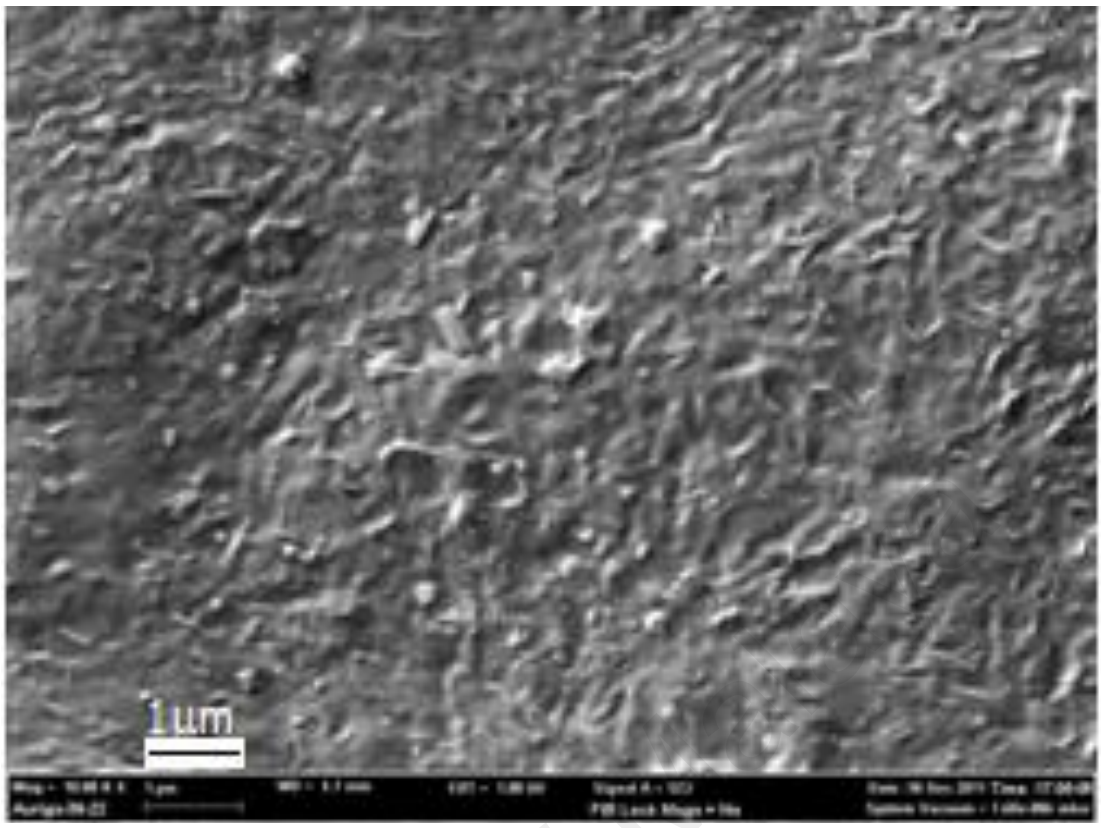

(c)

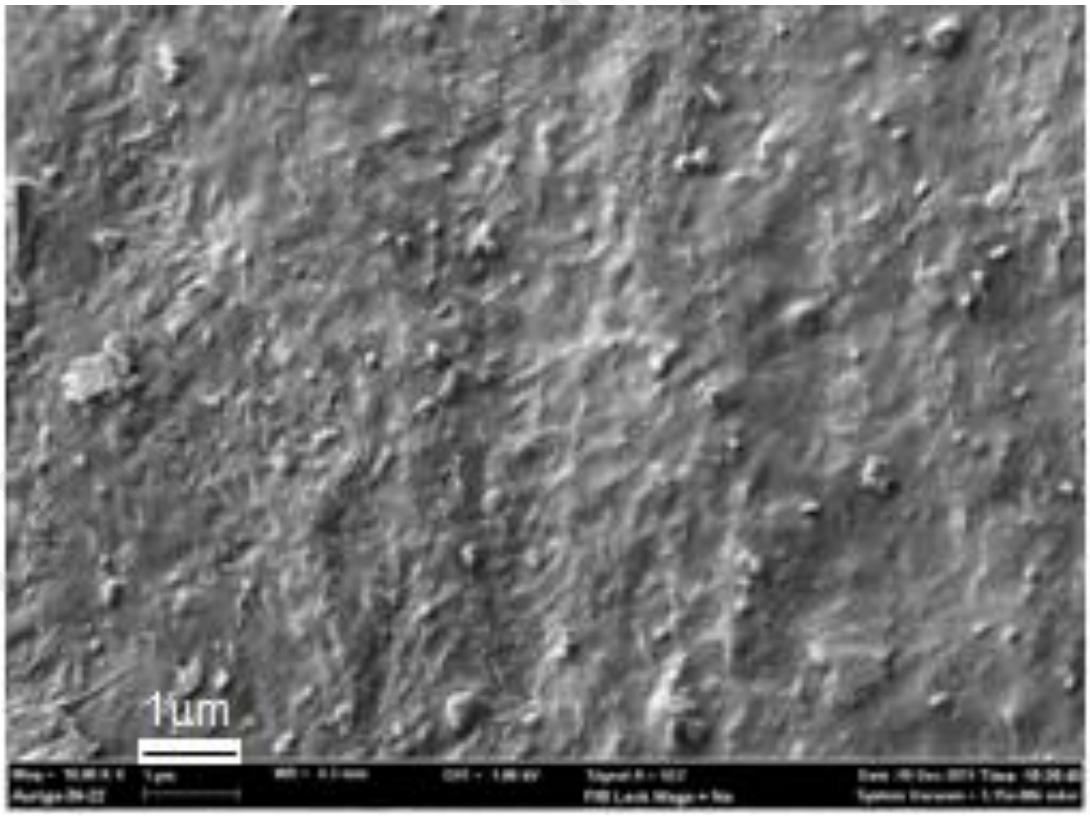

(d)

Figure 4.11, continued: FESEM images of PVA/ Na^{+}-MMT nanocomposite cryogels containing (c) 5 and (d) 10wt. % nanoclay

Figure 4.12 shows the XRD patterns of Na^+-MMT, pure PVA cryogel, and PVA/ Na^+-MMT nanocomposite cryogels containing 1, 5 and 10 wt% nanoclay. At first glance, the existence of nanoclay causes significant changes to be made in crystalline arrangement of the PVA. The XRD pattern of PVA cryogel at 2ɵ = 2–25° showed a broad peak at about 20° that is attributed to the semi-crystalline nature of PVA (Nanda et al. 2010, Bhargav et al. 2009).

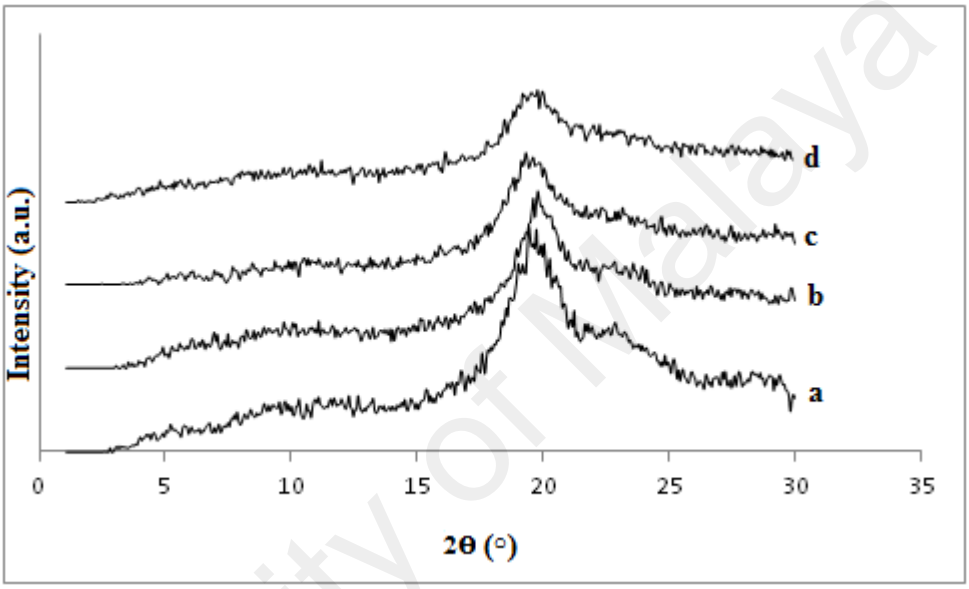

Figure 4.12: XRD patterns of (a) the pure PVA cryogel, (b) PVA/ Na^+-MMT cryogel containing 1, (c) 5, (d) 10 wt. % nanoclay

Physical interactions between PVA and nanoclay layers' surfaces can occur through the hydrogen bonding between Si-O-Si and -OH groups in nanoclay with the -OH groups of PVA chains and their dipole-dipole bonding. According to the XRD results, it can be seen that the presence of Na^+-MMT caused the new crystalline phase and changes on the crystalline domain of the PVA matrix (Strawhecker & Manias, 2000, Jeong et al. 2005). From the literature, MMT has been found having a role as crystalline nucleating agent for PVA chains (Bandi & Schiraldi, 2006, Paranhos et al., 2007). It was also found that the crosslinking with nanoclay leads to a decrease in crystalline phase of PVA, in other words, causes an expansion in amorphous regions. These findings were in good agreement with the swelling results.

DMA thermograms of pure PVA cryogel and the PVA/Na^+-MMT nanocomposite cryogels containing 1, 5 and 10 wt. % nanoclay are shown in Figure 4.13. The figure compares the values of tan δ within the temperature range of -50 to 200 °C for the pure PVA cryogel and three samples of nanocomposite cryogels containing 1, 5 and 10 wt.% nanoclay, respectively. At first glance, it can be seen that the tan δ is decreased as the nanoclay increased. Glass transition temperatures (T_g) can be obtained from the peak position in the tan δ curve. In Figure 4.13, the thermograms show the glass transition temperatures of the pure PVA cryogel, and their nanocomposite cryogels containing 1, 5 and 10 wt. % nanoclay to be 40, 42, 45 and 50 °C respectively. It was found that the tan δ peak positions are shifted toward higher temperatures as the amount of nanoclay increases; this behavior is due to the hydrogen bonding of the -OH and Si-O-Si groups in nanoclay with the -OH groups in PVA chains and hence more chain stiffness being produced. The height of the damping peak in the DMA curve shows the amount of mobility for the polymer molecular chains that leads to damping of energy. The higher the peak, the less restriction there is toward the polymer chain motions. The damping peak height decreases as the nanoclay content increases. The thermograms show that the tan δ values of the pure PVA cryogel, and nanocomposite cryogels containing 1, 5 and 10 wt. % nanoclay to be 0.24, 0.23, 0.19 and 0.17 respectively.This is due to the restriction to the polymer chain motions, created by nanoclay. Also, the peak is shifted toward higher temperatures as the amount of nanoclay increases. This behavior is due to the hydrogen bonding causing to free volume restriction created by crosslinking sites in the polymer network. More crosslinking leads to more free volume restriction and decreasing the mass transfer of water molecules which consequently caused to restriction for sorption and desorption of water.

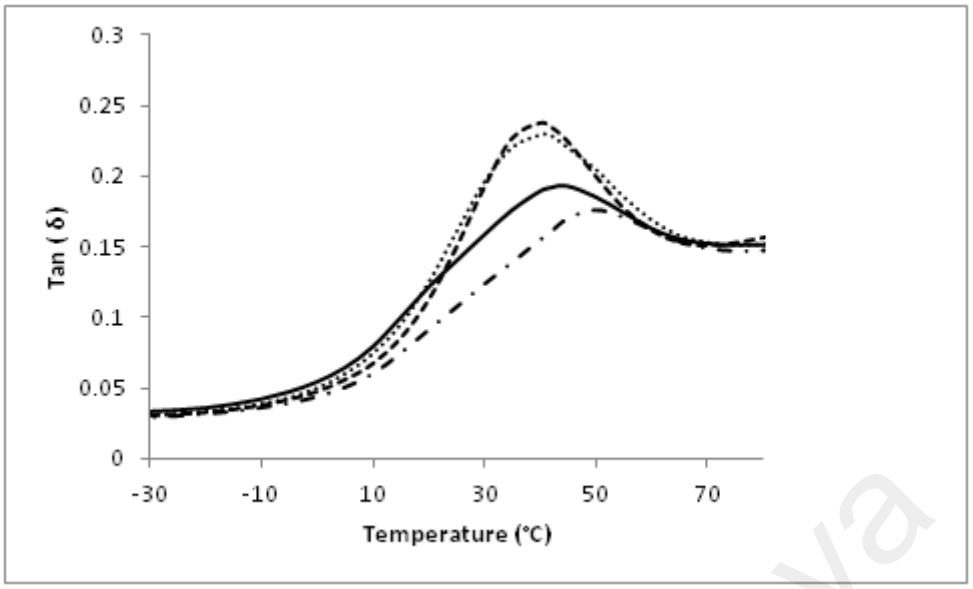

Figure 4.13: Temperature dependence of tan δ for the pure PVA cryogel (- - - - -) and PVA/ Na^{+}-MMT nanocomposite cryogels containing 1(.....), 5 (——) and 10 wt. % nanoclay (– · –)

4.3.2. Effect of nanoclay content on sorption and Barrier behaviors

4.3.2.1. Swelling ratios and Equilibrium water content

Figure 4.14 compares the swelling ratios versus time for the cryogels at 37 °C. It is observed that swelling ratios of nanocomposites are decreased as clay content increases, except for nanocomposites containing 1-2% nanoclay. It can be seen in figure 4.26 that the use of an optimized concentration of nanoclay (1 wt. %) as a crosslinker causes a significant increase in the swelling ratio of cryogels.

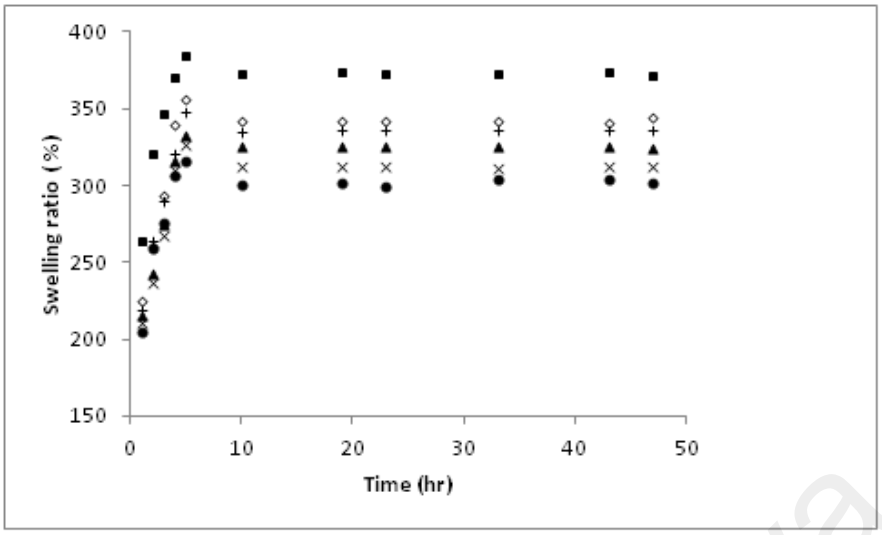

Figure 4.14: Sorption kinetics in deionized water media for the pure PVA cryogel (◇) and PVA/ Na^+-MMT nanocomposite cryogels containing 1(■), 3 (+), 5 (▲), 7 (×) and 10% (●) nanoclay at 37 °C

The results in Figure 4.15 indicate that the EWC of PVA nanocomposite cryogel containing 1% nanoclay at 37 °C has contained the most water content (about 74%) compared to the other nanocomposites.

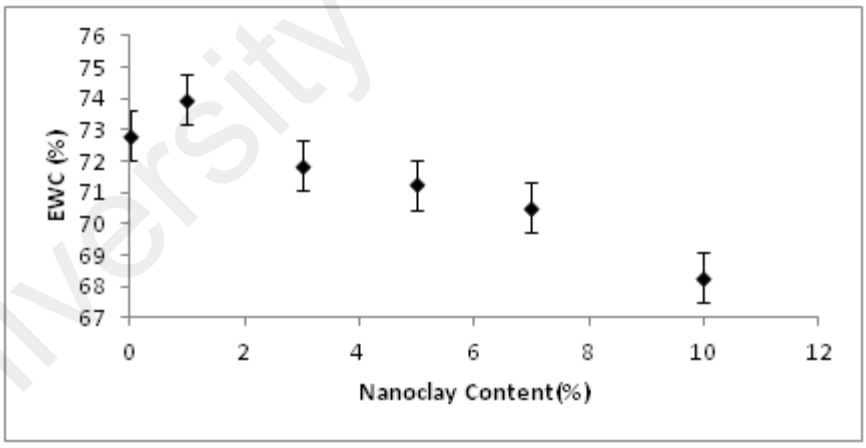

Figure 4.15: Equilibrium water content of the pure PVA cryogel and PVA/ Na^+-MMT nanocomposite cryogels containing 1, 3, 5, 7 and 10% nanoclay at 37 °C

It is observed that Equilibrium water contents and swelling ratios of nanocomposites are decreased as clay content increases, except for nanocomposites containing 1-2% nanoclay. This behavior is due to the Na^+-MMT nanoparticles acting as a crystalline nucleating agent and co-crosslinker for PVA chains (Bandi & Schiraldi, 2006). It means that as more Na^+-MMT nanoclay is incorporated in the PVA matrix, the number of

crosslinking points of the PVA network increases. It can be assumed that increasing the amount of Na^+-MMT leads to the increase in the crosslinking density of the network and more chain entanglement. Increasing the crosslinking causes a decrease in the available pores of the network within nanocomposite cryogels. It means that the available free volume is decreased for the mass transfer of water molecules by incorporating the Na^+-MMT to the PVA matrix. The unexpected behavior of PVA nanocomposite cryogel containing 1-2% nanoclay is attributed to ionic dissociation of Na^+-MMT (polycationic clay) and its strong swelling in the water. The osmotic pressure of counter ions has a predominant effect than the free volume restriction created by crosslinking sites. In contrast, the free volume restriction imposed by more crosslinked sites is the most important factor in reducing the swelling of PVA/Na^+-MMT nanocomposite cryogels containing more than 1-2% nanoclay (Paranhos et al., 2007). Thus, the PVA nanocomposite cryogel having 1% Na^+- MMT is more efficient and suitable for use as wound dressing and skin treatment applications.

4.3.2.2 Barrier properties and Permeation analysis

Figure 4.16 compares the values of the WVTR for pure PVA cryogel and PVA/Na^+-MMT nanocomposite cryogels containing 1, 3, 5, 7 and 10% nanoclay at 37 °C (35% RH). It was observed that the WVTR decreases as the nanoclay content increases; this behavior is due to the increase of the path tortuosity for the penetrating molecules passing through the nanoclay layers. It is known the WVTR for normal skin is 8.5 g/m^2/h and that for injured skin is beyond 11.6 g/m^2/h (Mi et al., 2001). The results in Figure 4.16 indicate that the WVTR of PVA nanocomposite cryogels containing 0–1% nanoclay at 37 °C is within 8.52 g/m^2/h to 11.22 g/m^2/h. Thus, the nanocomposite cryogels having up to 1% nanoclay are suitable for use as wound dressings.

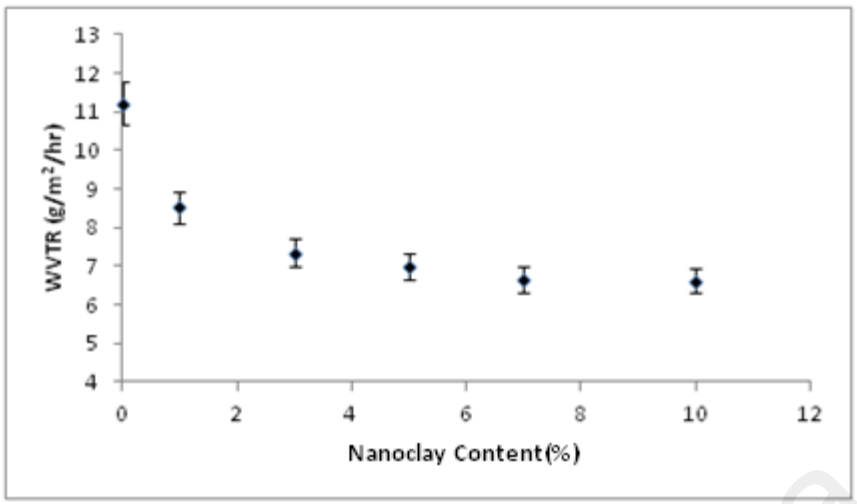

Figure 4.16: Comparison of WVTR for the PVA/ Na^+-MMT nanocomposite cryogels containing 0, 1, 3, 5, 7 and 10% nanoclay at 37 °C

4.3.3 Sorption and desorption kinetics

4.3.3.1. Sorption kinetics in deionized water media

The results show that the sorption kinetics of the pure PVA cryogel and nanocomposite PVA cryogels follows the diffusion mechanism. In order to find a diffusion model for the cryogels, the following equation was fitted to the swelling data (Berens & Hopfenberg, 1978):

$$\frac{W_t}{W_\infty} = kt^n \qquad \textbf{(4-1)}$$

where, w_t and w_∞ are the water intakes at time t and at the equilibrium time; k is a constant and n is the characteristic exponent describing the transport mode of water in the nanocomposites. This can indicate whether it is a Fickian, non-Fickian or anomalous sorption mechanism.When the rate of diffusion is much slower than the relaxation of polymeric chains, the exponent n has a value of 0.5 or below, and the kinetics is Fickian. When the relaxation of polymeric chains is slower than diffusion, the value of n can be a number within the range of 0.5 to 1. This is then described as an anomalous or non-Fickian sorption mechanism. The ‘n’ and ‘k’ can be calculated from the slope and intercepts of the plot of log W_t/W_∞ against log t.

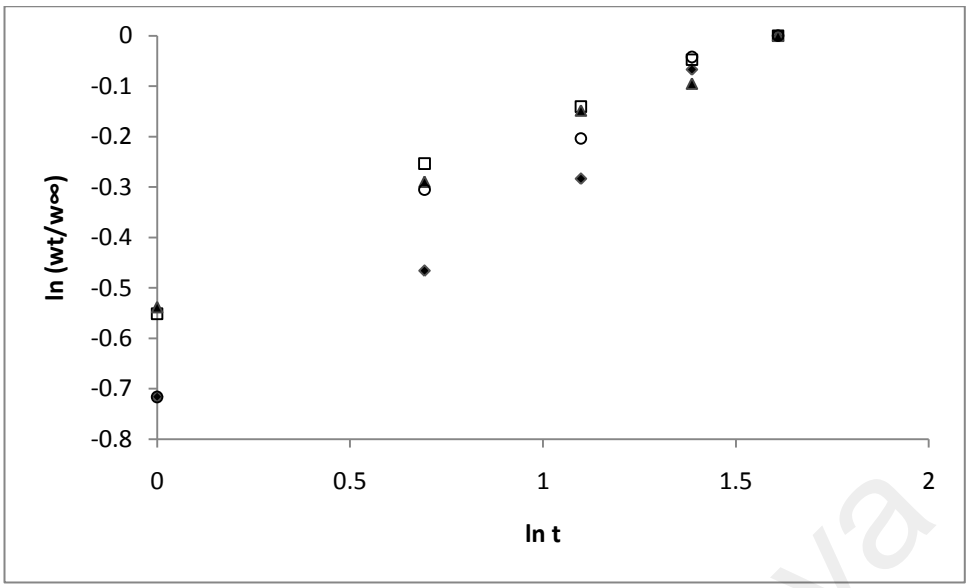

Figure 4.17: Plots of ln (W_t/W_∞) versus ln (t) for the pure PVA cryogel (♦) and PVA/ Na^+-MMT nanocomposite cryogels containing 1 (□), 5 (▲) and 10% (○) nanoclay at 37°C

According to calculated *n* values from plots of ln (W_t/W_∞) versus ln (t) in Figure 4.17, the sorption mechanism of nanocomposite cryogels at 37 °C for pure PVA cryogel and nanocomposite PVA cryogels is Fickian. The sorption kinetics parameters using regression method are summarized in Table 4.2.

Table 4.2: Sorption kinetics characteristics for the pure PVA cryogel and PVA/Na^+-MMT nanocomposite cryogels at 37 °C

Sample	Equation	n	k	R^2
PVA	y= 0.4579 x- 0.7448	0.45	2.11	0.98
1% Na^+-MMT	y= 0.3434 x- 0.5247	0.34	1.69	0.99
3% Na^+-MMT	y= 0.4469 x- 0.7339	0.44	2.08	0.99
5% Na^+-MMT	y= 0.3281 x- 0.5282	0.32	1.69	0.99
7% Na^+-MMT	y= 0.3420 x- 0.5683	0.34	1.76	0.96
10% Na^+-MMT	y= 0.4456 x- 0.6802	0.44	1.97	0.98

4.3.3.2. Kinetics of water desorption for swollen gels

Figure 4.18 shows the ratio of the absolute accumulated amount of the water desorbed at any time *t* to the initial amount of water inside the nanocomposite cryogel (M_t/M_∞)

versus time at 37 °C for the pure PVA cryogel and PVA/Na^+-MMT nanocomposite cryogels containing 1, 5 and 10% nanoclay. It can be seen that increasing the amount of Na^+-MMT leads to a decrease in desorption ability of nanocomposite cryogels. This shows that nanocomposite cryogels containing more nanoclay exhibit a longer duration of desorption. This behavior is related to decreasing the available pores in the network and more crosslinking in the nanocomposite cryogel network. In other words, a higher density of crosslinking causes more chain entanglement in the PVA chains of the nanocomposite cryogels containing more nanoclay. Increasing the degree of crosslinking causes a decrease in the pores of the network and the free volume available in the network. Therefore the mass transfer of water molecules would be restricted during the desorption process. It indicates that the desorption kinetics of PVA/Na^+-MMT nanocomposite cryogels are slower than those of pure PVA cryogels, and that they need more time to reach a certain level of water desorption compared to pure PVA cryogel.

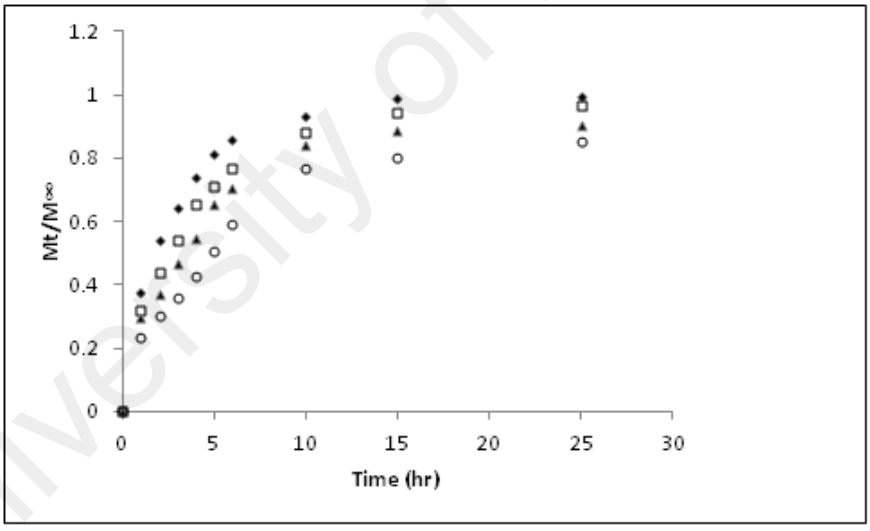

Figure 4.18: Desorption kinetics of the pure PVA cryogel (♦) and PVA/ Na^+-MMT nanocomposite cryogels containing 1(□), 5 (▲), and 10% (○) nanoclay at 37°C

To determine the desorption model, the power law equation (The Ritger-Peppas model) was fitted to the desorption kinetics data (Ritger & Peppas, 1987).

$$\frac{M_t}{M_\infty} = kt^n \qquad \textbf{(4-2)}$$

Where, M_t *and* M_∞ are the absolute accumulated amount of the water desorbed at any time *t* and the initial amount of water inside the nanocomposite cryogel, respectively, *k*

is the desorption characteristic constant and *n* is the characteristic exponent that is indicative of Fickian and non-Fickian or anomalous desorption mechanisms. When the rate of diffusion is much slower than the relaxation of the polymeric chains the exponent *n* has a value of 0.5 or less, and the kinetics is Fickian. If the value of *n* is between 0.5 and 1, it means that the relaxation of polymeric chains is slower than diffusion, and it has an anomalous or non-Fickian desorption mechanism.

The 'n' and 'k' values were obtained from the slope and intercepts of the plot of log M_t/M_∞ against log *t* respectively.

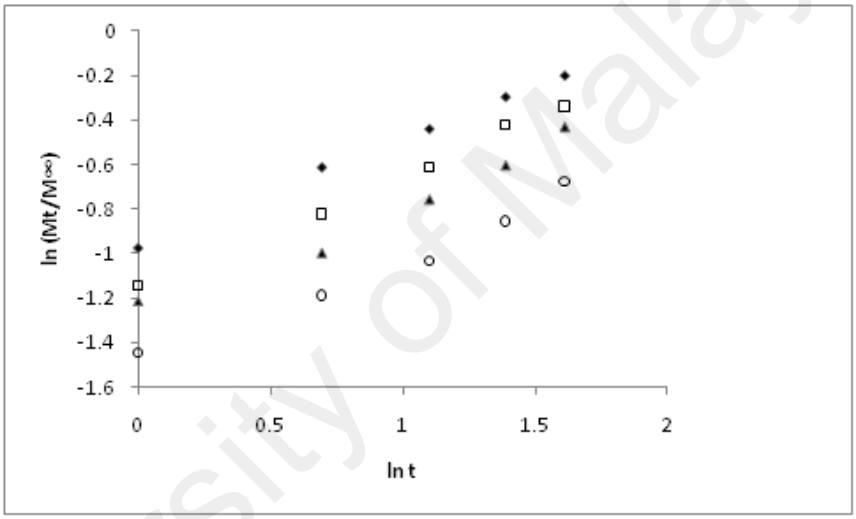

Figure 4.19: Plots of ln ($^{M_t}/_{M_\infty}$) versus ln (t) for pure PVA cryogel (◆) and nanocomposite cryogels with 1(□), 5(▲) and 10 % (○) Na^+-MMT) at 37°C

According to calculated *n* values presented in Figure 4.19, the desorption mechanism of nanocomposite cryogels are Fickian at 37 °C. The desorption kinetics parameters calculated based on regression method are presented in Table 4.3.

Table 4.3: Desorption kinetics characteristics for the pure PVA cryogel and PVA/Na^+-MMT nanocomposite cryogels at 37°C

Sample	Equation	n	k	R^2
PVA	y= 0.4806 x- 0.9694	0.48	2.64	0.99
1% Na^+-MMT	y= 0.5096 x- 1.156	0.50	3.18	0.99
5% Na^+-MMT	y= 0.4863 x- 1.2657	0.49	3.54	0.97
10% Na^+-MMT	y= 0.4612 x- 1.4808	0.46	4.39	0.97

4.4 PART 3: Comparison the Properties of PVA/Na^+-MMT Nanocomposite Hydrogels Prepared by Physical and Physicochemical Cross linking

4.4.1 Stractural characterization and morphology

The FTIR spectra for the pure PVA hydrogel together with those for the physical and the physicochemical crosslinked PVA/MMT hydrogels containing 1% nanoclay are shown in Figure 4.20. The most characteristic bands for PVA are –OH stretching at 3270-3300 cm^{-1}, –CH2 stretching at 2900-2922 cm^{-1} and C–O stretching at 1075-1087cm^{-1}, and $C-H$ bending vibration at around 839 cm^{-1} and 1326cm^{-1}; while those for MMT are Si-O stretching at 1000-1050cm^{-1},. The peak around 1650 cm^{-1} is related to –OH deformation vibrations. The stretching vibration band of C-C-C appeared at 1141-1142 cm^{-1} (Wu & Wisecarver, 1992). This band, which is present in all of the spectra, is attributed to the crystalline domains of PVA. It was also observed that the band 1142 cm^{-1} did not show any shift or any height changes as an effect of the clay, suggesting that there is no interaction between the PVA matrix and MMT nanoparticles in the crystalline domains of PVA.

Interaction between PVA chains and MMT and the presence of hydrogen bonding between the Si-O group of MMT and the –OH group of PVA has reduced the intensity of the Si-O stretching band at 1000-1050 cm^{-1}, while the intensity of the C–O stretching band of PVA at 1075-1087 cm^{-1} decreases due to the presence of MMT (Ogata et al., 1997). Figure 1 shows that the presence of the nanoclay caused a decrease in the intensity of –OH stretching bands at 3000-3600 cm^{-1}. This behavior is due to the weaker hydrogen bonding of the hydroxyl groups of PVA and MMT than interactions between –OH groups of PVA chains. In Figure 4.20, a broader absorption band at 980 to 1100 cm^{-1} can be seen instead of the C-O stretching at about 1100 cm^{-1} in pure PVA, which is related to the formation of C-O (ether) and C-O-C (acetal) bands due to

the crosslinking reaction of PVA with glutaraldehyde (Strawhecker & Manias, 2000). Moreover, duplet absorption with two peaks at about 2800 cm^{-1} to 2900 cm^{-1} is related to the alkyl chain (Reisa, et al., 2006, Hickey & Peppas, 1995). The C–H stretching bands are attributed to aldehydes. These evidences prove the chemical crosslinking of glutaraldehyde with PVA.

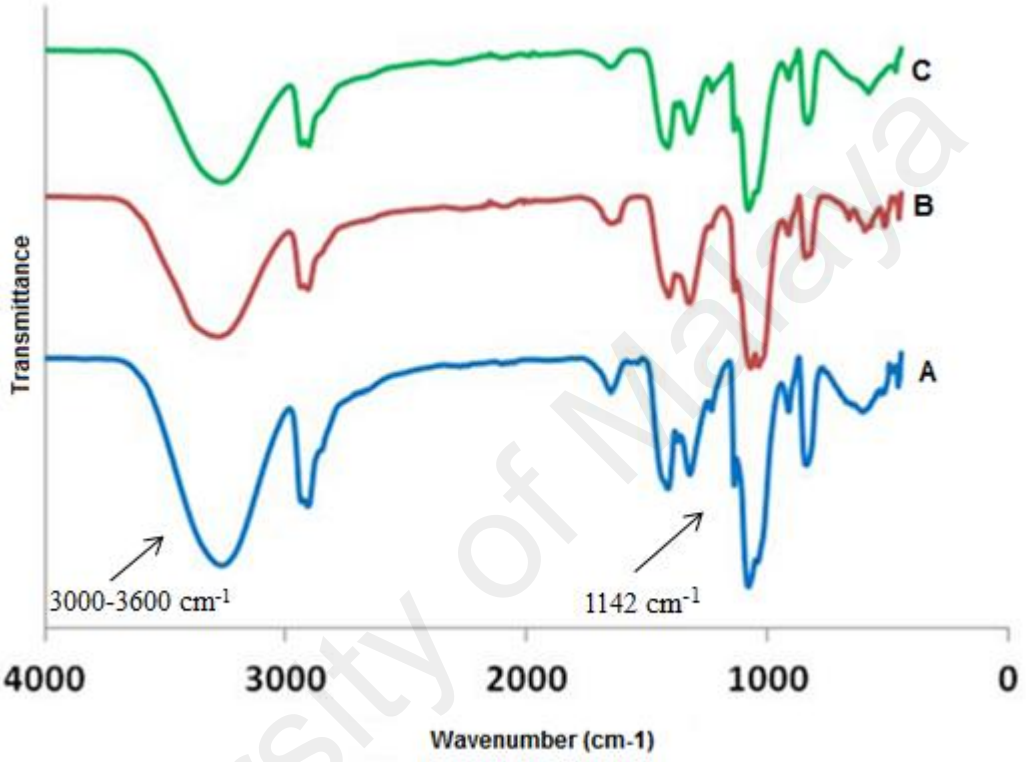

Figure 4.20: FT-IR spectra of the pure PVA hydrogel (A), physical (B) and physicochemical (C) crosslinked PVA/MMT hydrogel containing 1% nanoclay.

Figure 4.21 shows the X-ray diffraction patterns (XRD) of MMT, physical crosslinked pure PVA hydrogel, physicochemical crosslinked pure PVA hydrogel, physical crosslinked PVA/MMT hydrogel containing 1% nanoclay and physicochemical crosslinked PVA/MMT hydrogel containing 1% nanoclay. At first glance, the presence of glutaraldehyde causes a significant decrease in the crystalline domain of the PVA so there is an increase in its amorphous phase. In the case of physicochemical crosslinked PVA/MMT nanocomposite hydrogel containing 1% nanoclay, the crystallinity and

crystallite sizes of the PVA were observed to decrease and the amorphous fraction increased. In addition, the pattern did not show any diffraction peaks in 2Θ = 2–10° (7.12°) and 28.40°, but there was a shift at 2Θ = 19.69° (*d*-spacing= 4.57 Å) towards a smaller angle of about 19.12° (*d*-spacing= 4.70Å). These results indicate that the increase in the distance between the platelets is due to the presence of PVA chains that are intercalated and exfoliated into the individual silicate layers of Na-MMT. It appears that these phenomena were due to the effective dispersion of Na-MMT into the PVA matrix by sonication and also the high compatibility of PVA chains and Na-MMT. The chemical and physical interactions between the PVA and nanoclay layers can occur through hydrogen bonding of the OH and Si-O-Si groups of nanoclay with the OH groups of PVA chains and their dipole-dipole bonding. Therefore, strong interactions, good compatibility and high dispersion of the components can lead to the exfoliation. These results have been confirmed by TEM.

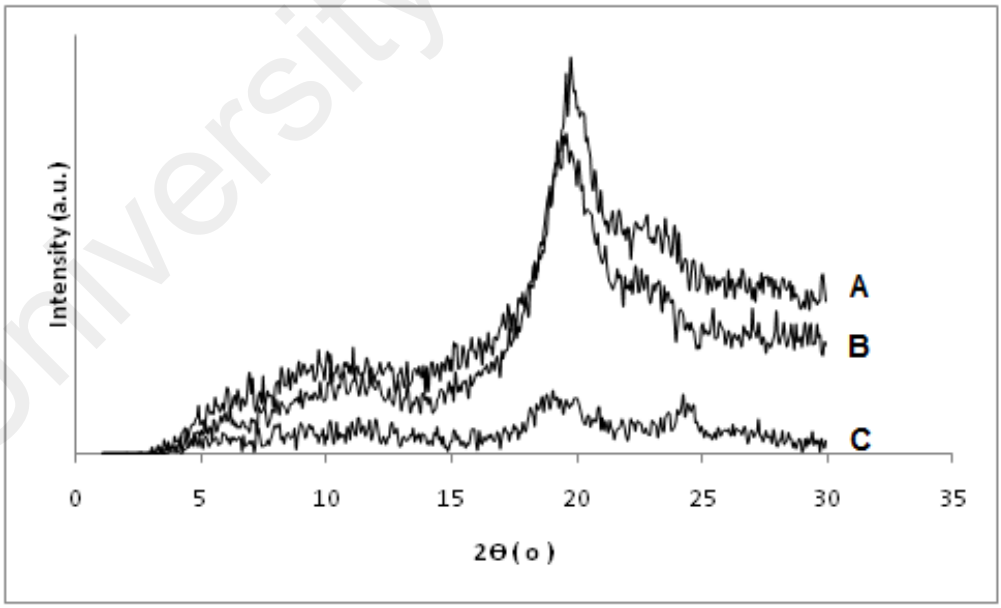

Figure 4.21: XRD patterns of the pure PVA hydrogel (A), physical crosslinked (B) and physicochemical crosslinked (C) PVA/MMT hydrogel containing 1% nanoclay.

The morphological image of the nanocomposite hydrogels was generated by FESEM. Sample preparation was done and they were fractured and mounted to expose the bulk before examination. FESEM images of the physicochemical crosslinked PVA nanocomposite in Figure 4.22 show that the matrix has connected pores. As can be seen, the nanoclay MMT (white color) is homogeneously incorporated into the PVA matrix and the morphology of physicochemical crosslinked PVA nanocomposites becomes more porous than that of pure PVA. This was due to the effective dispersion of MMT into the PVA matrix by sonication and also the good compatibility of PVA and MMT. It was also found that physicochemical crosslinking leads to an increase in the number and size of pores, causing a decrease of the PVA crystalline phase, and resulting in growth of the amorphous phase. These observations were in agreement with the XRD and swelling results.

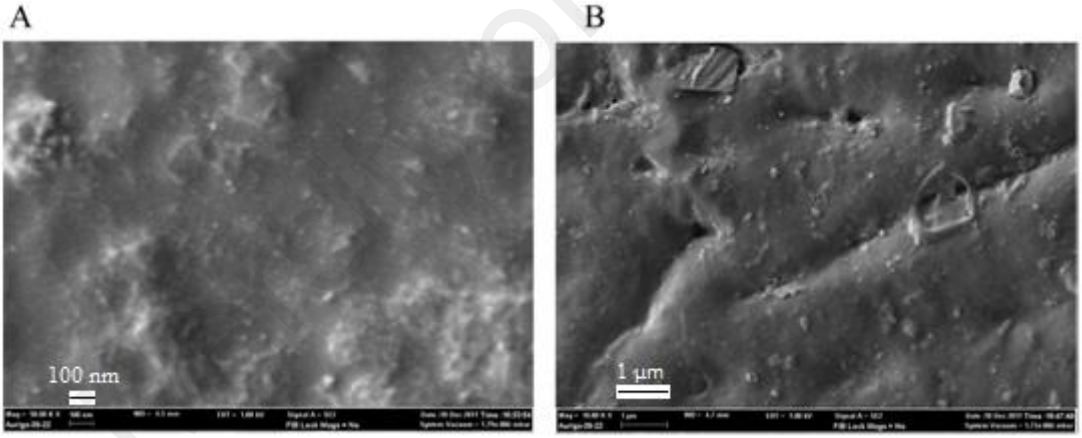

Figure 4.22: FESEM images of (A) physical and (B) physicochemical crosslinked PVA/MMT nanocomposites.

4.4.2 Thermal and mechanical analysis

The TGA thermographs of the pure PVA hydrogel and the PVA/Na-MMT nanocomposite hydrogel containing 1% nanoclay are shown in Figure 4.23. The first region in the TGA curve appeared in the temperature range of 80-150°C, and is due to the evaporation of H_2O molecules being physical or chemical bounded to the PVA molecules. The weight loss of the nanocomposites in this area was approximately 2.9–

3.55 wt. %. The second region was formed as a result of the matrix side-chain degradation of the PVA/Na-MMT nanocomposite at about 250-390°C; the weight loss in this area was around 50–70 wt. %. The third region is related to breaking of the C-C polymer backbone of the PVA/Na-MMT nanocomposite at about 440°C, with a total weight loss of approximately 75-95 wt. % at 600°C. In general, decomposition of the pure PVA and PVA/Na-MMT nanocomposite occurred in the temperature range of about 200 to 500°C; above 600°C, the curve became flat for the PVA/Na-MMT nanocomposite due to the presence of inorganic residue. The results showed that the thermal decomposition of the PVA/Na-MMT containing 1% nanoclay shifts slightly toward the higher temperature, in comparison with pure PVA. It can be concluded that the presence of nanoclay leads to the thermal stability of PVA due to hydrogen bonding between the OH and Si-O-Si groups of nanoclay with the OH groups in PVA chains and their dipole-dipole bonding due to the chemical and physical interactions between the PVA chains and nanoclay layers.

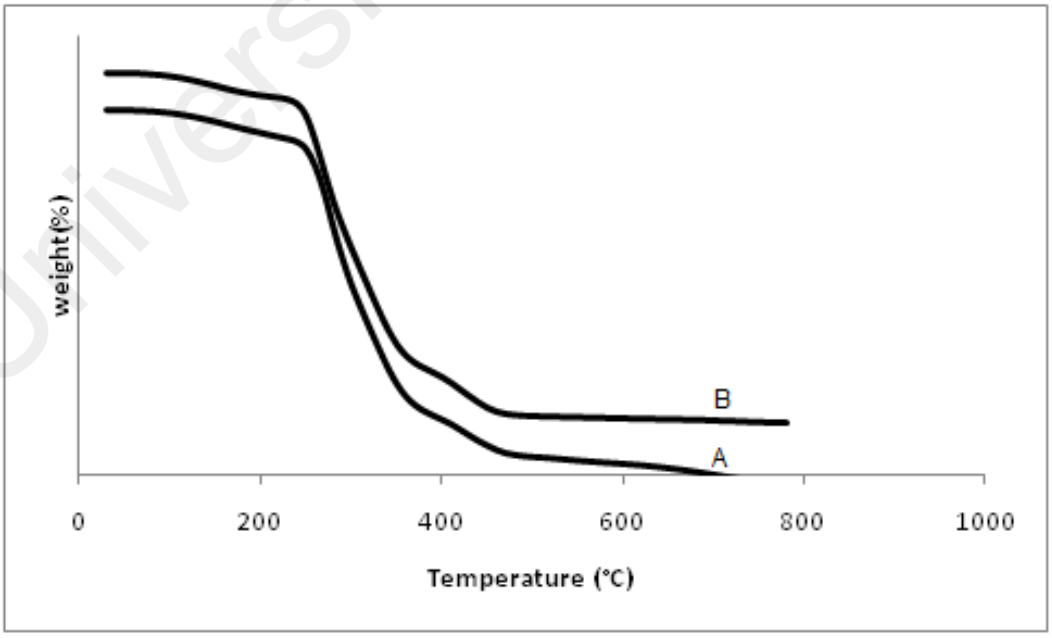

Figure 4.23: TGA curves for the pure PVA hydrogel (A) and physicochemical crosslinked PVA/MMT nanocomposite (B).

Figure 4.24 shows the DSC thermograms of the PVA/MMT nanocomposite hydrogel containing 1% nanoclay (physical crosslinking and physicochemical crosslinking using the freezing-thawing process and glutaraldehyde) and the pure PVA hydrogel. In Figure 4.24, the pure PVA hydrogel exhibits an endothermic peak at 223°C, corresponding to the melting temperature of the pure PVA hydrogel. This peak is shifted to 217°C and 205°C for the physical and physicochemical crosslinked nanocomposite hydrogel containing 1% nanoclay, respectively. This provides evidence for the role of nanoclay as a nucleating agent in the crystallization of PVA chains. Two new melting peaks appeared at lower temperatures for physicochemical crosslinked nanocomposite hydrogels containing 1% nanoclay. These peaks at 159°C and 180°C were broader, showing a change between the semi-crystalline phase and the amorphous phase due to crosslinking by glutaraldehyde. It was also found that physicochemical crosslinking led to a decrease in crystallinity due to a change between a semi-crystalline phase and an amorphous phase; these results were in agreement with the observations from XRD.

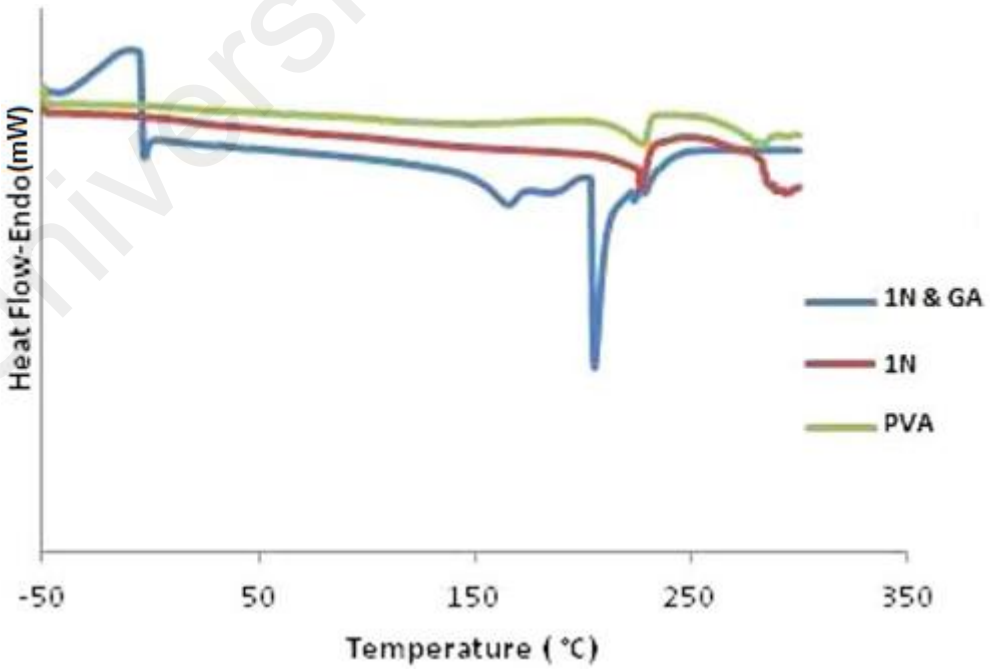

Figure 4.24: DSC curves for the pure PVA hydrogel, and their physical (1N) and physicochemical (1N & GA) crosslinked nanocomposite hydrogels.

Dynamic mechanical analysis (DMA) can be applied for measuring the response of a polymeric material such as a nanocomposite to cyclic deformation as a function of temperature. The deformation modes are usually tension, torsion and three-point bending (flexure) type deformations. There are three main parameters as a result of DMA: (i) the elastic (storage) modulus, (E'), corresponding to the elastic response to the deformation; (ii) the viscous (loss) modulus, (E"), corresponding to the plastic response to the deformation, and (iii) tan δ, which is the (E"/E') ratio. Tan δ can be used to calculate the glass transition temperature (T_g).

The DMA thermograms of the pure PVA hydrogel and the physical and physicochemical crosslinked PVA/Na^+-MMT nanocomposite hydrogels containing 1% nanoclay are shown in Figure 4.25. This figure compares the values of the mechanical loss tangent, tan δ, in the temperature range of -50 to 200°C for the hydrogels. It can be observed that tan δ is decreased for the physical crosslinked nanocomposite hydrogel containing 1% nanoclay. The peak of the tan δ curve shows the glass transition temperatures (T_g). In Figure 4.25, the thermogram shows the glass transition temperatures of the pure PVA hydrogel, the physical and physicochemical crosslinked nanocomposite hydrogels containing 1% nanoclay at 40, 40 and 35°C, respectively. The peak was shifted towards lower temperatures for the physicochemical crosslinked hydrogel due to an increase in the network porosity. This observation was in good agreement with the DSC results. The results indicated that the T_g values obtained by this method were higher than those obtained by DSC.

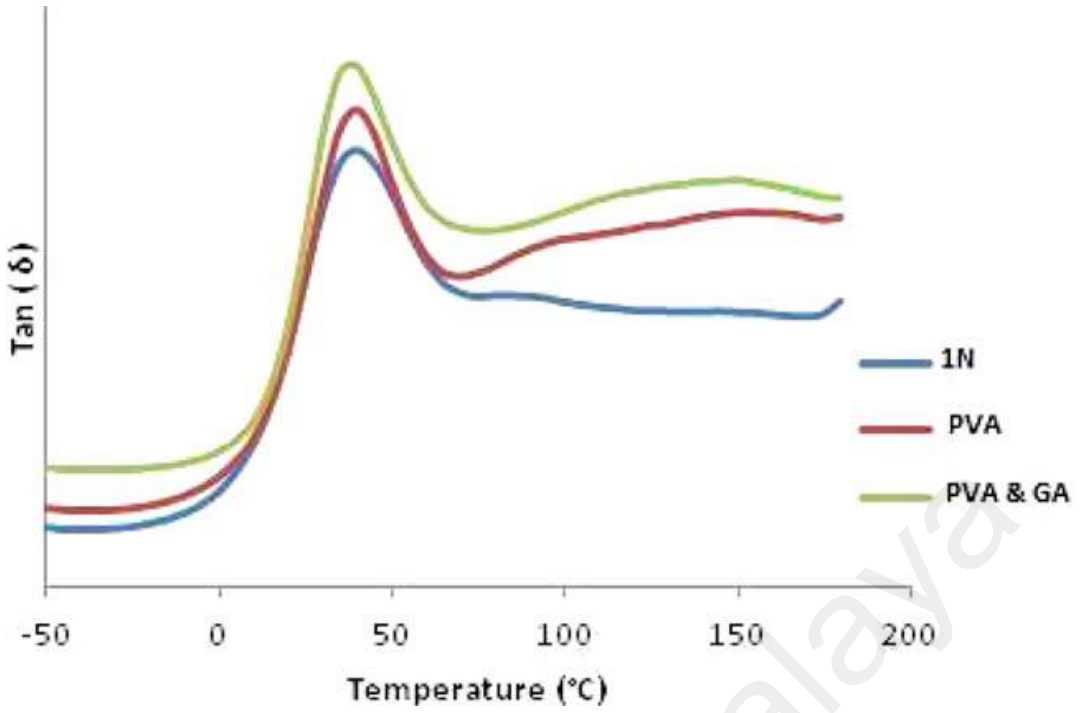

Figure 4.25: Temperature dependence of tan d for the pure PVA hydrogel, their physical (1N) and physicochemical (PVA & GA) cross linked PVA/MMT nanocomposite hydrogels.

Figure 4.26 shows the hardness data of pure PVA hydrogel, and the physical and physicochemical crosslinked nanocomposite hydrogels containing 1%, 3%, 5%, 7% and 10% nanoclay. Following the addition of 1, 3, 5, 7 and 10% by weight of Na-MMT, it was observed that the hardness of the pure PVA hydrogel increased to 23.81, 40.48, 66.67, 92.86 and 109.52%, respectively, due to physical crosslinking, whereas the PVA hardness grew to 22.33, 33.98, 49.51, 66.99 and 80.58%, respectively, because of physicochemical crosslinking. In comparison of the hardness of the physical crosslinked and the physicochemical crosslinked nanocomposite hydrogels, it was found that the hardness of the physicochemical crosslinked nanocomposite hydrogels containing 1%, 3%, 5%, 7% and 10% nanoclay was increased by 22.62, 21.15, 16.95, 10, 6.17 and 5.68%, respectively, compared to the corresponding physical crosslinked hydrogels. These results show the function of nanoclay content and the chemical crosslinking formed by glutaraldehyde following the freezing-thawing process, that make more chain

entanglements and crosslinking, causing the hardness of the polymer network to be increased. Also, the results are due to the chemical and physical interactions between the PVA and nanoclay layer surfaces occurring through hydrogen bonding between the OH and Si-O-Si groups in nanoclay with the OH groups in PVA chains and their dipole-dipole bonding.

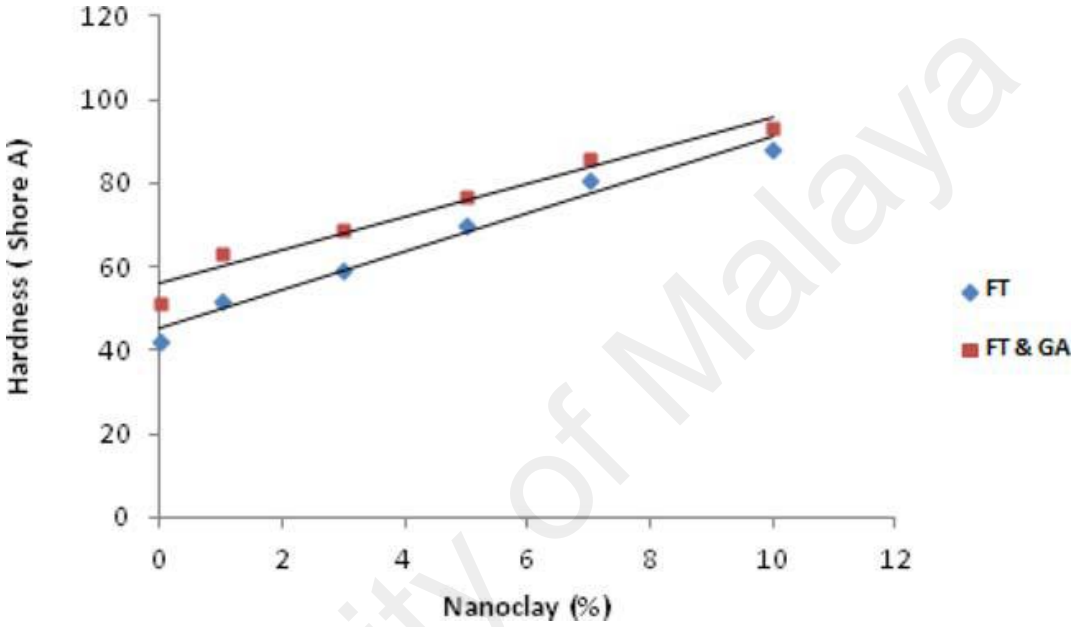

Figure 4.26: Hardness of physical (FT) and physicochemical (FT & GA) crosslinked PVA/MMT nanocomposite hydrogels versus nanoclay content, those for pure PVA hydrogels being at 0% nanoclay.

Barrier properties

Figure 4.27 compares the values of WVTR for pure PVA hydrogel with those for the physical and physicochemical crosslinked PVA/Na^+-MMT nanocomposite hydrogels containing 1% nanoclay at 25°C (43%, RH), 37°C (35%, RH) and 50°C (18%, RH). It was found that WVTR was increased by elevating the temperature, because the kinetic energy of the molecules increases at higher temperatures. On the other hand, it was found that WVTR was increased by using the glutaraldehyde as a chemical crosslinker but conversely, it was shown to decrease when using the 1% nanoclay; these behaviors are due to the increase in the network porosity of physicochemical crosslinked

nanocomposites and the increasing path tortuosity for the penetrant molecules that pass through the nanoclay layers. It has been found that the WVTR for normal skin is 8.5 g/m^2/h and that for injured skin is above 11.6 g/m^2/h (Ostuka et al., 2011). The results in Figure 4.27 show that the WVTR at 37°C for pure PVA hydrogel, and physical and physicochemical crosslinked PVA/Na$^+$-MMT nanocomposite hydrogels containing 1% nanoclay are 8.5, 10.15 and 11.22 g/m^2/h, respectively. Therefore, the hydrogels are suitable for wound dressing.

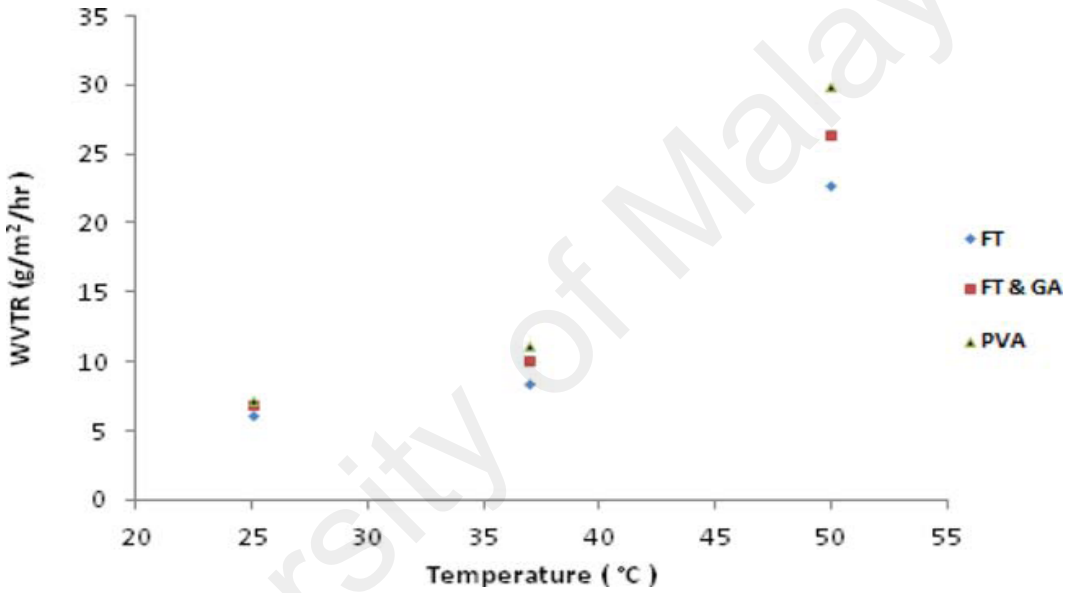

Figure 4.27: Comparison of WVTR for the pure PVA hydrogel, and physical (FT) and physicochemical (FT & GA) crosslinked PVA/MMT nanocomposite hydrogels at 25°C, 37°C, and 50 °C.

4. 4. 3 Sorption and desorption behavior

4. 4. 3. 1 Water sorption kinetics in deionized water media

In Figure 4.28, the swelling ratio curves versus time at 25°C for the physical crosslinked PVA/Na$^+$-MMT nanocomposite hydrogel containing 1% nanoclay are compared with those for physicochemical crosslinked PVA/Na$^+$-MMT nanocomposite hydrogels containing 1% nanoclay. It can be seen that the use of an optimized concentration of glutaraldehyde as a chemical crosslinker causes a significant increase in the swelling

ratio for physicochemical crosslinked hydrogels. This behavior is related to the increased number of available pores in the nanocomposite network and means that the available free volume is increased for the mass transfer of water molecules in physicochemical crosslinked hydrogels.

The results show that the swelling kinetics of both the physical crosslinked and the physicochemical crosslinked nanocomposite hydrogels obey the diffusion mechanism and need the diffusion time to reach an equilibrium level for water sorption.

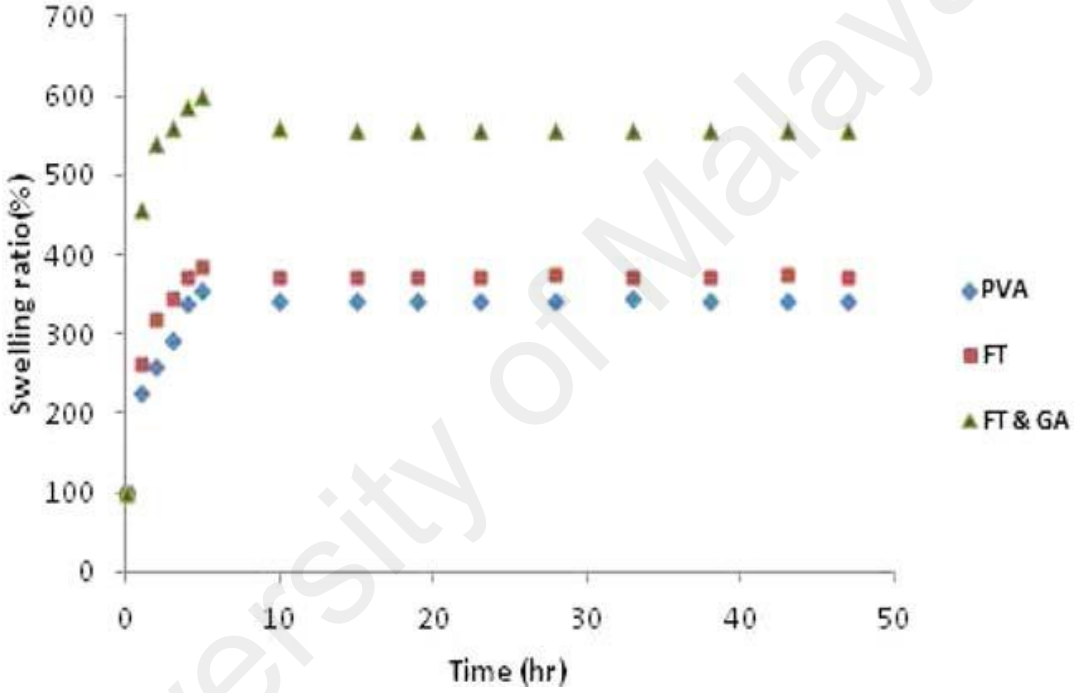

.

Figure 4.28: Comparison of water sorption kinetics for pure PVA hydrogel and its nanocomposites: physical (FT) and physicochemical (FT & GA) crosslinked hydrogels at 25C.

To determine the diffusion model, the equation (4-1) was fitted to the sorption kinetics data for the hydrogels (Chang et al., 2003).

If the exponent n has a value of 0.5 or less, and the rate of diffusion is much slower than the relaxation of polymeric chains, the kinetics is Fickian. On the contrary, when the relaxation of polymeric chains is slower than the diffusion and the value of n lies between 0.5 and 1, then the sorption mechanism is anomalous or non-Fickian. The values of n and k can be obtained from the slope and intercepts of the plot of $\ln W_t / W_\infty$

versus ln t. It is indicated from Figure 4.29 that, according to calculated n values, the sorption mechanism of both nanocomposite hydrogels is Fickian at 25°C.

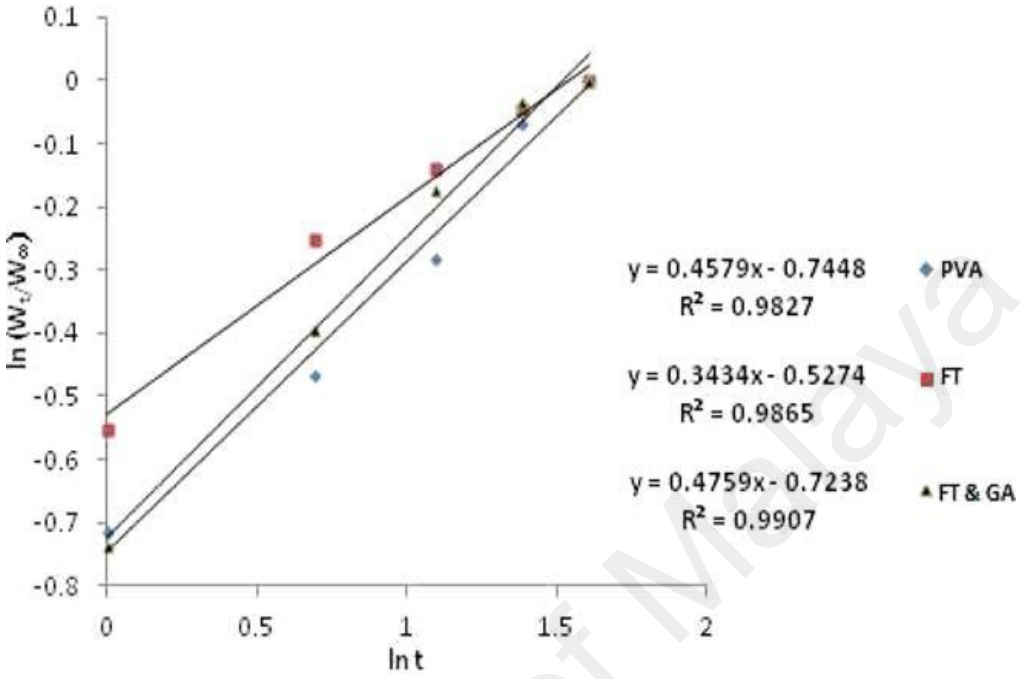

Figure 4.29: Plots of ln (W_t/W_∞) versus ln (t) for pure PVA hydrogel and its nanocomposites: physical (F-T) and physicochemical (FT & GA) crosslinked hydrogels at 25°C.

4.4.3.2 Water desorption kinetics of swollen gels

Figure 4.30 compares the absolute accumulated amount of the water desorbed at any time, t, and the initial amount of water inside the nanocomposite hydrogel ($^{M_t}/_{M_\infty}$) versus time at 25°C for the PVA/Na-MMT nanocomposite hydrogels containing 1% nanoclay (physical and physicochemical crosslinked). It can be observed that desorption ability of nanocomposite hydrogels decreases by using glutaraldehyde as a chemical crosslinker followed by the freezing-thawing process. In other words, the physicochemical crosslinked nanocomposite hydrogel exhibits longer desorption periods. This behavior is related to the increase in the number of available pores in the network and more crosslinking in the physicochemical crosslinked nanocomposite hydrogel. Therefore, the pores could entrap the water molecules and the mass transfer of

water molecules during desorption would be restricted. This indicates that the desorption kinetics of the physicochemical crosslinked nanocomposite hydrogel is slower than that of the physical crosslinked hydrogel, meaning that it needs more time to reach a certain level of water desorption.

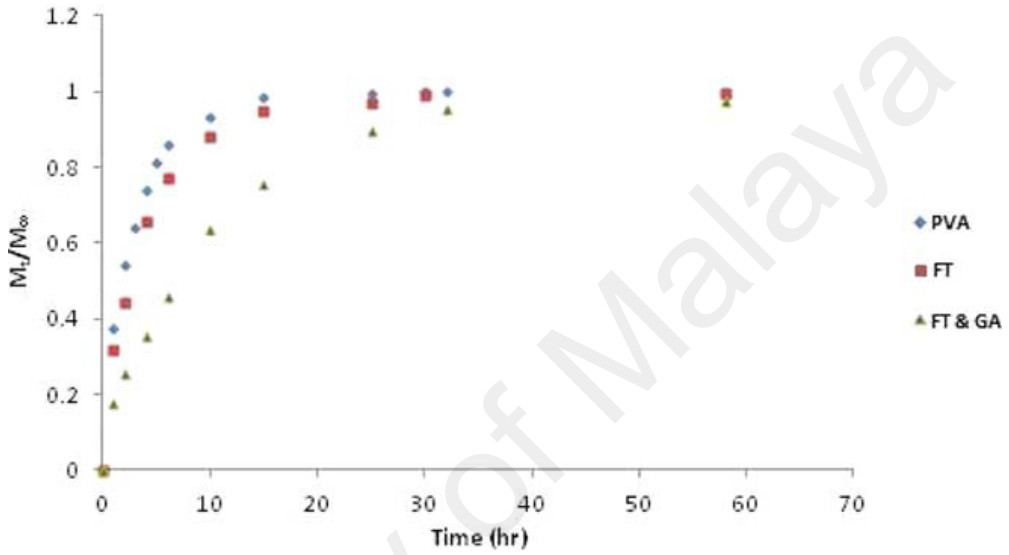

Figure 4.30: Comparison of desorption kinetics for pure PVA hydrogel and its nanocomposites: physical (FT) and physicochemical (FT & GA) crosslinked hydrogels at 25°C.

In order to identify a diffusion model, the kinetic data for the hydrogels desorption was fitted into a power law equation (4-2) named Ritger-Peppas model (Blumstein, 1965). When the rate of diffusion is much slower than the relaxation of polymeric chains, the exponent n would be a value of 0.5 or less, and the kinetics is Fickian. If the relaxation of polymeric chains is slower than diffusion, the value of n is between 0.5 and 1, and the desorption mechanism would be anomalous (non-Fickian).

The values for 'n' and 'k' can be calculated from the slope and intercepts of the plot of ln M_t/M_∞ against ln t, respectively. According to the calculated n values from the plot of ln M_t/M_∞ versus ln t in Figure 4.31, it can be seen that the desorption mechanism of both nanocomposite hydrogels is Fickian at 25°C.

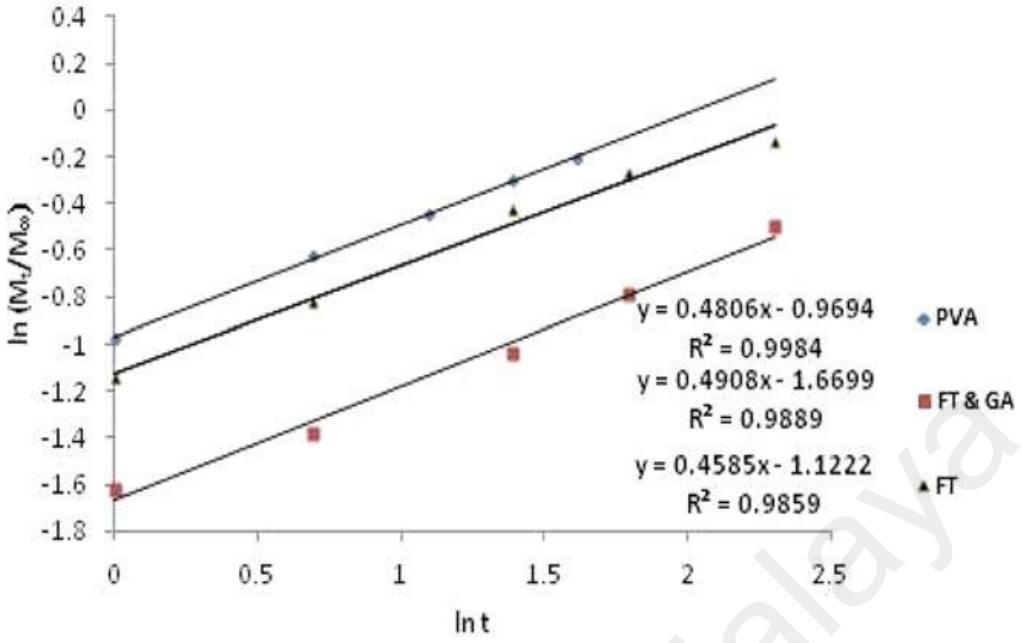

Figure 4.31: Plots of ln (Mt/M_∞) versus ln (t) for pure PVA hydrogel and its nanocomposites: physical (F-T) and physicochemical (FT & GA) crosslinked hydrogels at 25°C.

4.5 PART 4: Fabrication of (PVA/Na^+-MMT/ PVP-Iodine) nanocomposite hydrogel system and study of its in vitro antibacterial properties for wound dressing application

4.5.1 Equilibrium content and Equilibrium time of pure PVA hydrogel and its nanocomposite hydrogel at 37 °C in physiological saline solution

Figure 4.32 compares the values of the equilibrium content versus time for pure PVA cryogel and PVA/Na^+-MMT nanocomposite cryogel containing 1% nanoclay at 37 °C in physiological saline solution. At first glance it was observed that the equilibrium content of the PVA/Na^+-MMT nanocomposite cryogel containing 1 % nanoclay, has decreased up to 3.1% and its equilibrium time has prolonged up to 7.7 % compared to the pure PVA cryogel. This behavior is due to the differences in the ionic osmotic pressures between the nanocomposite hydrogel and the swelling medium compared to pure PVA hydrogel that can be lead to the reduction in the equilibrium content of the PVA/Na^+-MMT nanocomposite cryogel containing 1 % nanoclay. However the results indicate that the equilibrium content of PVA/Na^+-MMT nanocomposite cryogel containing 1 % nanoclay at the steady equilibrium time is 65 % that is within the acceptable range for biomedical applications such as skin treatment and wound dressing (Mitchell et al., 1945; Von zglinicki et al., 1993).

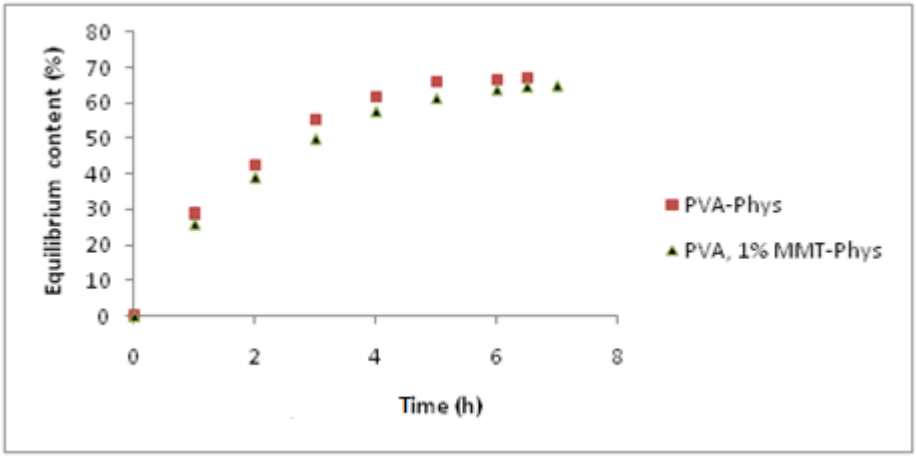

Figure 4.32: Equilibrium content versus time for pure PVA cryogel and PVA/Na+-MMT nanocomposite cryogel containing 1 % nanoclay at 37 °C in physiological saline solution

4.5.2 Desorption of physiological saline solution (PSS)

Figure 4.33 shows the absolute residual of physiological saline solution (PSS) amount versus time at 37 °C for the pure PVA cryogel and PVA/Na^+-MMT nanocomposite cryogel containing 1% nanoclay. It can be seen that presence of the Na^+-MMT nanoclay leads to a decrease in desorption ability of nanocomposite cryogels. This shows that nanocomposite cryogels containing nanoclay exhibits a higher ability to holding of the physiological solution. This behavior is related to decreasing the available pores in the network and more crosslinking in the nanocomposite cryogel network. In other words, a higher density of crosslinking causes more entanglement in the PVA chains of the nanocomposite cryogel. Increasing the degree of crosslinking causes a decrease in the pores of the network and the free volume available in the network. In addition increase of the path tortuosity for the penetrating molecules passing through the nanoclay layers leads to the decrease in desorption ability and in contrast increase in holding ability of physiological solution by nanocomposite cryogel. Therefore the mass transfer of molecules would be restricted during the desorption process. It indicates that the desorption kinetics of PVA/Na^+-MMT nanocomposite cryogels are slower than those of

pure PVA cryogels, and that they need more time to reach a certain level of water desorption compared to pure PVA cryogel.

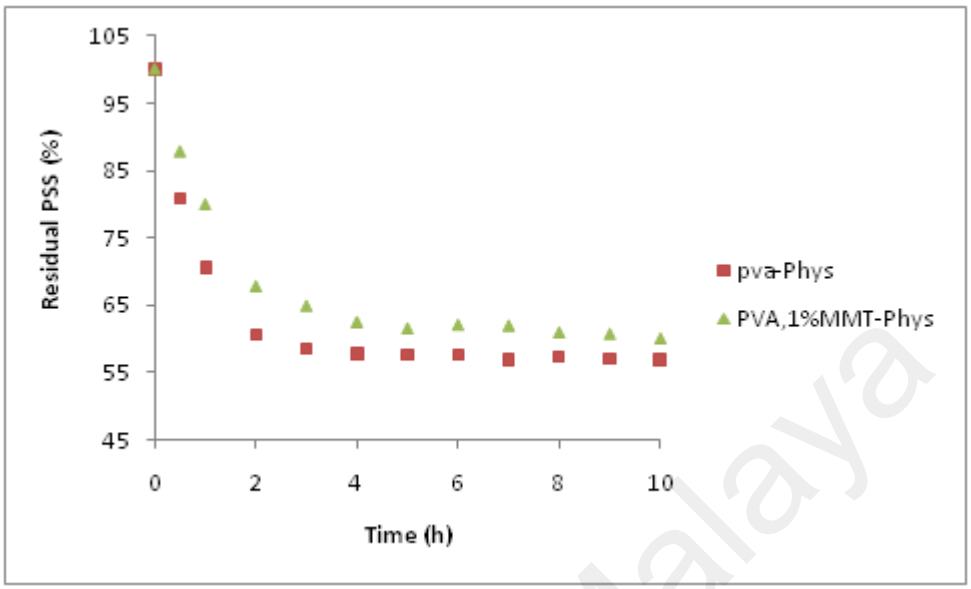

Figure 4.33: Residual of physiological saline solution (PSS) amount versus time at 37 °C for the pure PVA cryogel and PVA/Na^+-MMT nanocomposite cryogel containing 1% nanoclay

4. 5. 3 Effect of nanoclay content on release of antibacterial agent

Figure 4.34 compares the antibacterial activity zone of pure PVA cryogel and PVA/Na^+-MMT nanocomposite cryogel containing 1, 3, 5, 7, and 10 % nanoclay loaded by PVP- Iodin as an antibacterial agent at 37 °C after 24 hours. At first glance it is observed that the antibacterial activity of nanocomposites against Escherichia coli (E-coli); as a gram negative bacteria and Staphylococcus aureus (S- aureus); as a gram positive bacteria are decreased as clay content increases, except for nanocomposite containing 1% nanoclay. This behavior is due to the Na^+-MMT nanoparticles acting as a crystalline nucleating agent and co-crosslinker for PVA chains (Bandi & Schiraldi, 2006). It means that as more Na^+-MMT nanoclay is incorporated in the PVA matrix, the number of crosslinking points of the PVA network increases. It can be assumed that increasing the content of Na^+-MMT leads to the increase in the crosslinking density of the network and more chain entanglement. Increasing the crosslinking density causes a

decrease in the network of available pores in nanocomposite cryogels. It means that the available free volume is decreased for the mass transfer of antibacterial agent molecules by incorporating the Na^+-MMT to the PVA matrix. The results in Figure 4.34 indicate that the antibacterial activity of PVA nanocomposite cryogel containing 1% nanoclay has the most compared to the other nanocomposites and also to pure PVA cryogel. The unexpected behavior of PVA nanocomposite cryogel containing 1% nanoclay is attributed to ionic dissociation of Na^+-MMT (polycationic clay) and its strong swelling in the water and also more loading of PVP-Iodin that consequently leads to a larger release of antibacterial agent. The osmotic pressure of counter ions has a predominant effect than the free volume restriction created by crosslinking sites. In contrast, the free volume restriction imposed by more crosslinked sites is the most important factor in reducing the swelling of PVA/Na^+-MMT nanocomposite cryogels containing more than 1 % nanoclay (Paranhos et al., 2007).

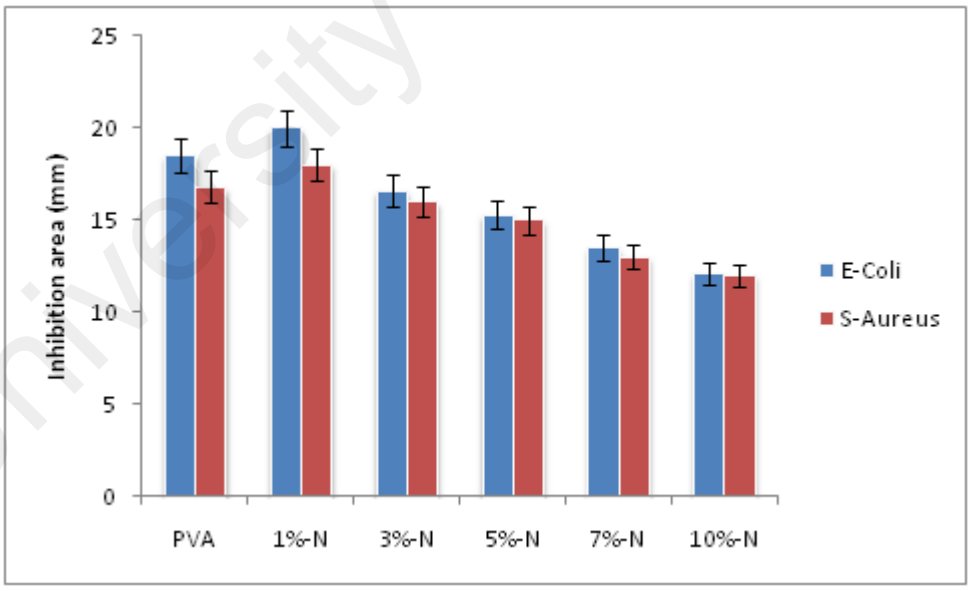

Figure 4.34: Antibacterial activity of pure PVA cryogel and PVA/Na^+-MMT nanocomposite cryogels containing 1, 3, 5, 7, and 10 % nanoclay loaded by PVP- Iodin at 37 °C after 24 hours

Figures 4.34, 4.35 and 4.36 also show that the pure PVA cryogel and PVA/Na^+-MMT nanocomposite cryogels have good sensitivity against the two types of bacteria but they are more sensitive to E-coli as a gram negative bacteria compared to the S- aureus as a gram positive bacteria. The figure 4.37 compares the antibacterial activity of the nanocomposite cryegels containing same nanoclay content against E. coli. and S-aureus bacteria.The results are summarized in table 4.4.

Table 4.4 Antibacterial activity of pure PVA cryogel and PVA/Na^+-MMT nanocomposite cryogels against gram positive and gram negative bacteria

Sample	**Inhibition zone (mm)**	
	gram positive (S-aurouse)	gram negative **(**E-coli)
PVA	16.8	18.5
1 % Na^+-MMT	18	20
3 % Na^+-MMT	16	16.6
5 % Na^+-MMT	15	15.3
7 % Na^+-MMT	13	13.5
10 % Na^+-MMT	12	12.1

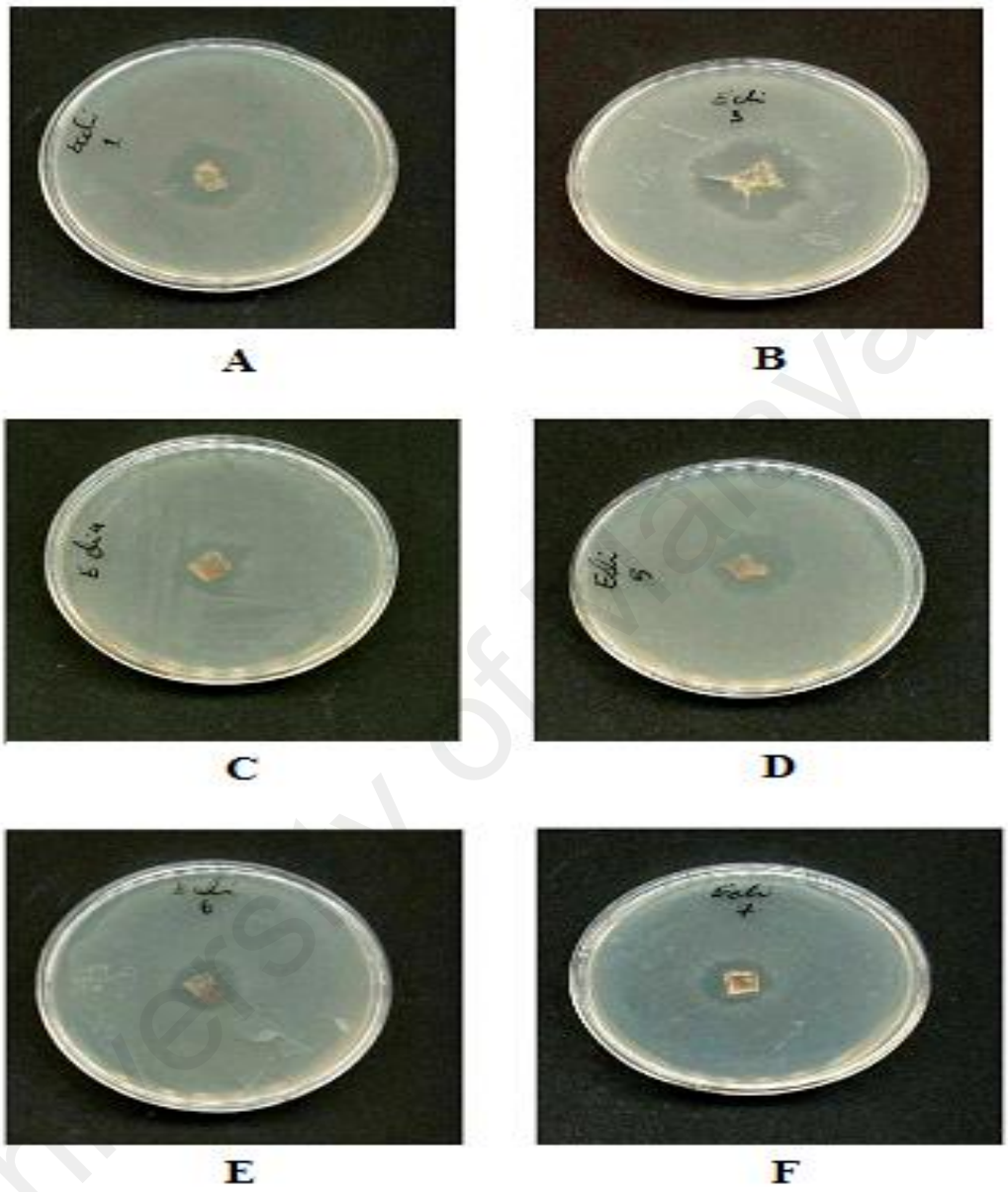

Figur 4.35: The antibacterial activity of the pure PVA cryogel (A), and nanocomposite cryegels containing 1 (B), 3 (C), 5(D), 7 (E) and 10 (F) wt. % nanoclay against E. coli. Bacteria, based on their inhibition zone.

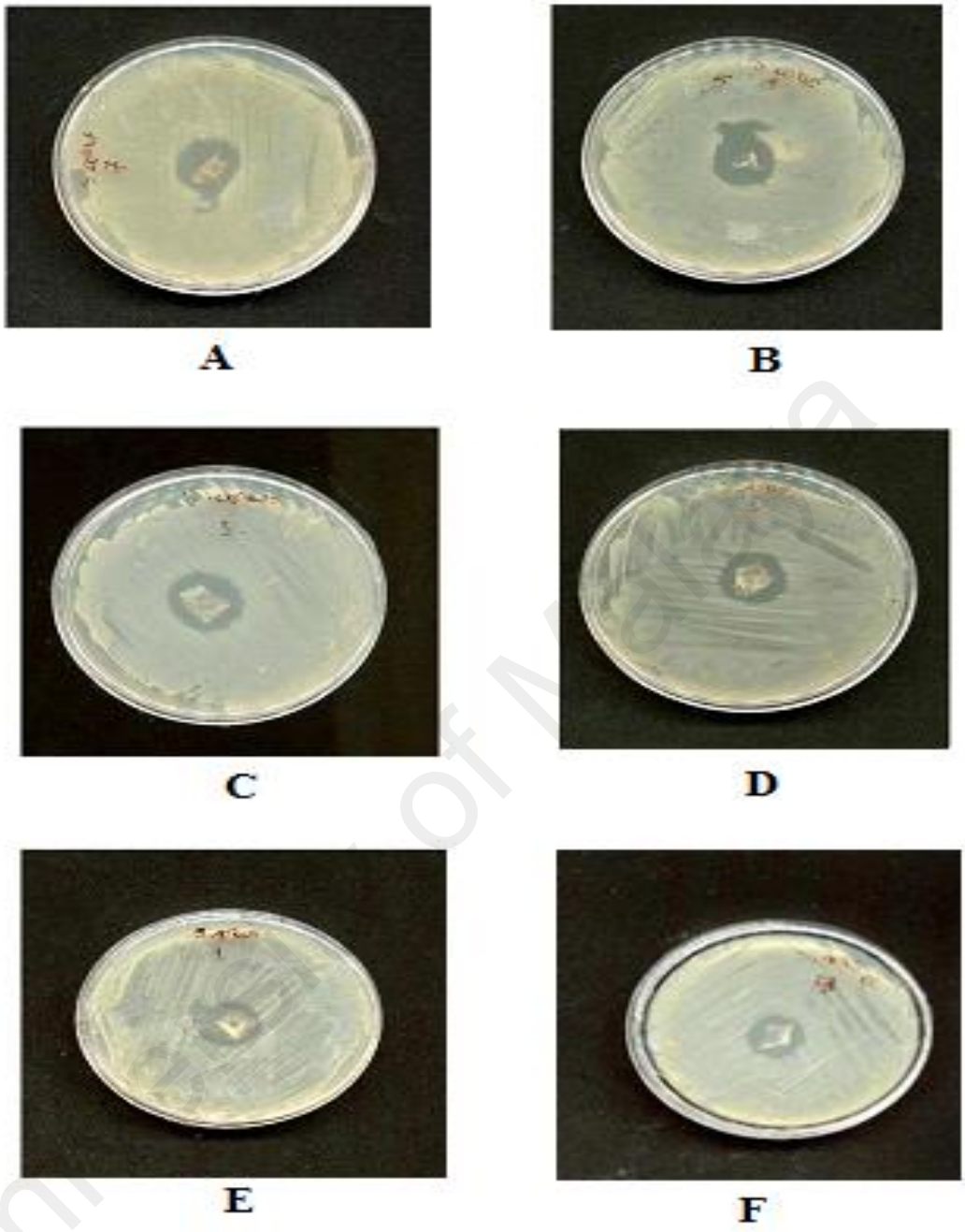

Figur 4.36: The antibacterial activity of the pure PVA cryogel (A), and nanocomposite cryegels containing 1 (B), 3 (C), 5(D), 7 (E) and 10 (F) wt. % nanoclay against S-aureus bacteria, based on their inhibition zone.

S- aureus **E- coli**

Figur 4.37: Comparison the antibacterial activity of nanocomposite cryogels containing the same amount of nanoclay against E. coli. and S-aureus bacteria.

CHAPTER 5: CONCLUSION AND RECOMMENDATION FOR FUTUR WORKS

5.1 CONCLUSION

In the present thesis in order to obtain nontoxic, tissue-compatible and efficient hydrogels for biomedical applications, a new series of nanocomposite hydrogels were prepared by a cyclic freeze-thaw process (physical method), using polyvinyl alcohol (PVA) as polymer matrix and 0–10 wt.% of hydrophilic natural Na-montmorillonite (Na^+-MMT), free from any modification, as nanocomposite aggregates. Investigations were performed on the nanostructure, morphology, barrier and swelling properties of the nanocomposites and it was shown that Na^+-MMT can act as a co-crosslinker. According to the results, the swelling characteristics of nanocomposite cryogels increases with the nanoclay content up to 1-2 wt.% nanoclay, after that they start to decrease uniformly. In contrast, the water removal from cryogels decreased and its time of removal prolonged on increasing the nanoclay content. These results are in good agreement with FESEM findings. Based on the results of WVTR measurements, it is concluded that the barrier properties of the nanocomposites can be improved by increasing the nanoclay content. According to the kinetics results, the sorption and desorption mechanisms for all of the nanocomposites are Fickian. The results of EWC (above 60%) and WVTR (at about 8.5 g/m2/h) are within the acceptable range for biomedical applications. Thus achieving the optimal swelling and WVTR properties of nanocomposite cryogels that required for desired applications, the nanoclay content and ultrasonic mixing conditions can be optimized. As the results show an optimum amount of nanoclay content for maximized EWC was observed at 1%, also it was found that the optimum range of nanoclay for having optimum WVTR is up to 1% nanoclay. Thus it is concluded that the optimum amount of nanoclay that is most suitable for wound healing

can be the same as nanoclay concentration (1 wt. %) that makes both properties optimum.

In order to study the effect of physical crosslinking and physicochemical crosslinking on the structure, morphology, thermal, mechanical, swelling and deswelling properties of nanocomposite hydrogels, a novel PVA nanocomposite hydrogel was synthesized by a physicochemical method and its behaviors were compared with those of a PVA nanocomposite hydrogel obtained using the physical method. The XRD and TEM results showed that Na^{+}- MMT nanoparticles formed intercalated and exfoliated structures with PVA matrix which act as crystallization nuclei and co-crosslinkers. Interactions between the silanol groups in MMT and the hydroxyl groups of PVA chains was evaluated by FT-IR, DSC, and XRD. Using 0.04% of glutaraldehyde as a chemical crosslinker in PVA caused the polymer crystallinity to decrease and its amorphous phase to increase; these results were confirmed by XRD and DSC. The FESEM and DMA results showed that chemical crosslinking with glutaraldehyde followed by physical crosslinking in a physicochemical crosslinked nanocomposite hydrogel led to an increase in the number of pores in the nanocomposite network. The swelling, water vapor transmission rate, and hardness measurements showed that the physicochemical crosslinked nanocomposite hydrogel has a higher swelling ratio, lower cumulative water loss, higher hardness, and WVTR than the physical crosslinked nanocomposite hydrogel. These behaviors are due to the high dispersion of nanoclay by sonication and controlled chemical crosslinking of PVA hydrogel containing 1wt. % nanoclay. The sorption and desorption kinetics in both methods were based on diffusion mechanisms and obey the Fickian model. According to the results obtained it is possible to optimize the unmodified nanoclay content, sonication process and controlled chemical crosslinking followed by physical crosslinking to obtain suitable products for biomedical applications, especially those with higher swelling capacity.

In order to investigate the possibility of biomedical applications of polyvinyl alcohol/Na^+-Montmorillonite (PVA/Na^+-MMT) nanocomposite hydrogels, the swelling behavior and swelling kinetics of PVA/Na^+-MMT nanocomposite hydrogels in deionized water and in the physiological saline solution at 37 ºC were examined. The isothermal kinetic curves of the swelling of a PVA/Na^+-MMT nanocomposite hydrogel in deionized water and in physiological saline solution at 37 ºC were determined. The differences in the ionic osmotic pressures between the nanocomposite hydrogel and the swelling medium can be lead to the reduction in the equilibrium water content and residual water of the nanocomposite hydrogel in the physiological saline solution compared to swelling in deionized water. Moreover, the increase of the initial swelling rate in the physiological saline solution compared to swelling in deionized water might be explained by an increased density of charges at the network and so increasing the affinity of the hydrogel network towards the water molecules. The obtained results were within the acceptable range for biomedical applications such as skin treatment and wound dressing.

The effect of nanoclay content on release of antibacterial agent for loaded hydrogels by poly (vinyl pyrrolidone) – Iodine (PVP- Iodine) was also investigated in vitro and found to be dependent on crosslinking amount due to interaction between PVA and nanoclay. It was concluded that nanocomposite hydrogel based on PVA/ Na^+-MMT loaded by PVP- Iodine has antibacterial effects against Escherichia coli (E-Coli); as a gram negative bacteria and Staphylococcus aureus (S-Aureus); as a gram positive bacteria respectively. Moreover, it is non toxic and suitable for wound dressing and skin treatment.

Therefore, it was summed up that according to the results, upon using the polyvinyl alcohol and unmodified Na^+-montmorillonite, controlled physical or physicochemical crosslinking, optimized the unmodified Na^+-MMT nanoclay content and suitable

ultrasonic mixing, it is possible to prepare a non toxic, biocompatible and efficient hydrogel. Also it was concluded that regarding to the in vitro sorption and desorption of this nanocomposite in physiological saline solution as well as in vitro their antibacterial properties, it can be considered being a good candidate for biomedical applications such as; wound dressing, skin treatment and tissue engineering.

5.2 RECOMMENDATION FOR FUTUR WORKS

The following recommendations are suggested for future works:

The research experiments in ionic media

The swelling behavior of hydrogels and their swelling kinetics are important in different media based on their applications. Due to effects of ions on the swelling behavior of hydrogels, the influence of electrolyte media on the swelling behavior of hydrogels can be investigated.

Considering other kinetics models

In this research sorption and desorption kinetics for both physical and physicochemical methods of preparation were investigated based on diffusion mechanism and it is found that they obey the Fickian model in the deionized water and physiological solution. Other kinetic mechanism and models can be considered for the behavior study of the hydrogels, based on their applications.

Optimization of these hydrogel properties for other biomedical applications

PVA/ Na^{+}-MMT nanocomposite hydrogels that prepared in this research have many desired properties such as; biocompatible, nontoxic, non-carcinogenic and inert in body fluids. In addition these hydrogels have desirable mechanical, swelling and optical properties which make them suitable for example as drug delivery applications.

REFERENCES

Abd El-Mohdy, H.L. (2013). Radiation synthesis of nanosilver/polyvinyl alcohol/cellulose acetate/gelatin hydrogels for wound dressing. *J. Polym. Res.*, 20: 177–188.

Abdurrahmanoglu, S., Can, V. & Okay, O. (2008). Equilibrium swelling behavior and elastic properties of polymer-clay nanocomposite hydrogels. *J. Appl. Polym. Sci.*, 109: 3714-3724

Adoor, S.G., Sairam, M., Manjeshwar, L.S., Raju, K.V.S.N. & Aminabhavi, T.M. (2006). Sodium montmorillonite clay loaded novel mixed matrix membranes of poly(vinyl alcohol) for pervaporation dehydration of aqueous mixtures of isopropanol and 1,4-dioxane. *J Membr Sci*, 285:182–95.

Ajji, Z. (2005). Preparation of poly (vinyl alcohol) hydrogels containing citric or succinic acid using gamma radiation. *Radiat Phys Chem*, 74: 36-41

Al, E., Guclu, G., Iyim,T.B., Emik, S. & Ozgumus, S. (2008). Synthesis and properties of starch-graft-acrylic acid/Namontmorillonite superabsorbent nanocomposite hydrogels. *J. Appl. Polym. Sci.*, 109: 16-22.

Alexandre,. M. & Dubois, P. (2000). Polymer layered silicate nanocomposites: preparation, properties and uses of a new class of materials.*Mater Sci Eng*, 28(1-2); 1-63.

Andrews, R. & Wisenberger, M.C. (2004). Carbon nanotube polymer composites *Curr Opin Solid State Mater Sci*, 8: 31-7.

Aranda, P. & Ruiz-Hitzky, E. (1992). Poly(ethylene oxide)- silicate intercalation materials. *Chem Mater*, 4: 1395-1403.

Avadhani, C.V. & Chujo, Y. (1997). Polyimide–Silica Gel Hybrids Containing Metal Salts: Preparation via the Sol–Gel Reaction. *Appl Organomet Chem.*, 11(2): 153-161.

Aymonier, C., Bortzmeyer, D. & Thomann, R.M. Lhaupt. (2003). Poly (methyl methacrylate)/palladium nanocomposites: synthesis and characterization of the morphological, thermomechanical, and thermal properties. *Chem Mater*, 15 (25): 4874-4878.

Backfolk,K., Rosenholm, J.B., Husband, J.& Eklund, D. (2006). the influence of surface chemical properties of kaolin surfaces on the adsorption of poly (vinyl alcohol). *Colloid Surf* A, 275: 133.

Bafna, A., Beaucage, G., Mirabella, F., & Mehata, S. (2002). Shear induced orientation and associated property enhancement in polymer/clay nanocomposites. *Proc Nanocomposites, September 23–25. San Diego, California, USA, ECM Publication.*

Bafna, A., Beaucage, G., Mirabella, F., & Mehata, S. (2003). 3D hierarchical orientation in polymer-clay nanocomposite films. *Polymer*, 44: 1103-15.

Bandi, S., & Schiraldi, D.A. (2006). Glass Transition Behavior of Clay/Poly(vinyl alcohol) Composites. *Macromolecules*, 39: 6537.

Becker, O., Varley, R., & Simon, G., (2002). Morphology, thermal relaxation and mechanical properties of layered silicate nanocomposites based upon highfunctionality epoxy resins. *Polymer*, 43: 4365-73.

Benamer, S., Mahlous, M., Boukrif, A., Masouri, B.& Larbi, Y. S. (2006). Synthesis and Characterisation of Hydrogels Based on Poly(Vinyl Pyrrolidone). *Nucl Instrum Methods Phys Res B*,248: 284-290.

Berens A. R., & Hopfenberg, H. B. (1978). Diffusion and relaxation in glassy polymer powders: 2. Separation of diffusion and relaxation parameters. *Polymer*, 19: 489.

Bhajantri,S. F., Ravindachary, V., Harisha, A., Crasta, V., Nayak, S.P. & Poojary B. (2006). Microstructural studies on BaCl2 doped poly (vinyl alcohol). *Polymer*, 47: 3598.

Bhargav, P. B., Mohan, V. M., Sharma, A. K. & Rao, V. (2007). Structural and electrical studies of sodium iodide doped poly(vinyl alcohol) polymer electrolyte films for their application in electrochemical cells. *Ionics*, 13, 173–178.

Bhargav, PB., Mohan, VM., Sharma, AK., & Rao, VVRN. (2009). Investigations on electrical properties of (PVA:NaF) Polymer electrolytes for electrochemical cell applications. *Current Applied Physics*, 9 (1): 165–171.

Bignotti, F., Sartore, L., Penco, M., Ramorino, G. & Peroni, I. (2004). Effect of montmorillonite on the properties of thermosensitive poly(N-isopropylacrylamide) composite hydrogels. *J Appl Polym Sci,* 93:1964.

Biswas,M.& Sinha Ray, S. (2001). Recent Progress in Synthesis and Evaluation of Polymer-Montmorillonite Nanocomposites. *Adv Polym Sci*, 155: 167-221.

Blumstein, A. (1965). Polymerization of adsorbed monolayers: II. Thermal degradation of the inserted polymers. *J Polym Sci A,* 3:2665–73.

Caro, V., Paik Sung, C.S. & Merrill, E.W. (1976). Reaction of hexamethylene diisocyanate with poly(vinyl alcohol) films for biomedical applications. *J Appl Polym Sci,* 20:3241.

Carrado, K.A. & Xu, L.Q. (1998). In situ synthesis of polymer-clay nanocomposites from silicate gels. *Chemistry of Materials*, 10(5): 1440-1445.

Carrado, K.A., Thiyagarajan, P. & Elder, D.L. (1996). Polyvinyl alcohol-clay complexes formed by direct synthesis. *Clay Clay Miner*, 44: 506.

Cha, Won –Ill., Hyon,Suong-Hyu., Graiver, Daniel., & Ikada, Yoshito. (1993). Sticky poly (vinyl Alcohol) Hydrogels. *J.of.Appl. Poly. Sci,* 47:339-343.

Chang, J., Jang, T., Ihn, KJ., Lee, W., & Sur, G.S. (2003). Poly (vinyl alcohol) nanocomposites with different clays: Pristine clays and organoclays. *J. Appl. Polym. Sci*, 90: 3208-3214.

Chang, J.H., Seo, B.S., & Hwang, D.H. (2002). An exfoliation of organoclay in thermotropic liquid crystalline polyester nanocomposites.*Polymer*, 43: 2969-74.

Chen, DH,, Leu, J.C. & Huang TC. (1994). Transport and hydrolysis of urea in a reactor–separator combining an anion exchange membrane and immobilized urease. *J Chem Technol Biotechnol.,* 61:351–357.

Chen, J.S., Poliks, M.D., Ober, C.K., Zhang, Y., Wiesner, U. & Giannelis, E.P. (2002). Study of the interlayer expansion mechanism and thermal-mechanical properties of surface-initiated epoxy nanocomposites. *Polymer*, 43: 4895-904.

Chiellini,E., Corti, A., Politi, B. & Solaro, R. (2000). Adsorption/Desorption of Polyvinyl Alcohol on Solid Substrates and Relevant Biodegradation. *J Polym Environ*, 8: 67-79

Christie, M.H., Jennifer, E.S & Nikolaos, A.P. (2000). Diffusional characteristics of freeze/thawed poly(vinyl alcohol) hydrogels: Applications to protein controlled release from multilaminate devices. *European Journal of Pharmaceutics and Biopharmaceutics*. 49: 161-165.

Churochkina, N.A., Starodoubtsev. S.G. & Khokhlov, A.R. (1998). Swelling and Collapse of the Gel Composite Based on Neutral and Slightly Charged Poly (acrylamide) Gels Containing Na-Montmorilonite. *plym. GELS. Networks*, 6: 205-215.

Cohen, Y., Ramon, O., Kopelman, I.J., & Mizrahi, S.J. (1992). Characterization of inhomogeneous polyacrylamide hydrogels. *Polym Sci Polym Phys Ed*, 30: 1055-1067. 33.

Coviello, T., Matricardi, P., Marianecci, C., & Alhaique, F. (2007). Polysaccharide hydrogels for modified release formulations. *J. Controlled Release*, 119: 5-24.

Davis, C.H., Mathias, L.J., Gilman, J.W., Schiraldi, D.A., Shields, J.R., Trulove, P., Sutto, T.E., & Delong, H.C. (2002). Effects of melt-processing conditions on the quality of poly (ethylene terephthalate) montmorillonite clay nanocomposites. *J Polym Sci Part B Polym Phys*, 40: 2661-2666.

De Bussetti, S.G. & Ferreiro, E.A. (2004). Adsorption of Poly (Vinyl Alcohol) onMontmorillonite. *Clay and Clay Miner*, 52(3): 334 – 340

Di Lorenzo, M.L., Errico, M.E. & Avella, M. (2002). Thermal and morphological characterization of poly (ethylene terephthalate)/calcium carbonate nanocomposites. *J. Mater Sci*, 37(11): 2351 2358.

Doppers, L-M., Breen, Ch. & Sammon, Ch. (2004). Diffusion of water and acetone into poly(vinyl alcohol)–clay nanocomposites using ATR-FTIR. *Vibrat Spectrosc*, 35:27–32.

Ekici, S., Isikver, Y. & Saraydın, D. (2006). Poly(Acrylamide-Sepiolite) Composite Hydrogels: Preparation, Swelling and Dye Adsorption Properties. *Polym Bull*, 57:231.

Elizabeth, F.D.R. & Fabia, S.C. (2006). Synthesis and characterization of poly (vinyl alcohol) hydrogels and hybrids for rMPB70 protein adsorption. *Mat.Res*. 9 (2): 185-191.

Evora, V.M.F. &Shukla, A. (2003). Fabrication, characterization, and dynamic behavior of polyester/TiO2 nanocomposites. *Mater Sci Eng*, 361(1-2): 358-366.

Fornes, T.D., Yoon, P.J., Hunter, D.L., Keskkula, H., & Paul, D.R. (2002). Effect of organoclay structure on nylon-6 nanocomposite morphology and properties. *Polymer*, 43: 5915-33.

Fornes, T.D., Yoon, P.J., Keskkula, H., & Paul, D.R. (2001). Nylon 6nanocomposites: the effect of matrix molecular weight. *Polymer,* 42: 9929-40.

Fukumori, T., & Nakaoki, T. (2013). Significant Improvement of Mechanical Properties for Polyvinyl Alcohol Film Prepared from Freeze/Thaw Cycled Gel *Sci. Res*., 3, 110-116.

Gaboune, A., Sinha Ray, S., Ait-Kadi, A., Riedl, B. & Bousmina, M. (2006). Polyethylene/Clay Nanocomposites Prepared by Polymerization Compounding Method. *Journal of nanoscience and nanotechnology*, 6 (2): 530-535.

Gamiz, E., Linares, J., Delgado, R. (1992). Assessment of two Spanish bentonites for pharmaceutical uses. *Appl Clay Sci*. 6:359.

Gao, D., Heimann, R.B., Lerchner, J., Seidel, J.& Wolf, G. (2001). Development of a novel moisture sensor based on superabsorbent poly(acrylamide)-montmorillonite composite hydrogels. *J Mater Sci.* 36:4567-4571.

Gao, D., Heimann, R.B., Williams, M.C., Wardhaugh, L.T., Muhammad, M. (1999). Rheological properties of poly(acrylamide)-bentonite composite hydrogels, J Mater Sci 34:1543-1552.

Giannelis, E.P. Krishnamoorti, R. & Manias, E. (1999). Polymer-silicate nanocomposites: model systems for confined polymers and polymer brushes. *Adv Polym Sci*, 138: 107-47.

Giannelis, E.P. (1996). Polymer Layered Silicate Nanocomposites. *Adv Mater*, 8: 29-35.

Gilmann, . J.W. (1999). Flammability and thermal stability studies of polymer- layered –silicate (clay) nanocomposites. *Appl Clay Sci*, 15(1-2): 31-49.

Gimenez, V., Mantecon, A., Ronda, J.C. & Cadiz, V. (1997). Poly(vinyl alcohol) modified with carboxylic acid anhydrides: crosslinking through carboxylic groups. J Appl Polym Sci,65:1643-1651

Ginzburg, V.V. & Balazs, A.C. (1999). Calculating phase diagram of polymer–platelet mixtures using density functional theory: implication for polymer/clay composites. *Macromolecules*, 32: 5681-5688.

Giusti, P., Lazzeri, L., Barbani, N., Narducci, P., Bonaretti, A., Palla, M. & L. Lelli, (1993). Hydrogels of poly (vinyl alcohol) and collagen as new bioartificial materials. *J. Mater. Sci.: Materials in Medicine*, 4: 538.

Gonzalez, J. S., Maiolo, A. S., Hoppe, C. E., & Alvarez, V. A. (2012). Composite gels based on poly (vinyl alcohol) for biomedical uses. *Proc. Mater. Sci*, 1: 483.

Gonzalez, J.S., Maiolo, A.S., Ponce, A.G., & Alvarez, V.A. (2011). Composites based on poly(vinyl alcohol) hydrogels for wound dressing. The Argentine Congress of Bioengineering and Clinical Engineering Conference VII, SABI, 1

Greenland,D.J. (1963). Adsorption of poly(vinyl alcohols) by montmorillonite.*J.Colloid Sci*, 18: 647– 64.

Grunlan, J.C., Grigorian, A., Hamilton, C.B., & Mehrabi, A.R. (2004). Effect of clay concentration on the oxygen permeability and optical properties of a modified poly(vinyl alcohol. *J. Appl. Polym. Sci.*, 93: 1102.

Hackett, E., Manias, E. & Giannelis, E.P. (2000). Computer simulation studies of PEO/layered silicate nanocomposites. *Chem. Mater*, 12: 2161-2167.

Hackett, E., Manias, E. & Giannelis, E.P. (1998). Molecular dynamics simulations of organically modified layered silicates. *J Chem. Phys*, 108: 7410-7415.

Hajizadeh, S., Xu, C., Kirsebom, H., Ye, L. & Mattiasson, B. (2013). Cryogelation of molecularly imprinted nanoparticles: A macroporous structure as affinity chromatography column for removal of β-blockers from complex samples. *Journal of Chromatography A*, 1274: 6-12.

Hamidi, M.et al. (2008). Hydrogel nanoparticles in drug delivery. *Adv Drug Del Rev*, 60: 1638-1649.

Haraguchi, K. & Takehisa, T. (2002). Nanocomposite Hydrogels: A Unique Organic–Inorganic Network Structure with Extraordinary Mechanical, Optical, and Swelling/De-swelling Properties. *Adv. Mater*, 14: 1120-1124.

Haraguchi, K. (2007). Nanocomposite hydrogels. *Curr. Opin. Solid State Mater. Sci*, 11: 47-54.

Haraguchi, K., Farnworth, R., Ohbayashi, A. & Takehisa, T.(2003). Compositional Effects on Mechanical Properties of Nanocomposite Hydrogels Composed of Poly (N,N-dimethylacrylamide) and Clay. *Macromolecules*, 36: 5732-5741.

Hassan, C. M. & Peppas, N. A. (2000). Structure and applications of poly (vinyl alcohol) hydrogels produced by conventional crosslinking or by freezing-thawing methods. *Advances in Polymer Science,* 153: 37–65.

Hassan, C. M., Stewart, J. E., & Peppas, N. A. (2000). Diffusional characteristics of freeze/thawed poly (vinyl alcohol) hydrogels: applications to protein controlled release from multilaminate devices*Eur. J. Pharm. Biopharm*, 49: 161.

Hassan, C.M. & Peppas, N.A. (2000). Structure and morphology of freeze/thawed PVA hydrogels. *Macromolecules*., 33: 2472-2479.

Hassan, C.M., Ward, J.H. & Peppas, N.A. (2000). Modeling of crystal dissolution of poly (vinyl alcohol) gels produced by freezing/thawing processes. *Polymer*, 41:6729.

Hatakeyema, T., Uno, J., Yamada, C., Kishi, A. & Hatakeyama, H. Thermochim. (2005). Gel-sol transition of poly(vinyl alcohol) hydrogels formed by freezing and thawing. *Thermochim. Acta*, 431:144-148.

Hennink, W. E. & van Nostrum, C. F. (2002). Novel crosslinking methods to design hydrogels. Advanced Drug Delivery Reviews, 54: 13–36.

Hernandez, M.C., Suarez, N., Martınez, L.A., Feijoo, J.L., Monaco, S.L., & Salazar, N. (2008). Effects of nanoscale dispersion in the dielectric properties of poly(vinyl alcohol)-bentonite nanocomposites, *Phys. Rev.* E, 77: 051801.

Hickey A. S., & Peppas, N. A. (1995). Screening of potentially mucoadhesive polymer microparticles in contact with rat intestinal mucosa. *J. Membr. Sci,* 107: 229.

Hiroi,R., Sinha Ray, Okamoto, M. & Shiroi, T. (2004). Organically modified layered titanate: a new nanofiller to improve the performance biodegradable polylactide. *Macromol Rapid Commun*, 25: 1359-63.

Hoffman, A. S. (2001). Hydrogels for biomedical applications. *Annals of the New York Academy of Science*, 944:62–73.

Huang, X., Xu, S., Zhong, M., Wang, J.,Feng, S. & Shi, R. (2009). Modification of Na-bentonite by polycations for fabrication of amphoteric semi- IPN nanocomposite hydrogels, *J. Appl. Polym. Sci*, 42: 455-459.

Hyon, S.H., Cha, W.I., Ikada, Y., Kita, M., Ogura, Y. & Honda, Y. (1994). Poly(vinyl alcohol) hydrogels as soft contact lens material. *J Biomater Sci Polym Ed*, 5:397–406.

Iwaseya, M., Katsuyama, N., Yamaura, K. & Dai L-X. (2006). Effect of degree saponification on the properties of films obtained from PVA/NaCl/H2O systems. *Journal of Materials Science*, 41, 1979–1982.

Iwaseya, M., Watanabe, M., Yamaura, K., Dai, L-X. & Noguchi, H. (2005). High performance films obtained from PVA/Na2SO4/H2O and PVA/CH3COOONa/H2O systems. *Journal of Materials Science*, 40:5695–5698.

Jackson, C.L., Bauer, B.J., Nakatani, J. A.I. & Barnes, D. (1996). Synthesis of hybrid organic-inorganic materials from interpenetrating polymer network chemistry.*Chem Mater*, 8(3): 727-733.

Jeong H. M., Kim B. C., Kim E.H.(2005). Structure and properties of EVOH/organoclay nanocomposites. J. Mater. Sci, 40 (14) 3783-3787.

Jimenez, G., Ogata, N., Kawai, H. & Ogihara, T. (1997). Structure and thermal/ mechanical properties of poly (ε-caprolactone) - clay blend. *J Appl Polymer Sci*, 64, 2211-2220.

Kamigaito, O.J. (1991). What can be improved by nanometer composites?. *Japan Soc Powder Metallurgy*, 38: 315-321.

Kamoun, E. A., Kenawy, E.-R., Tamer, T. M., El- Meligy, M. A., & Mohy Eldin, M. S. (2015). Poly (vinyl alcohol)-alginate physically crosslinked hydrogel membranes for wound dressing applications: characterization and bio-evaluation. *Arab. J. Chem,* 8 (1): 38–47.

Karimi, A. (2008). Investigation the Effect of Cross Linking Agent on Equilibrium Swelling and Kinetics of Water Absorption and Desorption for pH and pH-Temperature Sensitive Hydrogels. *Asian Journal of Chemistry,* 20 (5): 3482-3488.

Karimi, A. & Wan Daud, WMA. (2014). Comparison the Properties of PVA/Na^{+}-MMT Nanocomposite Hydrogels Prepared by Physical and Physicochemical Cross-Linking. *Polymer Composites*, DOI: 10.1002/pc.

Kasgoz, H. & Durmus, A. (2008). Dye removal by a novel hydrogel-clay nanocomposite with enhanced swelling properties. Polym. *Adv. Technol*, 19: 838-845.

Kawasumi, M., Hasegawa, N., Kato, M., Usuki, A. & Okada, A. (1997). Preparation and mechanical properties of polypropylene-clay hybrids. *Macromolecules,* 30(20): 6333-6338.

Kenawy, E.-R., El-Newehy, M. H., & Al-Deyab, S. S. (2010). Controlled release of atenolol from freeze/thawed poly(vinyl alcohol) hydrogel. *J. Saudi Chem. Soc*, 14: 237-240.

Kenawy, E.-R., Kamoun, E. A., Mohy Eldin, M. S., & El-Meligy, M. A. (2014). Physically crosslinked poly(vinyl alcohol)-hydroxyethyl starch blend hydrogel membranes: Synthesis and characterization for biomedical applications. *Arab. J. Chem*, 7: 372–380.

Kickelbick, G. (2003). Concepts for the incorporation of inorganic building blocks into organic polymers on a nanoscale. *Progr Polym Sci*, 28(1):83-114.

Kim, J. O., Park, J. K., Kim J. H., Giujin, S., Yong, C. S., Li, D. X., Choi, J. Y., Woo, J. S., Yoo, B. K., Lyoo, W. S., Jung-Ae, K.& Han-Gon, C. (2008). Development of polyvinyl alcohol–sodium alginate gel-matrix-based wound dressing system containing nitrofurazone. Int, J, Pharm, 359: 79-86

Kim, S.W., Bae, Y.H., & Okano, T., (1992). Hydrogels: Swelling, drug loading and release. *Pharm Res*, 9(3): 283-290.

Kobayashi, H.et al. (1992). Tissue reactions induced by modified poly(vinyl alcohol) hydrogels in rabbit cornea. *J. Biomed Mater Res*, 26: 1583-1598.

Kojima, Y., Usuki, A., Kawasumi, M., Okada, A., Fukushima, Y., Kurauchi, T.et al. (1993). Mechanical properties of nylon 6-clay hybrid. *J Mater Res*, 8: 1185-9.

Kokabi, M., Sirousazar M., & Hassan, Z.M. (2007). PVA-clay nanocomposite hydrogels for wound dressing. *European Polymer Journal*, 43: 773-781.

Komiya, S., Otsuka, E., Hirashima, Y. & Suzuki A. (2011). Salt effects on formation of microcrystallites in poly(vinyl alcohol) gels prepared by cast-drying. *Progress in Natural Science: Materials International*. 21: 375-379.

Kopecek, J. (2003). Smart and genetically engineered biomaterials and drug delivery systems. *Eur J Pharm Sci*, 20: 1-16.

Korsmeye, R.W. & Peppas, N.A. (1981). Effect of the morphology of hydrophilic polymeric matrices on the diffusion and release of water soluble drugs. *J Membr Sci*, 9 (3):211-227.

Krishnamoorti,R., Vaia, R.A. & Giannelis, E.P. (1996). Structure and dynamics of polymer-layered silicate nanocomposites.*Chem. Mater*, 8: 1728-1734.

Lagaly, G. (1986). Interaction of alkylamines with different types of layered compounds. *Solid State Ionics*, 22:43-51.

Lavin E., & Snelgrove, L. (1983). "Vinyl Polymers," in Encyclopedia of Chemical Technology, *K. Othmer, Ed., John Wiley, New York*, 808.

LeBaron, P.C., Wang, Z.& Pinnavaia, T.J. (1999). Polymer-layered silicate nanocomposites: an overview. *Appl Clay Sci*, 15: 11-29.

Lee, J.H., Park, T.G., Park, H.S., Lee, D.S., Lee, Y.K., Yoon, S.C., & Nam, J.D. (2003). Thermal and mechanical characteristics of poly (L-lactic acid) nanocomposite scaffold, *Biomaterials*, 24: 2773.

Lee, J.Y., Baljon, A.R.C., Loring, R.F.& Panagiopoulos, A.Z. (1998). Simulation of polymer melt intercalation in layered nanocomposites. *J Chem Phy*, 109: 10321-30.

Lee, W.& Jou, L. (2004). Effect of the intercalation agent content of montmorillonite on the swelling behavior and drug release behavior of nanocomposite hydrogels. *J Appl Polym Sci*, 94: 74.

Lee, W.F. & Chen, Y.C. (2004). Effect of bentonite on the physical properties and drug-release behavior of poly(AA-co-PEGMEA)/bentonite nanocomposite hydrogels for mucoadhesive. *J. Appl. Polym. Sci*, 91: 2934-1941.

Lee, W.F. & Lee, S.C. (2006). Effect of hydrotalcite on the swelling and mechanical behaviors for the hybrid nanocomposite hydrogels based on gelatin and hydrotalcite. *J. Appl. Polym. Sci*, 100: 500-507.

Lee, W.F.& Fu, Y.T. (2003). Effect of montmorillonite on the swelling behavior and drug release behavior of nanocomposite hydrogels. *J. Appl. Polym. Sci.,* 89: 3652-3660.

Lepoittevin, B., Devalckenaere, M., Pantoustier, N., Alexandre, M., Kubies, D., Calberg C., Jerome, R. & Dubois, P. (2002). Poly (1-caprolactone)/clay nanocomposites prepared by melt intercalation: mechanical, thermal and rheological properties. *Polymer*, 43: 4017-4023.

Lepoittevin, B., Pantoustier, N., Devalckenaere, M., Alexandre, M., Kubies, D., Calberg C.,et al., (2002). Pol(e-caprolactone)/clay nanocomposites prepared by melt intercalation: mechanical thermal and rheological properties. *Macromolecules*, 35: 8385-8390. 44.

Li, C., Fu, R., Yu, C., Li, Z., Guan, H., Hu, D., Zhao, D., & Lu, L. (2013). Silver nanoparticle/chitosan oligosaccharide/poly(vinyl alcohol) nanofibers as wound dressing: a preclinical study. *Int. J. Nanomed.,* 8: 4131.

Li, J.K., Wang, N. & Wu, X.S. (1998). Poly(vinyl alcohol) nanoparticles prepared by freezing–thawing process for protein/peptide drug delivery. *J Control Rel*, 56:117–126.

Lim, S.T., Hyun, Y.H., Choi, H.J., & Jhon, M.S. (2002). Synthetic biodegradable aliphatic polyester/montmorillonite nanocomposites. *Chem. Mater*, 14: 1839-1844.

Lin, J.M., Wu, J.H., Yang, Z.F. & Pu, M.L. (2001). Synthesis and Properties of Poly(acrylic acid)/Mica Superabsorbent Nanocomposite. *Macromol Rapid Commun*, 22: 422.

Litvinov, V. M. & De, P. P. (2002). Spectroscopy of Rubbers and RubberyMaterials. *Rapra, Shawbury, U.K.*

Liu, J., Gao, Y., Wang, F., Li, D . & Xu, J. (2002). Preparation and characteristic of a new class of silica/polyimide nanocomposites. *J Mater Sci*, 37(14): 3085-3088.

Liu, Y., Zhu, M., Liu, X., Zhang, W., Sun, B.,Chen, Y. et al. (2006). High clay content nanocomposite hydrogels with surprising mechanical strength and interesting deswelling kinetics. *Polymer*, 47: 1.

Liu,Y., Zhu, M., Liu, X., Jiang, Y.M., Ma, Y., Qin, Z.Y., Kuckling, D. & Adler, H.J.P. (2007). Mechanical Properties and Phase Transition of High Clay Content Clay/Poly(N-isopropylacrylamide) Nanocomposite Hydrogel. *Macromol. Symp*, 254: 353-360.

Loo, L.S. & Gleason, K.K. (2003). Fourier transforms infrared investigation of the deformation behavior of montmorillonite in nylon 6/nanoclay nanocomposites. *Macromolecules*, 36: 2587-2590.

Lozinsky, V. I. (1998). Cryotropic gelation of poly (vinyl alcohol) solutions.*Russ. Chem. Rev*, 67: 573.

Lozinsky, V. I., Domotenko, L. V., Zumbov, A.L. & Simenel, I.A. (1996). Study of cryostructuration of polymer systems. XII. Poly(vinyl alcohol) cryogels: Influence of low-molecular electrolytes. *Journal of Applied Polymer Science*, 61: 1991–1998.

Lozinsky, V. I., Korotaeva, G. F, . Vainerman, E. S., & Rogozhin, S. V. (1984). Study of cryostructurization of polymer systems. *Colloid Polym. Sci*, 262: 617.

Lozinsky, V.I. & Damshkaln, L.G. (2000). Study of cryostructuration of polymer systems. XVII. Poly(vinyl alcohol) cryogels: Dynamics of the cryotropic gel formation. *J Appl Polym Sci*, 77:2017.

Lozinsky, V.L., Galaev, I.Yu ., Plieva, F.M., Savina, I.N., Jungvid, H. & Mattiasson, B. (2003). Polymeric cryogels as promising materials of biotechnological interest. *Trends Biotechno*, 21: 445–451.

Mahdavi, H., Mirzadeh, H., Zohuriaan-Mehr, M. J., & Talebnezhad, F. (2013). Poly(vinyl alcohol)/chitosan/clay nanocomposite films: Preparation, properties and anti-bacterial activities. *J. Am. Sci*, 9(8): 203.

Mallam, S., Horkay, F., Hecht, A.M., & Geissler, E. (1989). Scattering and swelling properties of inhomogeneous polyacrylamide gels. *Macromolecules*, 22: 3356-3361.

Mansur, H. S., & Mansur, A. P. (2005). Small Angle X-Ray Scattering, FTIR and SEM Characterization of Nanostructured PVA/TEOS Hybrids by Chemical Crosslinking Mater. *Res. Soc. Symp. Proc*, 873E (K1.9.1), 20.

Mansur, H. S., Sadahira, C. M., Souza, A. N., & Mansur, A. A. P. (2008). FTIR spectroscopy characterization of poly (vinyl alcohol) hydrogel with different hydrolysis degree and chemically crosslinked with glutaraldehyde. *Mater. Sci. Eng. C*, 28 (4) 539–548.

Martens, P. & Anseth, K. S. (2000). Characterization of hydrogels formed from acrylate modified poly(vinyl alcohol) macromers. *Polymer*, 41: 7715-7722.

Mathias, L.J., Davis R.D., & Jarrett, W.L. (1999). Observation of a- and g-crystal forms and amorphous regions of nylon 6-clay nanocomposites using solid-state 15N nuclear magnetic resonance.*Macromolecules*, 32: 7958-7960.

Mbhele, Z.H., Salemane, M.G., Van Sittert, C.G.C.E., Nedeljkovic, J.M., Djokovic, V. & Luyt, A.S. (2003). Fabrication and characterization of silver-polyvinyl alcohol nanocomposites. *Chem. Mater,* 15 (26): 5019-5024.

Mc Gann, M. J., Higginbotham, C. L., Geever, L. M. & Nugent, M. J. D. (2009). The synthesis of novel pH-sensitive poly(vinyl alcohol) composite hydrogels using a freeze/thaw process for biomedical applications. *Int. J. Pharm*, 372:154.

Messersmith,P.B. & Giannelis, E.P. (1993). Polymer Layered Silicate Nanocomposites: in situ intercalative polymerization of ε–caprolactone in layered silicates. *Chem. Mater*, 5(8): 1064-1066.

Messersmith, P.B. & Giannelis, E.P. (1994). Synthesis and Characterization of Layered Silicate-Epoxy Nanocomposites. *Chem. Mater*, 6 (10): 1719-1725.

Mi, F.-L., Shyu, S. S., Wu, Y. B., Lee, S. T., Shyong, J. Y., & Huang, R. N. (2001). Fabrication and characterization of a sponge-like asymmetric chitosan membrane as a wound dressing. *Biomaterials,* 22: 165-173.

Michael Nugent . J.D., et al., (2007). Preparation of a novel freeze thawed poly(vinyl alcohol) composite hydrogel for drug delivery applications. *European Journal of Pharmaceutics and biopharmaceutics,* 67: 377-386.

Mirzan, T. R., Darmawan, D.& Zainuddin, S. (2001). Irradiation of polyvinyl alcohol and polyvinyl pyrrolidone blended hydrogel for wound. *Radiat. Phys. Chem,* 62: 107-113.

Mitchell, C.A., Bahr, J.L., Arepalli, S., Tour, J.M. & Krishnamoorti, R. (2002). Dispersion of functionalized carbon nanotubes in polystyrene. *Macromolecules,* 35: 8825-8830.

Mitchell, H.H., Hamilton, T. S., Steggerda, F. R., & Bean, H. W. (1945). The Chemical Composition of the Adult Human Body and Its Bearing on the Biochemistry of Growth. *J. Biol. Chem*, 158:625-637.

Miyataa, T., Uragamia, T. & Nakamaeb, K (2002). Biomoleculesensitive hydrogels. *Adv Drug Deliv Rev*, 54: 79-98.

Mohanty, A.K., Drzal, L.T. & Misra, M. (2003). Nano-reinforcement of bio-based polymers-the hope and reality. *Polym Mater Sci Eng*, 88: 60-61.

Morgan, A.B. & Gilman, J.W. (2003*).* Characterization of poly-layered silicate (clay) nanocomposites by transmission electron microscopy and X-ray diffraction: a comparative study. *J Appl Polym Sci*, 87: 1329-38.

Mouhoub, L., Sedgelmaci, M., Ammi, N., Benslimane Mansouri, M., & Mameri,S. (2013). Evaluation of healing activity of PVA/chitosan hydrogels on deep second degree burn: Pharmacological and toxicological tests. *BURNS,* 39: 98-104.

Nacer Khodja, A., Mahlous, M.,Tahtat, D., Benamer, S., Larbi Youcef, S., Chader, H., Nagura, M., Hamano, T. & Ishikawa, H. (1989). Structure of poly(vinyl alcohol) hydrogel prepared by repeated freezing and melting. *Polymer,* 30:762-765

Nacer Khodja, A., Mahlous, M., Tahtat, D., Benamer, S., Larbi Youcef, S., Chader, H., Mouhoub, L., Sedgelmaci, M., Ammi, N., Benslimane Mansouri M., & Mameri, S. (2013). Evaluation of healing activity of PVA/chitosan hydrogels on deep second degree burn: Pharmacological and toxicological tests, *BURNS,*39: 98.

Nam, . P.H., Maiti, P., Okamoto, M., Kotaka, T., Nakayama, T., Takada, M., Ohshima, M., Usuki, A., Hasegawa, N., & Okamoto, H. (2002). Foam processing and cellular structure of polypropylene/clay nanocomposites. *Polym Eng Sci,* 42: 1907-18.

Nanda, P., De, SK., Manna, S., De, U., & Tarafdar, S. (2010). Effect of gamma irradiation on a polymer electrolyte: Variation in crystallinity, viscosity and ion-conductivity with dose. *Nuclear Instruments and Methods in Physics Research Section B* 268 (1): 73–78.

Nho, Y. C., Lim, Y. M., Gwon, H. & Choi, E. K. (2009). Preparation and characterization of PVA/PVP/glycerin/antibacterial agent hydrogels using γ-irradiation followed by freeze-thawing. *Korean J. Chem. Eng.* , 26: 1675-1678.

Nie, J., Du, B. & Oppermann, W. (2005). Swelling, Elasticity, and Spatial Inhomogeneity of Poly(N-isopropylacrylamide)/Clay Nanocomposite Hydrogels. Macromolecules, 38: 5729-5736.

Nuget, M. J. D., Hanley, A., Tomkins, P. T. & Higginbotham, C. L. (2005). Investigation of a novel freeze-thaw process for the production of drug delivery hydrogels. *Journal of Materials Science: Materials in Medicine,* 16: 1149–1158. DOI: 10.1007/s10856-005-4722-7

Ogata, N., Kawakage, S. & Ogihara, T. (1997). Poly(vinyl alcohol)-clay and poly(ethylene oxide)–clay blend prepared using water as solvent. *J Appl Polym Sci*, 66:573–81.

Okada,A., Kawasumi, M., Usuki, A., Kojima, Y., Kurauchi, T. & Kamigaito, O. (1990). Synthesis and properties of nylon-6/clay hybrids. *MRS Symposium Proceedings*, Pittsburgh,171: 45-50.

Okamoto, M., Morita, S., Kotaka, T. (2001). Dispersed structure and ionic conductivity of smectic clay/polymer nanocomposites. *Polymer*, 42(6); 2685-2688.

Okamoto, M., Morita, S., Taguchi, H., Kim, Y.H., Kotaka, T. & Tateyama, H. (2000). Synthesis and structure of smectic clay/poly(methyl methacrylate) and clay/polystyrene nanocomposites via in situ intercalative polymerization. *Polymer*, 41(10): 3887-3890.

Okazaki, M., Hamada, T., Fujii, H., Mizobe, A. & Matsuzawa,S. (1995) . Development of PVA Hydrogel for Wast Water Cleaning.I.Study of PVA Gel as a carrier for Immobilizing Microorganism. *J.of.Appl.Poly. Sci*, 58: 2235-2241.

Ossipov, D. A. & Hilborn, J. (2006). Poly(vinyl alcohol)-based hydrogels formed by "click chemistry''. *Macromolecules*, 39: 1709-1718.

Ostuka, E., Sugiyama, M., & Suzuki, A. (2011). Formation and destruction of physical crosslinks by mild treatments in chemically crosslinked poly(vinyl alcohol) gels. *Polym. Bull.* 67: 1215-1226.

Pal, K., Banthia, A.K., & Majumdar, D.K. (2008). Effect of heat treatment of starch on the properties of the starch hydrogels. *Mater Lett*, 62; 215-218.

Pantoustier, N., Lepoittevin, B., Alexandre, M., Kubies, D., Calberg, C., Jerome, R. et al., (2002). Biodegradable polyester layered silicate nanocomposites based on poly(e-caprolactone). *Biodegradable Polym Eng Sci*, 42: 1928-37.

Paradossi, G., Cavalieri, F., & Chiessi, E. (2003). Poly(vinyl alcohol) as versatile biomaterial for potential biomedical applications. *J. Mater. Sci. Mater. Med*, 14: 687-691.

Paranhos, C.M., et al., (2007a). Microstructure and free volum evaluation of poly (vinyl alcohol) nanocomposite hydrogels. *Eur Polymer J*, 43: 4882-4890.

Paranhos C.M., Soares, B.G., Oliveira, R.N., & Pessan, L.A. (2007b). Poly (vinyl alcohol)/clay-based nanocomposite hydrogels: swelling behavior and characterization, *Macromol Mater Eng*, 292: 620-626.

Park, J.-S., Park, J.-W., & Ruckenstein, E. (2001). Thermal and dynamic mechanical analysis of PVA/MC blend hydrogels. *Polymer*, 42: 4271-4280.

Park, S.S., Bernet, N., De La Roche, S. & Hanh, H.T. (2003). Processing of iron oxide-epoxy vinyl ester nanocomposites *J Comp Mater*, 37(5): 465-465.

Patachia S.,Florea C., Friedrich Chr. & Thomann Y. (2005). *e XPRESS Polymer Letters* 3(5) : 320-331.

Patachia, S. (2003). Blends based on poly(vinyl alcohol) and the products based on this polymer. in: 'Handbook of polymer blends and composites' (eds.: Vasile C., Kulshreshtha A. K.). *Rapra Technology, Shawbury,* 288–365.

Patachia, S., et al., (2009). Tailoring of poly(vinyl alcohol) cryogels properties by salts addition, eXPRESS Polymer Letters, 3(5): 320-331.

Patachia, S., Valente, A.J.M. & Baciu, C. (2007). *European Polymer Journal*, 43 (2):460-467.

Paul, M-A., Alexandre, M., Degee, P., Henrist, C., Rulmont A., & Dubois, P. (2003). New nanocomposite materials based on plasticized poly(L-lactide) and organo-modified montmorillonites: thermal and morphological study. *Polymer*, 44: 443-50.

Peppas, N. A. & Mongia, N. K. (1997). Ultrapure poly (vinyl alcohol) hydrogels with mucoadhesive drug delivery characteristics. *Eur J Pharm Biopharm*, 43; 51-58.

Peppas, N. A., Bures, P., Leobandung, W. & Ichikawa, H. (2000). Hydrogels in pharmaceutical formulations. *European Journal of Pharmaceutics and Biopharmaceutics*, 50: 27–46.

Peppas, N.A. & Tennenhous, D. (2004). Semicrystalline poly (vinyl alcohol) films and their blends with poly (acrylic acid) and poly (ethylene glycol) for drug delivery applications. *J. Drug. Del. Sci. Tech*, 14 (4): 291-297.

Peppas, N.A.& Simmons, R.E.P. (2004). Mechanistic analysis of protein delivery from porous poly (vinyl alcohol) systems. *J. Drug Del. Sci. Tech.,* 14(4): 285-289.

Pines, E.& Prins, W. (1973). Structure- property Relations of Thermoreversible Macromolecular Hydrogels. Macromolecules,6:888-895.

Potschke, P., Bhattacharyya, A., Janke, A. & Goering, H. (2003). Melt-mixing of polycarbonate/multi-wall carbon nanotube composites. *Compos Interfaces,* 10: 389-404.

Purss, K. H., Qiao G. G. & Solomon, D. H. (2005). Effect of "glutaraldehyde" functionality on network formation in poly(vinyl alcohol) membranes. *J. Appl Polym Sci*, 96: 780-792.

Ratner, B., Hoffman, A. S., Schoen, F. J. & Lemons, J. E. (2004). Biomaterials science: An introduction to materials in medicine. *Elsevier Academic Press*, San Diego.

Razzak, M.T., Darwis, D. & Sukirno, Z. (2001). Irradiation of poly(vinyl alcohol) and poly(vinyl pyrrolidone) belended hydrogel for wound dressing. *Radiat Phys Chem.* 62:107–13.

Reisa, E. F., Camposa, F. S., Lagea, A. P., Leitea, R. C., Heneineb, L. G., Vasconcelosc, W. L., Lobatoa, Z. P., & Mansurc, H. S. (2006).Synthesis and Characterization of Poly(Vinyl Alcohol) Hydrogels and Hybrids for Rmpb70 Protein Adsorption. *Mater. Res*, 9(2): 185-191.

Ricciardi, R., Gailet, C., Ducouret, G., Lafuma, F. & Lauporete, F. (2003). Investigation of the relationships between the chain organization and rheological properties of atactic poly(vinyl alcohol) hydrogels. *Polymer*, 44: 3375-3380

Ritger P. L., & Peppas, N. A. (1987). A Simple Equation for Description of Solute Release I Fickian and Non-Fickian Release from Non-Swellable Devices in the form of Slabs, Spheres, Cylinders or Discs. *J. Control. Release*, 5: 23.

Rosiak, J.M.& Ulan ski, P. (1999). Synthesis of hydrogels by irradiation of polymers in aqueous solution.*Radiat Phys Chem*, 55: 139-51.

Roy, I. & Gupta, M.N. (2003). Smart polymeric materials:emerging biochemical applications. *Chem Biol*, 10: 1161-71.

Sapalidis, A.A., Katsaros, F.K., & Kanellopoulos, N.K. (2011). PVA /Montmorillonite Nanocomposites: Development and Properties, in Nanocomposites and Polymers with Analytical Methods, ISBN: 978-953-307-352-1, *InTech*.

Schexnailder, P. & Schmidt, G. (2009). Nanocomposite Polymer Hydrogels. *Colloid Polym. Sci*, 287: 1-11.

Schosseler, F., Skouri, R., Munch, J.P., & Candau , S.J.. (1994). Swelling and cross-linking density effects on the structure of partially ionized gels. *J Phys II*, 4: 1221-1239.

Schuetz, Y.B., Gurny, R.& Jordan, O. (2008). A novel thermoresponsive hydrogel of chitosan. *Eur. J. Pharm. Biopharm*, 68:19-25.

Shaffer, M.S.P., & Windle, A.H. (1999). Fabrication and characterization of carbon nanotube/poly (vinyl alcohol) composites. *Adv Mater*, 11: 937-941.

Shaheen, S. M., Ukai, K., Dai, L.-X., & Yamaura, K. Properties of hydrogels of atactic poly (vinyl alcohol)/NaCl/H2O system and their application to drug release, *Polymer International*. (2002) 51 (12): 1390-1397.

Shaheen, S.M. & Yamaura, K. (2002). Preparation of theophylline hydrogels of atactic poly(vinyl alcohol)/NaCl/H2O system for drug delivery system. *J. Controlled Release*, 81: 367-377.

Shaheen, S.M. & Yamaura, K. (2006). In vitro Parameters Evaluation of Theophyline Release from the Hydrogels of a-PVA/NaCl/H2O. *International Journal of Pharmacology*, 2 (3): 286-292, 42. K.T.

Shalumon, K.T., Anulekha, K.H., Nair, S.V., Chennazhi, K.P., & Jayakumar, R. (2011). Sodium alginate/poly(vinyl alcohol) nano ZnO composite nanofibers for antibacterial wound dressing, *Int. J. Biol. Macromol.*, 49: 247.

Shibayama, M., Tanaka, T., & Han, C.C. (1992). Small-angle neutron scattering study on weakly charged temperature sensitive polymer gels. *J Chem Phys*, 97: 6842-6854. 34.

Silva FEF, Di-Medeiros MCB, Batista KA, & Fernandes KF. (2013). PVA/polysaccharides blended films: mechanical properties. *J. Mater*. 2013: 1-6.

Simon, G .& Schneider, H. (1991). MC-determination in elastomers by 1H-NMR relaxation and 2H-NMR spectroscopy. *Makromol Chem Macromol Symp*, 52:233-246.

Sinha Ray, Okamoto, K., Okamoto, M. (2003). Structure–propertyrelationship in biodegradable poly(butylene succinate)/layered silicate nanocomposites. *Macromolecules*, 36: 2355-2367.

Sinha Ray, Okamoto, S. M. (2003). Polymer/layered silicate nanocomposites: a review from preparation toprocessing. *Prog Polym Sci*, 28: 1539-641.

Sinha Ray, S., Maiti, P., Okamoto, M., Yamada, K., & Ueda, K. (2002). New polylactide/layered silicate nanocomposites. 1. Preparation, characterization and properties.*Macromolecule,* 35: 3104-3110.

Sinha Ray, S., Yamada, K., Okamoto, M., & Ueda, K. (2002). Polylactide-layered silicate nanocomposite: A novel biodegradable material. *Nano Lett.,* 2: 1093-1096.

Sinha Ray, S., Yamada, K., Okamoto, M., Ogami, A., & Ueda, K. (2003). New polylactide/layered silicate nanocomposites. 3. High performance biodegradable materials. *Chem Mater,* 15: 1456-1465.

Sirousazar, M..& Yari, M. (2010). Dehydration Kinetics of Polyvinyl Alcohol Hydrogel Wound Dressing During The Wound Healing Process. *Chinese J. Polym. Sci,* 28: 573-580.

Song, L., Zhu, M., Chen, Y. & Haraguchi K. (2008). Temperature- and pH-Sensitive Nanocomposite Gels with Semi-Interpenetrating Organic/Inorganic Networks. *Macromol. Chem. Phys*, 209: 1564-1575.

Stasko, J., Kalniņs M., Dzene, A. & Tupureina, V. (2009). Poly(vinyl alcohol) hydrogels. *Proc Estonian Acad Sci,* 58(1): 63-66.

Stathi, P., Papadas, I.T., Enotiadis, A., Gengler, R.Y.N., Gournis, D., Rudolf, P., & Deligiannakis, Y. (2009). Effects of Acetate on Cation Exchange Capacity of a Zn- Containing Montmorillonite: Physicochemical Significance and Metal Uptake. *Langmuir.,* 25: 6825-6833.

Stauffer, S.R. & Peppas, N.A. (1992). Poly (vinyl alcohol) hydrogels prepared by freezing-thawing cyclic processing. *Polymer,* 33(18): 3932-3936.

Strawhecker K.E., & Manias, E. (2001). AFM of Poly(vinyl alcohol) Crystals Next to an Inorganic Surface. *Macromolecules*, 34: 8475-8482.

Strawhecker, K.E.,&Manias,E. (2000). Structure and properties of poly (vinyl alcohol)/Na+-montmorillonite. *chem. Mater*, 12:2943-2949.

Sur, G.S., Lyu, S.C. & Chang, J.H. (2003). Synthesis and LCST behavior of thermosensitive poly (N-isopropylacrylamide)-clay nanocomposites. *J. Ind. Eng. Chem*, 9: 58-62

Sur, G.S., Sun, H.L., Lyu, S.G., & Mark, J.E. (2001). Synthesis, structure, mechanical properties,and thermal stability of some polysulfone/organoclay nanocomposites. *Polymer*, 42: 9783-9789.

Tager. A. (1978). Physical chemistry of polymers, *Moscow (Russia), Mir Publishers.*

Takeshita, H., Kanaya, T., Nishida, N. & Kaji, K. (1999). Gelation Process and Phase Separation of PVA Solutions As Studied by a Light Scattering Technique. *Macromolecules,* 32:7815-7819.

Tomasko, D.L., Han, X., Liu, D.H. & Gao, W. (2003). Supercritical fluid applications in polymer nanocomposites. *Curr Opin Solid State Mater Sci*, 7(4-5): 407-412.

Traitel, T., Cohen, Y. & Kost, J. (2000). Characterization of glucosesensitive insulin release systems in simulated in vivo conditions. *Biomaterials*, 21: 1679-1687.

Tretinnikov, O.N., Sushko, N.I. & Zagorskaya, S.A. (2015). Effect of salt concentration on the structure of Poly (vinyl alcohol) cryogels obtained from aqueous salt solutions. *Appl.Spectrosc,* 82 (1) : 40-45.

Upadhyay, D.J., & Bhat, N.V. (2005). Separation of azeotropic mixture using modified PVA membrane, *J. Membr. Sci*, 255: 181-186.

Usuki, A., Kawasumi, M., Kojima, Y., Okada, A., Kurauchi, T. & Kamigaito, O. (1993). Swelling behavior of montmorillonite cation exchanged for x-amine acid by x-caprolactam. *J Mater Res*, 8: 1174-1184.

Usuki, A., Kojima, Y., Kawasumi, M., Okada, A., Fukushima, Y., Kurauchi, T. & Kamigaito, O. (1993). Synthesis of Nylon-6-clay hybrid. Synthesis of Nylon-6-clay hybrid. *J Mater Res*, 8(5): 1179-1183.

Vaia, R.A. & Giannelis, E.P. (1997). Polymer Melt Intercalation in Organically-Modified Layered Silicates: Model Predictions and Experiment. *Macromolecules,* 30: 7990-7999.

Vaia, R.A. & Giannelis, E.P. (1997). Polymer melt intercalation in organically modified layered silicates: model predictions and experiment. *Macromolecules,* 30: 8000-8009.

Vaia, R.A. Vasudevan, S., Krawiec, W., Scanlon, L.G. & Giannelis, E.P. (1995). New polymer electrolyte nanocomposites: melt intercalation of poly (ethylene oxide) in mica-type silicates. *Adv Mater*, 7(2): 154-156.

Vaia, R.A., Jant, K.D., Kramer, E.J., & Giannelis, E.P. (1996). Microstructural evaluation of melt-intercalated polymer-organically modified layered silicate nanocomposites. *Chem. Mater*, 8: 2628-2635.

Vaia, R.A., Ishii, H.& Giannelis, E.P. (1993). Synthesis and properties of two-dimensional nanostructures by direct intercalation of polymer melts in layered silicates. *Chem. Mater*, 5: 1694-1696.

Vaia, R.A., Price, G., Ruth, P.N., Nguyen, H.T.& Lichtenhan, (1999). Polymer/layered silicate nanocomposites as high performance ablative materials. J. *Appl Clay Sci*, 15: 67-92.

Vaia, R.A., Teukolsky, R.K.& Giannelis, E.P. (1994). Interlayer structure and molecular environment of alkylammonium layered silicates. *Chem. Mater*, 6: 1017-22.

Valenta, C. & Anver, B. G., (2004). The use of polymers for dermal and transdermal delivery.*Eur. J. Pharm. Biopharm*., 58: 279-289.

Valentine et al., (2009). Structure of Poly(vinyl alcohol) Cryo-Hydrogels as Studied by Proton Low-Field NMR Spectroscop. *Macromolecules*, 42: 263-272.

Van Krevelen. D.W. (1997). Properties of polymers, *Amsterdam (The Netherlands), Elsevier*.

Vander Hart, D.L., Asano, A. & Gilman, J.W. (2001). NMR measurements related to clay dispersion quality and organic-modifier stability in nylon 6/clay nanocomposites.*Macromolecule*, 38: 3819-22.

Varshney,L. (2007). Role of natural polysaccharides in radiation formation of PVA–hydrogel wound dressing. *Nucl. Instrum. Methods Phys. Res. Sec B: Beam Interactions with Materials and Atoms*, 255: 343-349.

Velazco-Diaz, M., Ruiz, F. A., Doria-Serrano, M. C., Gonzàlez-Montiel, A. & Zolotukin, M. (2005). Synthesis and Characterization of Hydrogels Based on Poly(vinyl alcohol)-g-Poly(styrene) Copolymers.*Ind. Eng. Chem. Res*., 44: 7092-7097.

Vicentini, D.S., Smania Jr, A.. & Laranjeira, M.C.M. (2010). Chitosan/poly(vinyl alcohol) films containing ZnO nanoparticles and plasticizers. Mater. Sci. Eng., C 30: 503-508.

Von zglinicki, T., Lindberg, M., Roomans, G. M., & Forslind, B. (1993). Water and Ion Distribution Profiles in Human Skin. *Acta Derm Venereol (Stockh)*, 73: 340-343.

Watase, M. & Nishinari, K. (1988). Thermal and rheological properties of poly(vinyl alcohol) hydrogels prepared by repeated cycles of freezing and thawing. *Makromol Chem*, 189:871-880.

Watkins, J.J. & Mccarthy, T.J. (1994). Polymerization in supercritical fluid-swollen polymers: a new route to polymer blends. *Macromolecules*, 27(17): 4845-4847.

Watkins, J.J. & Mccarthy, T.J. (1995 a). *Abstract of Papers of the American Chemical Society*, 210: 84 84.

Watkins, J.J. & Mccarthy, T.J. (1995 b). Polymer/metal nanocomposite synthesis in supercritical CO2.*Chem Mater*, 7(11): 1991-1994.

Watkins, J.J. & Mccarthy, T.J. (1995 c). Polymerization of styrene in supercritical CO2-swollen poly (chlorotrifluoroethylene). *Macromolecules*, 28(12): 4067-4074.

Willcox, P.J., Howie, Jr. D.W., Rohr, K.S., Hoagland, D.A., Gido,S.P., Pudjianto, S., et al. (1999). Microstructure of poly(vinyl alcohol) hydrogels produced by freeze/thaw cycling . *J Polym Sci, Part B: Polym Phys*, 37:3438-3454.

Wu, K. A., & Wisecarver, K. D. (1992). Cell immobilization using PVA crosslinked with boric acid, *Biotechnol. Bioeng*, 39: 447-449.

Xu, X., Yin, Y., Ge, X ., Wu, H. & Zhang, Z. (1999). γ-Radiation Synthesis of Poly (acrylic acid)-Metal Nanocomposites. *Mater Letters*, 37(6): 354-358.

Yamaura, K. & Naitoh, M. (2002). Preparation of high performance films from poly (vinyl alcohol)/NaCl/H2O systems. *Journal of Materials Science*, 37: 705–708.

Yamura, K., Itoh, M., Tanigami, T.& Matsuzawa, S. (1989). Properties of gels obtained by freezing/thawing of poly (vinyl alcohol) / water/ dimethyl sulfoxide, *J Appl Polym Sci*, 37:2709-2718.

Yang, C.-C., Lee, Y.-J., & Yang, J. M. (2009). Direct methanol fuel cell (DMFC) based on PVA/MMT composite polymer membranes, *J. Polym. Sour*, 188: 30-37.

Yao, K.J., Song, M., Hourston, D.J. & Luo, D.Z. (2002). Polymer/layered clay nanocomposites: 2- polyurethane nanocomposites. *Polymer*, 43(3): 1017-1020.

Yoshii, F., Makunchi, K. Darwis, D., Iriawan, T., Razzak, M.T. & Rosiak, J.M. (1995). Heat resistance poly (vinyl alcohol) hydrogel. *Radiat Phys* Chem, 46(2):169–174

Yoshii, F., Zhanshan, Y., Isobe, K., Shiozaki, K. & Makunchi, K. (1999). Electron beam crosslinked PEO and PEO/PVA hydrogels for wound dressing. *Radiat Phys Chem*.55:133–138.

Yu, H., & Xiao, C., (2008). Synthesis and properties of novel hydrogels from oxidized Konjac glucomannan cross linked gelation for in-vitro drug delivery. *Carbohyd Polym*, 72:479-489.

Yu, Y-H., Lin, Ch-Y., Yeh, J-M, Lin, W-H. (2003). Preparation and properties of poly(vinyl alcohol)–clay nanocomposite materials.*Polymer*,44:3553–3560.

Zhang, Li-Zhi., Wang, Yuan-Yuan., Wang, Cai-Ling. & Xiang, Hui. (2008). Synthesis and characterization of a PVA/LiCl blend membrane for air dehumidification. *J. Membr. Sci*, 308: 198-206.

Zhang, Y.T., Zhi, t.t., Zhi, T.T., Zhang, L., Huang, H. & Chen, H.L. (2009). Immobilization of carbonic anhydrase by embedding and covalent coupling into nanocomposite hydrogel containing hydrotalcite. *Polymer*, 50: 5693-5700.

Zhao, L., Mitomo, H., Zhai, M., Yoshii, F., Nagasawa, N., & Kume, T. (2003). Synthesis of antibacterial PVA/CM-chitosan blend hydrogels with electron beam irradiation. *Carbohydr. Polym.*, 53: 439-446.

Zhao, X., Urano, K. & Ogasawara, S. (1989) Adsorption of poly (ethylene vinyl alcohol) from aqueous solution on montmorillonite clays. *Colloid Polym Sci*, 267:899–906.

Zheng, J.P., Li, P. & Yao, K.D. (2002). Preparation and characterization of gelatin/montmorillonite nanocomposite. *J Mater Sci Lett*, 21: 779.

Zhu, J., Morgan, A.B., Lamelas F.J., & Wilkie, C.A. (2001). Fire properties of polystyrene–clay nanocomposites. *Chem. Mater*, 13: 3774-80.

APPENDICES

APPENDIX A

Table1: Raw data for sorption kinetics of pure PVA hydrogel and PVA/Na^+-MMT nanocomposite hydrogels containing 1, 3, 5, 7, and 10 % nanoclay:

time (h)	(W_t/W_∞)					
	PVA	1% MMT	3% MMT	5% MMT	7% MMT	10% MMT
1	0.4888	0.5761	0.4804	0.5839	0.5886	0.4885
2	0.6276	0.7760	0.6625	0.7488	0.6762	0.7369
3	0.7532	0.8688	0.7664	0.8622	0.8035	0.8157
4	0.9353	0.9535	0.8876	0.9095	0.9376	0.9587
5	1	1	1	1	1	1

Table 2: Raw data for sorption kinetics of pure PVA hydrogel and PVA/Na^+-MMT nanocomposite hydrogels prepared by physical and physicochemical crosslinking:

time (h)	(W_t/W_∞)		
	PVA	FT	FT & GA
1	0.4888	0.5761	0.4791
2	0.6276	0.7760	0.6742
3	0.7532	0.8688	0.8399
4	0.9353	0.9535	0.9647
5	1	1	1

Table3: Raw data for desorption kinetics of pure PVA hydrogel and PVA/Na^+-MMT nanocomposite hydrogels containing 1, 5 and 10 % nanoclay:

time (h)	(M_t/M_∞)			
	PVA	1% MMT	3% MMT	5% MMT
1	0.3753	0.3188	0.2961	0.2354
2	0.5396	0.4395	0.3684	0.3050
3	0.6412	0.5415	0.4695	0.3567
4	0.7403	0.6544	0.5478	0.4258
5	0.8149	0.7134	0.6521	0.5075

Table4: Raw data for desorption kinetics of pure PVA hydrogel and PVA/Na^+-MMT nanocomposite hydrogels prepared by physical and physicochemical crosslinking.

time (h)	(M_t/M_∞)		
	PVA	FT	FT & GA
1	0.3753	0.3188	0.1982
2	0.5396	0.4395	0.2520
3	0.6412	-	-
4	0.7403	0.6544	0.3544
5	0.8149	-	-
6		0.7687	0.4561
8		-	-
10		0.8795	0.6061

APPENDIX B

The physical properties of the nanoclay (Cloisite Na^+**)** used in this research:

Cloisite® Na^+

Typical Physical Properties Bulletin

Description:
Cloisite® Na^+ is a natural montmorillonite.

Designed Used:
Cloisite® Na^+ is an additive for plastics to improve various plastic physical properties, such as reinforcement, HDT, CLTE and barrier.

Typical Properties:

Treatment/Properties:	Organic Modifier	Modifier Concentration	% Moisture	% Weight Loss on Ignition
Cloisite® Na^+	None	None	4-9%	7%

Typical Dry Particle Sizes: (microns, by volume)

10% less than:	50% less than:	90% less than:
2µm	6µm	13µm

Color: Off White

Density:

Loose Bulk, lbs/ft^3	Packed Bulk, lbs/ft^3	Density, g/cc
12.45	20.95	2.86

LIST OF PUBLICATIONS AND PRESENTED PAPERS

Academic Journals

1) Ali Karimi, Wan Mohd Ashri Wan Daud, Comparison the Properties of PVA/Na+-MMT Nanocomposite Hydrogels Prepared by Physical and Physicochemical Cross linking, Polymer composites, Article first published online : 3 OCT 2014, DOI: 10.1002/pc.23248

2) Ali Karimi, Wan Mohd Ashri Wan Daud, Harmless hydrogels based on polyvinyl alcohol/Na+-Montmorillonite nanocomposites for biomedical applications: Fabrication & Characterization, Polymer Composites, Article first published online: 16 JUL 2015, DOI: 10.1002/pc.23676

3) Ali Karimi, Wan Mohd Ashri Wan Daud, Materials, preparation, and characterization of PVA/MMT nanocomposite hydrogels: A review, Polymer Composites, Article first published online: 21 AUG 2015, DOI: 10.1002/pc.23671

4) Ali Karimi, Wan Mohd Ashri Wan Daud, Nanocomposite cryogels based on poly (vinyl alcohol)/ unmodified Na^+-montmorillonite suitable for wound dressing application: optimizing nanoclay content, under review.

5) Ali Karimi, Wan Mohd Ashri Wan Daud, Fabrication of (PVA/Na^+-MMT/ PVP-Iodine) nanocomposite hydrogel system and study of its in vitro antibacterial properties for wound dressing application, submitted.

Conference Proceedings

1) Ali Karimi, Wan Mohd Ashri Wan Daud, Preparation techniqus and characterization of Poly (vinyl alcohol) – clay nanocomposite hydrogels, 4th Regional Conference on Chemical Engineering, Kuala Lumpur, Malaysia. February, 2012.

2) Ali Karimi, Wan Mohd Ashri Wan Daud, Babak Kaffashi, Ahmad Nalbandi, Comparison of the sorption and desorption kinetics of PVA/Na^+-MMT nanocomposite hydrogels in deionized water and physiological saline solution, Fourth International Conference on Multifunctional, Hybrid and Nanomaterials, Spain (Barcelona), March, 2015.

3) Ali Karimi, Wan Mohd Ashri Wan Daud, Fatemeh Mirsalimi, Behnam Rasekh,Antibacterial wound dressing based on PVA/ Na^+-MMT nanocomposite hydrogels, Fourth International Conference on Multifunctional, Hybrid and Nanomaterials, Spain (Barcelona), March, 2015.